ANTIOXIDANTS & REDOX SIGNALING
Volume 14, Number 6, 2011

DOI: 10.1089/ars.2010.3223

COMPREHENSIVE INVITED REVIEW

Redox Control of Molecular Motion in Switchable Artificial Nanoscale Devices

Alberto Credi, Monica Semeraro, Serena Silvi, and Margherita Venturi

Abstract

The design, synthesis, and operation of molecular-scale systems that exhibit controllable motions of their component parts is a topic of great interest in nanoscience and a fascinating challenge of nanotechnology. The development of this kind of species constitutes the premise to the construction of molecular machines and motors, which in a not-too-distant future could find applications in fields such as materials science, information technology, energy conversion, diagnostics, and medicine. In the past 25 years the development of supramolecular chemistry has enabled the construction of an interesting variety of artificial molecular machines. These devices operate *via* electronic and molecular rearrangements and, like the macroscopic counterparts, they need energy to work as well as signals to communicate with the operator. Here we outline the design principles at the basis of redox switching of molecular motion in artificial nanodevices. Redox processes, chemically, electrically, or photochemically induced, can indeed supply the energy to bring about molecular motions. Moreover, in the case of electrically and photochemically induced processes, electrochemical and photochemical techniques can be used to read the state of the system, and thus to control and monitor the operation of the device. Some selected examples are also reported to describe the most representative achievements in this research area. *Antioxid. Redox Signal*. 14, 1119–1165.

Reviewing Editors: *Amar Flood, Federico Gago, Angel Kaifer, Sergei V. Kalinin, Shoko Kume, Hiroshi Nishihara, and Rajendra Rathore*

Dipartimento di Chimica "G. Ciamician," Università di Bologna, Bologna, Italy.

I. Introduction

The development of civilization has always been strictly related to the design and construction of devices—from wheel to jet engine—capable of facilitating human movement and traveling. Nowadays the miniaturization race leads scientists to investigate the possibility of designing and constructing machines and motors at the nanometer scale, that is, at the molecular level. Many fields of technology, in particular information processing, have benefited from progressive miniaturization of the components of devices in the last 50 years. A common prediction is that further progress in miniaturization will not only decrease the size and increase the power of computers (165), but could also open the way to new technologies in the fields of medicine, environment, energy, and materials (130).

The top-down approach used so far for the construction of miniaturized devices is reaching fundamental and practical limits, which include severe cost limitations, for sizes below 50 nanometers (278). Miniaturization, however, can be pushed further on because "there is plenty of room at the bottom," as Richard Feynman stated in his famous talk in 1959 (138). Research on supramolecular chemistry has shown that molecules are convenient nanometer-scale building blocks that can be used, in a bottom-up approach, to construct ultraminiaturized devices and machines (199). Chemists are in an ideal position to develop such a molecular approach to functional nanostructures because they are able to design, synthesize, investigate, and operate with molecules—for instance, make them react or get them together into larger assemblies.

Much of the inspiration to construct molecular devices and machines comes from the outstanding progress of molecular biology that has begun to reveal the secrets of the natural nanomachines that constitute the material base of life (261). Surely, the supramolecular architectures of the biological world are themselves the premier, proven examples of the feasibility and utility of nanotechnology, and constitute a sound rationale for attempting the realization of artificial molecular devices (149, 176). The bottom-up construction of machines as complex as those present in the Nature is a prohibitive task. Therefore, chemists have tried (i) to construct much simpler systems, without mimicking the complexity of the biological structures, (ii) to undestand the principles and processes at the basis of their operation, and (iii) to investigate the challenging problems posed by interfacing artificial molecular machines with the macroscopic world, particularly as far as energy supply and information exchange are concerned. In the last few years the development of powerful synthetic methodologies, combined with a device-driven ingenuity evolved from the attention to functions and reactivity, have led to remarkable achievements in this field, as evidenced by several reviews (69, 89, 116, 119, 141, 182, 184, 191, 194, 212, 256, 257, 269, 275, 297) and a monograph (64).

This section is focused on redox-controlled artificial nanoscale machines and devices. The various design strategies and processes that have been employed so far to operate these systems will be illustrated with the help of some representative examples based on host–guest systems, rotaxanes, and catenanes. The important and still open problem, concerning the need to transfer these nanodevices from fluid solution to more organized and sophisticated environments, to operate them with some degree of control in space and in time, will be also discussed together with future directions and perspectives.

II. Basic Concepts

A. Definitions

In the macroscopic world, devices and machines are assemblies of components designed to achieve a specific function. Each component of the assembly performs a simple act, whereas the entire assembly performs a more complex, useful function, characteristic of that particular device or machine. In principle, the macroscopic concepts of a device and a machine can be extended to the molecular level (64). A molecular device can be defined as an assembly of a discrete number of molecular components designed to achieve a specific function. Each molecular component performs a single act, whereas the entire supramolecular assembly performs a more complex function, which results from the cooperation of the various components. It also follows that a molecular machine is a special type of molecular device.

The Nature shows, however, that nanoscale devices can hardly be considered as shrunk versions of macroscopic counterparts because several intrinsic properties of molecular-level entities are quite different from those of macroscopic objects, particularly in the case of the molecular machines. In fact, the design and construction of artificial molecular machines can take greater benefit from the knowledge of the working principles of natural ones rather than from sheer attempts to apply at the nanoscale macroscopic engineering principles (105).

Biomolecular machines are made of nanometer-sized floppy molecules that operate at constant temperature in the soft and chaotic environment produced by the weak intermolecular forces and the ceaseless and random molecular movements. Gravity and inertia motions we are familiar with in our everyday experience are fully negligible at the molecular scale; viscous forces resulting from intermolecular interactions (including those with solvent water molecules) largely prevail and it is difficult to obtain directed motion. This means that while we can describe the bottom-up construction of a nanoscale device as an assembly of suitable (molecular) components by analogy with what happens in the macroscopic world, we should not forget that the design principles and the operating mechanisms at the molecular level are different.

For the above reasons, it is not easy to define the functions related to artificial molecular motions. A simple and immediate categorization is usually based on an iconic comparison with motions taking place in macroscopic systems (*e.g.*, braking, locking, shuttling, and rotating). Such a comparison presents the advantage of an easy representation of molecular devices by cartoons that clearly explain their mechanical functions, but it also implies the danger of overlooking the substantial differences between the macroscopic and molecular worlds.

We suggest the use of a minimum set of terms and definitions as reported below, but we are well aware of dealing with a difficult and potentially controversial topic (182, 194).

- Mechanical device: a particular type of device designed to perform mechanical movements.*

*Mechanical movements at the molecular level result from nuclear motions caused by chemical reactions. Any kind of chemical reaction involves, of course, some nuclear displacement, but only large amplitude, nontrivial motion leading to real translocation of some component parts of the system should be considered

- Machine: a particular type of mechanical device designed to perform a specific mechanical movement under the action of a defined energy input.
- Motor: a machine capable of using an energy input to produce useful work.

Clearly, there is a hierarchy: a motor is also a machine, and a machine is also a mechanical device, but a mechanical device might not be a machine or a motor and a machine might not be a motor.

It is also useful to discuss briefly the relation between molecular switches, and molecular machines and motors. A switch is a multistate system whose properties and effects on the environment are a function of its state (121, 136, 151, 212, 213, 221, 222). Most often the interconversion between two given states of a molecular switch can take place by the same pathway that is traveled in opposite directions (Fig. 1a). In this case, any mechanical effect exerted on an external system is cancelled out when the switch returns to its original state. Switches exist, however, in which the forward and backward transitions between a pair of states follow different pathways. A typical example is provided by a rotary device undergoing a 360° unidirectional rotation through two directionally correlated half-rotations (160, 195) (Fig. 1b).

Switches of this kind can influence a system as a function of their switching trajectory, and a physical task performed in a cycle is not inherently undone.

This is a fundamental requirement if a molecular motor has to be constructed. Therefore, generally speaking, molecular machines are also switches, whose states differ from one another for the relative positioning of the various molecular components. However, to behave as motors, the above-described additional feature is required, namely, the forward and backward transitions between the states of the system have to occur by following different pathways. The vast majority of artificial molecular machines reported so far do not exhibit such a behavior and are therefore switches, but not motors. A more thorough discussion on this topic can be found in reference (182).

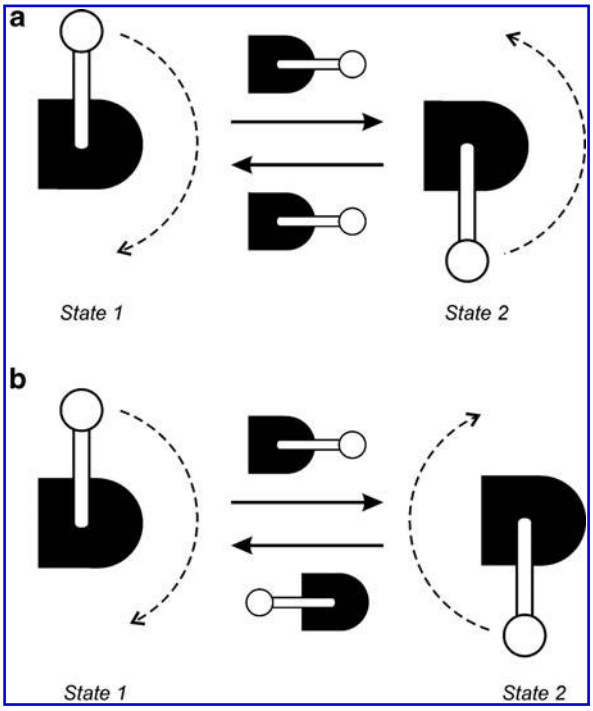

FIG. 1. Schematization of the difference between a rotary switch and a rotary motor. (a) Rotary switch: the interconversion between two states can take place by the same pathway traveled in opposite directions. **(b)** Rotary motor: the forward and backward transitions between two states follow different pathways.

B. Energy supply

As it happens in the macroscopic world, molecular-level devices and machines need energy to operate and signals to communicate with the operator (60). The most obvious way to supply energy to a chemical system is through an exergonic chemical reaction. Not surprisingly, the majority of the molecular motors of the biological world are powered by chemical reactions (*e.g.*, ATP hydrolysis) (149, 176, 261). Richard Feynman observed (138) that "[A]n internal combustion engine of molecular size is impossible. Other chemical reactions, liberating energy when cold, can be used instead." This is exactly what happens in our body, where the chemical energy supplied by food is used in long series of slightly exergonic reactions to power the biological machinery that sustains life.

If an artificial molecular machine has to work by inputs of chemical energy, it will need addition of fresh reactants (fuel) at any step of its working cycle, with the concomitant formation of waste products. Accumulation of waste products, however, will compromise the operation of the device unless they are removed from the system, as it happens in our body as well as in macroscopic internal combustion engines. The need to remove waste products introduces noticeable limitations in the design and construction of artificial molecular machines and devices based on chemical fuel inputs.

In the case of nano-machines and nano-devices whose working operation is based on redox processes, like those described in this section, however, light (through photoinduced electron-transfer processes) and electrical energy (through electrochemically induced redox processes) can be profitably used. They offer indeed several advantages in comparison with chemical energy inputs:

- photons and electrons power molecular devices and machines without formation of waste products;
- photochemical and electrochemical techniques are also useful to read the state of the system monitoring in this way its operation;
- photons and electrons can be switched on and off easily and rapidly;
- lasers provide the opportunity of working in very small space and very short time domains, and near-field techniques enable excitation with nanometer resolution;
- light energy can be transmitted to molecules without physically connecting them to the source (no wiring is necessary);
- electrodes represent one of the best way to interface molecular-level systems with the macroscopic world.

The use of light to power nanoscale devices and machines is relevant for another important reason. If and when a nanotechnology-based industry will be developed, its products will have to be powered by renewable energy sources, because it has become clear that the problem of energy supply is a crucial one for human civilization for the years ahead (23).

In this frame, the construction of nanodevices, including natural–artificial hybrids (272), that harness solar energy in the form of visible or near-ultraviolet light is indeed an important possibility.

C. Other particular features of molecular machines

In addition to the kind of energy input supplied to make them work and the way of monitoring their operation, molecular machines are characterized by other features such as (i) the type of motion—for example, translation, rotation, and oscillation—performed by their components, (ii) the possibility to repeat the operation in cycles, (iii) the time scale needed to complete a cycle, and (iv) the function performed.

An important property of molecular machines, related to energy supply and cyclic operation, is their capability to exhibit an autonomous behavior; that is, to keep operating, in a constant environment and without the intervention of an external operator, as long as the energy source is available. Natural motors are autonomous, but most of the artificial systems reported so far are not autonomous because, after the mechanical movement induced by a given input, they need another, opposite input to reset. Obviously, the operation of a molecular machine is accompanied by partial degradation of free energy into heat, regardless of the chemical, photochemical, and electrochemical nature of the energy input.

Finally, the functions that can be performed by exploiting the movements of the component parts in molecular machines are various and, to a large extent, still unpredictable. In natural systems the molecular motions are always aimed at obtaining specific functions, for example, catalysis, transport, and gating. The changes in the physicochemical properties related to the mechanical movements in molecular machines usually obey binary logic, and can thus be taken as a basis for information processing at the molecular level.

III. Systems Based on Host–Guest Complexes

Molecular self-assembly, a central concept to the Nature's forms and functions (115), is an important route toward the construction of artificial molecular-level devices and machines (62, 66, 69, 128, 142, 182, 198, 241, 256). The challenge for chemists engaged in this field resides in the programming (66, 199) of the system, that is, in the design and synthesis of components that carry, within their structures, the pieces of information necessary not only for construction of the desired supramolecular architecture, but also for the performance of the required function. In systems based on self-assembly, the machine-like function to be performed is often related to the occurrence of a reversible assembly–disassembly process.

The system must therefore be programmed to be able not only to self-assemble under thermodynamic control (process 1 in Fig. 2), but also to disassemble under the action of a suitable energy input (process 2 in Fig. 2). Disassembly implies, of course, chemical transformation of one of the assembled partners. To repeat the self-assembly/induced-disassembly process at will (cyclic process), reset of the system is needed after induced disassembly (process 3 in Fig. 2) (66).

For practical purposes, the state of the system must be well defined. This means that the self-assembly equilibrium (Fig. 2, process 1) must be strongly displaced toward the assembled species. The interaction driving the assembly must, therefore, be relatively strong. The designing principles include

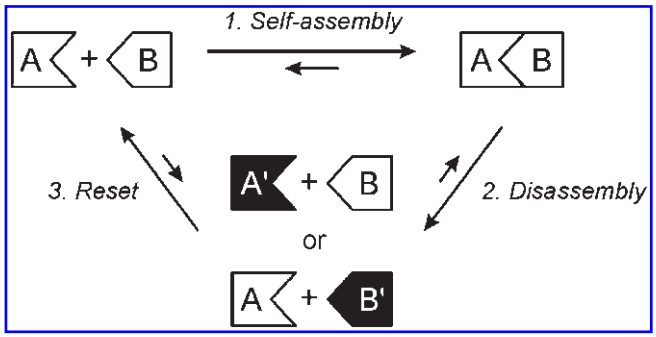

FIG. 2. Schematic representation of a self-assembling/induced-disassembling-reset process that can be used to design molecular-level devices.

- choice of molecular components that can give rise to an intimate supramolecular structure, usually in the form of a host–guest system;
- presence of complementary, strongly interacting (electron donor–electron acceptor, acid–base, *etc.*) units;
- multipoint interactions;
- choice of a suitable, weakly interacting solvent.

Disassembly of a thermodynamically stable supramolecular structure requires the destruction of the interaction responsible for the association process. This can be achieved by means of an appropriate chemical reaction that transforms one of the assembled partners (Fig. 2, process 2). For example, when the interaction responsible for complexation is donor–acceptor in nature, it can be destroyed by oxidation of the electron-donor unit or reduction of the electron-acceptor one. Once again, disassembly must be complete to avoid loss of definition of the system. The reaction needed to cause disassembly can be promoted by chemical, photochemical, or electrochemical stimulation (50, 69, 198).

Reset of the system implies reassembly, which can occur only after the occurrence of a chemical reaction opposite to that responsible for disassembly (Fig. 2, process 3). For example, if disassembly was achieved by reduction of an electron-acceptor unit, oxidation of such a unit must be performed to restore the donor–acceptor interaction and achieve reassembly.

In this section we will illustrate some examples of redox-induced self-assembly/induced-disassembly/induced-reassembly processes, translocation of metal ions between two different sites of a supramolecular system, and threading–dethreading movements in pseudorotaxane structures.

A. Redox-induced self-assembly/induced-disassembly/induced-reassembly processes

An interesting example of a redox regulation mechanism involving conformational changes is compound **1** (Fig. 3a) with two thiol groups inside the binding cavity (223). When dissolved in 1,2-dichloroethane solution, **1** can extract several soft metal ions from water, with strong selectivity for Ag(I). Disulfide **2**, obtained by oxidation of **1** with H_2O_2, does not have any extraction capacity, as expected, because its cavity is closed by the disulfide linkage. The oxidation reaction can be fully reversed by using $NaBH_4$ as reductant. The concept of switching between open and closed cavity discussed above is also relevant to gating of ion channels.

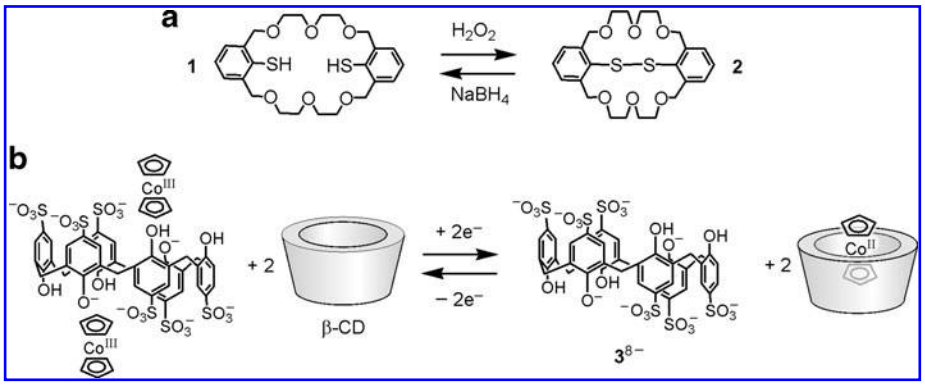

FIG. 3. Redox-controlled host-guest systems. (a) The capacity of compound **1** to extract metal ions from water is switched off by oxidation to **2**; **(b)** selection of either calixarene $\mathbf{3}^{8-}$ or β-cyclodextrin hosts by changing the oxidation state of the cobaltocenium ions.

Calixarenes, in the same way as cyclodextrins (CD), are electrochemically inactive receptors that can form inclusion complexes with a variety of redox-active guests. It has been found (307) that the water-soluble calixarene hexasulfonate $\mathbf{3}^{8-}$ forms (Fig. 3b) stable complexes with ferrocene and cobaltocene derivatives (289) and with bipyridinium-based compounds (81). In contrast with CD, however, binding to calixarenes such as $\mathbf{3}^{8-}$ becomes stronger when the guest is positively charged. This result has been exploited (289) in the design of a three-component supramolecular system, in which an electro-active guest can choose reversibly between two macrocyclic hosts, depending on its oxidation state. The cobaltocenium cation forms a strong 2:1 complex with $\mathbf{3}^{8-}$, even in the presence of an excess of β-CD. Reduction of the cobaltocenium guests, however, leads (Fig. 3b) to their inclusion in β-CD and subsequent oxidation back to the monocation affords the original complex.

Other interesting redox-controlled processes concern

- formation of a molecular loop starting from a pseudorotaxane consisting of a cucurbit[6]uril macrocycle and a hexamethylene bridged bis-bipyridinuim (171);
- mediation by cucurbit[8]uril of the self-assembling of bipyridinium-containing dendrimers (220);
- formation/dissociation of molecular capsules starting from calixarenes (219);
- molecular movements in a ferrocenyl appended cyclam copper complex (90).

Interesting examples of redox-controlled three-pole switches (Fig. 4a) have been reported (38, 86). A three-component supramolecular system, composed of tetrathiafulvalene (TTF), which can exist in three stable forms (TTF, TTF^+, and TTF^{2+}) and two hosts, specifically the π-electron accepting cyclophane cyclobis(paraquat-*p*-phenylene) $\mathbf{4}^{4+}$, and the π-electron donating crown ether **5**, has been investigated (Fig. 4b) (38).

In its role of an electron donor TTF forms, in acetonitrile solution, a 1:1 inclusion complex with $\mathbf{4}^{4+}$, which can be dissociated–reassociated reversibly by cyclic oxidation–reduction of TTF, while TTF^{2+} acts as a π-electron acceptor, giving a 1:1 inclusion complex with **5**. In contrast, TTF^+ is not bound by either of the two hosts. When the electrochemical potential applied to the solution that becomes more positive than $\sim+0.4$ V (relative to the saturated calomel electrode

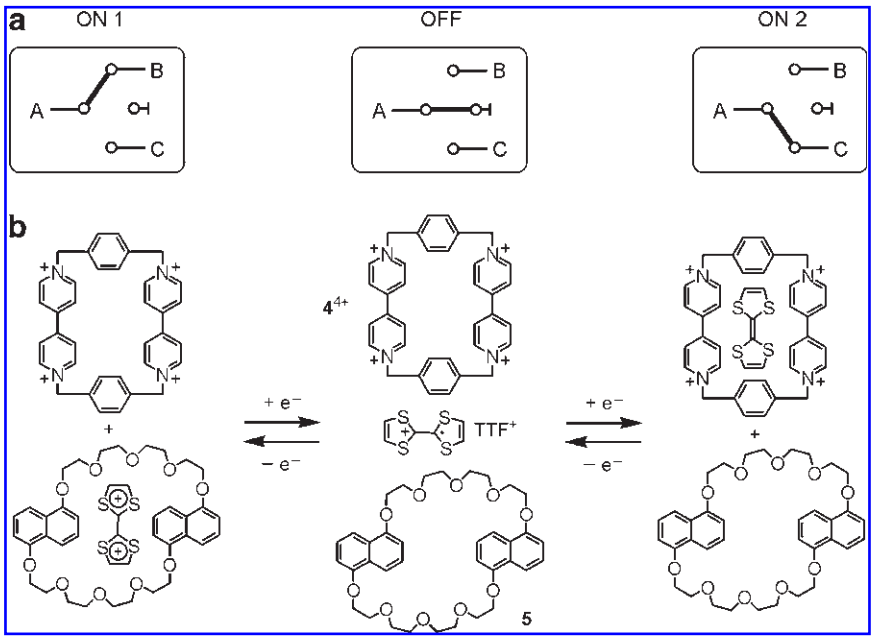

FIG. 4. A supramolecular three-pole switch. (a) Symbolic representation of a three-pole switch. **(b)** A supramolecular switch in which selection of either cyclophane $\mathbf{4}^{4+}$ or crown ether **5** hosts is achieved by changing the oxidation state of the TTF guest. TTF, tetrathiafulvalene.

[SCE]), TTF is oxidized to the monocation form and the complex disassembles to give three essentially noninteracting species. Further one-electron oxidation to TTF^{2+} at potentials more positive than $\sim +0.7$ V (relative to the SCE) leads to the insertion of the dication into the cavity of **5**. Because both oxidized forms of TTF are stable, the initial state can be restored by subsequent reduction. This system can therefore be switched reversibly between three distinct states by exercising electrochemical control on the guest behavior of TTF (Fig. 4b). The fact that the three states have different colors, coupled with the ease of their electrochemical interconversion, renders this supramolecular system suitable for electrochromic applications; the system could, moreover, form the basis for the construction of molecular devices in which energy- or electron-transfer processes between selected components can be controlled (38). This investigation suggests that carefully designed molecular machines could be employed to perform a variety of valuable functions that go far beyond their characteristic molecular motion.

The supramolecular complex composed of an enlarged version of the tetracationic cyclophane $\mathbf{4}^{4+}$, namely, cyclobis (paraquat-*p*-biphenylene), and a polyether-type thread containing a ferrocene unit in the center has been studied with the aim of developing new dual-mode switchable systems (56). By means of spectroscopic and electrochemical experiments it has been found that such a complex, which does not adopt a pseudorotaxane geometry, can be dissociated reversibly either by oxidation–reduction of the ferrocene unit of the guest, or by reduction–oxidation of the bipyridinium units of the host.

Redox-driven processes involving transition metal ions have also been investigated (14, 132, 134). Particularly interesting is the redox-driven intramolecular anion hopping between coordinated metal centers that occurs in compound $\mathbf{6}^{6+}$ (Fig. 5) (124).

This compound consists of two tetraazamacrocyclic (cyclam) moieties, each bearing a 2,2′-bipyridine unit; the cyclam rings can host Ni(II), whereas the bipyridine units, pointing outward, are available for coordination of a Cu(II) ion according to a 2:1 stoichiometry. The resulting species $\mathbf{6}^{6+}$ is therefore a trinuclear metal complex in which the Cu(II) ion, which prefers a five-coordination sphere, has a solvent molecule or an anion, A^-, in the fifth coordination position. In aqueous solution the Cu(II) center of $\mathbf{6}^{6+}$ has a particularly large affinity for triatomic anions such as N_3^-, NCO^-, and NCS^-, presumably because of its high positive charge (6+). Each proximate Ni(II) center, which has a low-spin d^8 electronic configuration, does not compete with the Cu(II) cation for the A^-anion. Thus, in a solution containing $\mathbf{6}^{6+}$ and A^-in 1:1 stoichiometry the anion stays on the copper center. On electrochemical oxidation, the Ni(II) metal ions hosted in the cyclam units are oxidized to Ni(III), which prefer an octahedral coordination environment. The A^- ion, therefore, translocates on an oxidized Ni(III) center, as pictorially illustrated in Figure 5. On Ni(III)-to-Ni(II) reduction, A^- returns to the central copper ion. The translocation distance is estimated to be $\sim$1 nm. Redox-driven intramolecular anion translocation between a metal center and a hydrogen-bond donating compartment has also been reported (6).

Other interesting processes concern assembling/disassembling of metal-based helicate complexes like those formed by ligands **7** and **8** with copper ions (8, 9, 12–14).

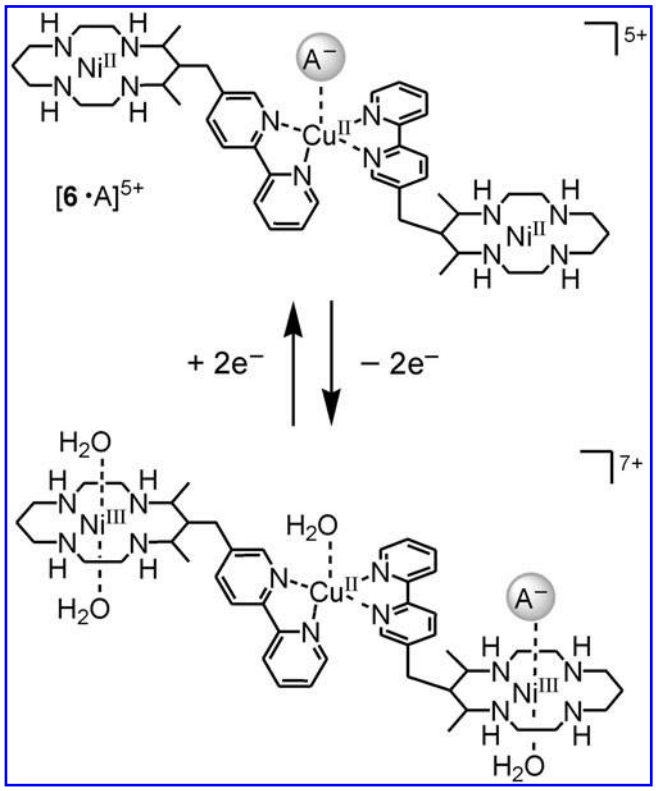

FIG. 5. Redox-controlled anion (A^-) translocation in the trinuclear metal complex $\mathbf{6}^{6+}$.

Ligand **7** (Fig. 6a) gives stable complexes with Cu(I) and Cu(II), both in acetonitrile solution and in the solid state. X-Ray diffraction studies evidence very clearly that Cu(I) forms a dinuclear complex, $[Cu_2(\mathbf{7})_2](CF_3SO_3)_2$, that shows a double-strand helix arrangement of the bis-bidentate ligand around the metal center (Fig. 6b), whereas Cu(II) prefers to form a mononuclear complex species, $[Cu(\mathbf{7})](CF_3SO_3)_2$, in which it reaches its convenient tetragonal coordination through the chelation by a single molecule of **7** (Fig. 6c).

On assuming that the above-described geometrical features are maintained in solution, the Cu(II)/Cu(I) redox change in solution would result in an assembling–disassembling equilibrium, as pictorially illustrated in Figure 7.

The occurrence of such redox-driven and reversible processes involving copper complexes of **7** has been verified through cyclic voltammetry experiments at a platinum electrode in an acetonitrile solution (10). The high irreversibility of the cyclic voltammetric profile depends upon the fact that the assembling–disassembling process is too fast with respect to the time scale of the voltammetric experiment, also when they are recorded at a scan rate of 20 V s^{-1}. This means that the transient species $[Cu_2(\mathbf{7})_2]^{4+}$ (upper right corner in the square scheme of Fig. 7) and $[Cu(\mathbf{7})]^+$ (lower left corner of square scheme) have a very short lifetime.

However, it has been recently demonstrated (234) that the lifetime of the di-copper(II) double-strand helicate $[Cu_2(\mathbf{7})_2]^{4+}$ can be significantly increased by introducing hindering substituents on the framework of **7**, as in the case of the bis-bidentate ligand **8** (Fig. 6a).

The bidentate ligand **8** forms with Cu(I) a double-strand helicate complex, $[Cu_2(\mathbf{8})_2]^{2+}$, very similar to the $[Cu_2(\mathbf{7})_2]^{2+}$

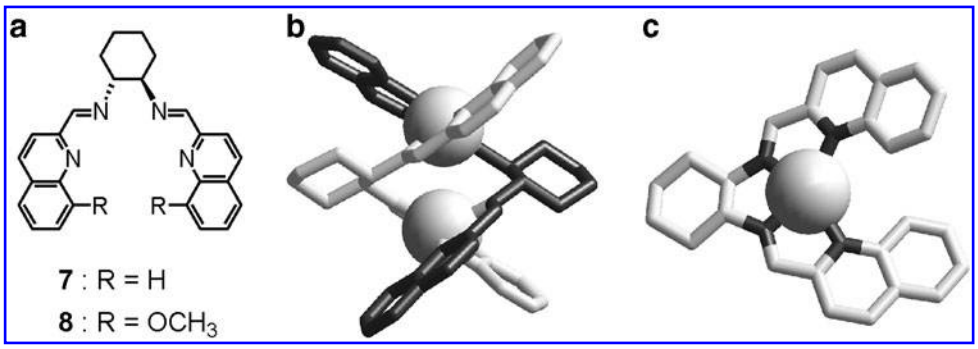

FIG. 6. Redox-active metal-based helicate complexes. (a) Structural formula of ligands **7** and **8**; **(b)** molecular structure of the $[Cu_2(\mathbf{7})_2]^{2+}$ double-strand helicate complex in which the Cu(I) metal centers are represented as spheres and the hydrogen atoms of the two strands have been omitted for clarity; **(c)** molecular structure of the $[Cu(\mathbf{7})]^{2+}$ complex in which the Cu(II) metal center is represented as a sphere and the hydrogen atoms of the two strands have been omitted for clarity (the metal center experiences a rather distorted square coordination geometry).

analog. Its cyclic voltammetric behavior in acetonitrile solution unambiguously indicates that on oxidation of the dicopper(I) helicate a dicopper(II) helicate forms according to two distinct one-electron oxidation steps:

$$[Cu^{I}_2(\mathbf{8})_2]^{2+} \leftrightarrows [Cu^{I}Cu^{II}(\mathbf{8})_2]^{3+} + e^-$$
$$[Cu^{I}Cu^{II}(\mathbf{8})_2]^{3+} \leftrightarrows [Cu^{II}Cu^{II}(\mathbf{8})_2]^{4+} + e^-$$

On the other hand, the electrochemical investigation on an acetonitrile solution containing the mononuclear $[Cu(\mathbf{8})]^{2+}$ complex, obtained from the interaction of Cu(II) with ligand **8**, gives totally different results that can be interpreted as follows: (i) on scanning the potential to negative values, the reduction of the mononuclear $[Cu(\mathbf{8})]^{2+}$ complex to the corresponding mononuclear $[Cu(\mathbf{8})]^{+}$ species results in a fast assembling to give the dicopper(I) double-strand helicate; (ii) on scanning the potential to positive values, the $[Cu_2(\mathbf{8})_2]^{2+}$ complex undergoes stepwise one-electron metal-based oxidation processes to give first $[Cu_2(\mathbf{8})_2]^{3+}$ and then $[Cu_2(\mathbf{8})_2]^{4+}$. The above evidence indicates that the $-OCH_3$ substituent in each quinoline moiety slows down the disassembling of the Cu(II) double-strand helicate complex, which persists in solution on the time scale of the voltammetric experiment (in the present case performed at a scan rate of 200 mV/s).

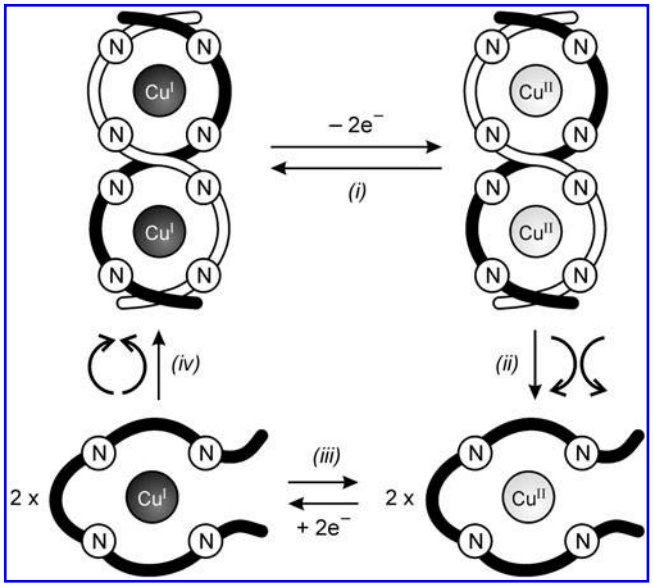

FIG. 7. The redox-driven disassembling of the $[Cu_2(\mathbf{7})_2]^{2+}$ double-strand helicate complex to give two mononuclear $[Cu(\mathbf{7})]^{2+}$ complexes, in which each strand behaves as a quadridentate ligand. On subsequent reduction, the two mononuclear complexes reassemble to give the di-copper helicate.

Double-strand dicopper helicate complexes are interesting systems because they may show hysteresis (as observed with ligand **7**), giving rise to a rare example of electrochemical bistability. It has been also shown that the hysteretic behavior can be controlled and modulated through simple synthetic modifications, as observed with ligand **8**.

B. Redox-induced translocation of metal ions

In the redox-driven metal translocation the movable metal center should have two consecutive, stable oxidation states, M^{n+} and $M^{(n+1)+}$, a quite common property in transition metal chemistry. On this basis a ditopic ligand could be designed in which a compartment, A, has selective affinity for the oxidized form, $M^{(n+1)+}$, whereas the other compartment, B, has a higher affinity for the reduced form, M^{n+}. The redox cycle can be performed either chemically or electrochemically. The rate of the process depends on the extent of reorganization required by the change in the coordination arrangement. Similar problems are encountered in the redox-driven mechanical movements in metal-based rotaxanes and catenanes described in sections "IV. Systems Based on Rotaxanes" and "V. Systems Based on Catenanes."

A classical example of redox-driven translocation of a transition metal ion is shown schematically in Figure 8 (306). The triple-stranded helical ligand contains internal, hard hydroxamate and external, soft bipyridine binding sites. Fe(III) prefers to reside in the hard coordination environment, [**9**•Fe], whereas Fe(II) has a large affinity for the bipyridine ligands $[\mathbf{10}\bullet Fe]^{2+}$. On chemical reduction of Fe(III) to Fe(II) by ascorbic acid the metal ion, therefore, translocates to the external soft bipyridine site. The translocation, which occurs with a change in color, can be reversed by adding peroxydisulfate. The ion translocation process is rather slow (minutes to hours, depending on the direction) because of the severe steric rearrangements that the ditopic system must experience in the course of the metal ion movement.

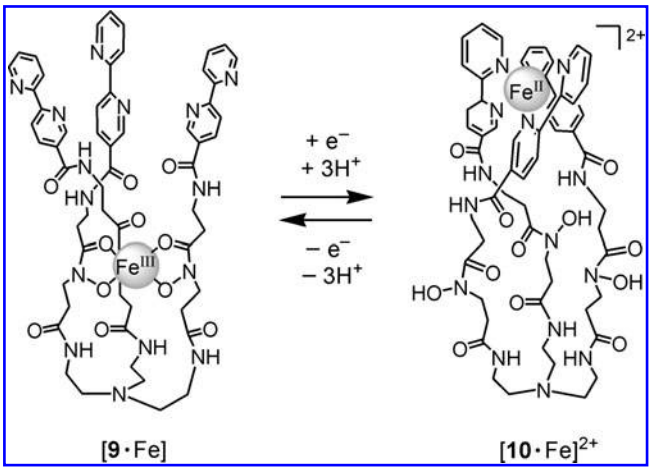

FIG. 8. Redox-driven translocation of an iron cation within a ditopic ligand.

An Fe(III)/Fe(II)-driven translocation process of different nature is illustrated in Figure 9 (77). Ligand **11** consists of a 4-methylphenol platform, to which two different terdentate subunits have been appended in 2 and 6 positions. One appendance is formed by a tertiary amine group and two phenolate oxygen atoms; deprotonation of all the phenolic group of **11** is guaranteed by the presence of the base 2,4,6-trimethylpyridine (collidine) in the acetonitrile solution. The other appendance possesses one tertiary amine group and two pyridine nitrogen atoms. When 1 equiv. of $Fe(ClO_4)_3$ is added to an acetonitrile solution of **11**, in the presence of collidine, the Fe^{3+} cation seeks for the coordination of the three available oxygen atoms, one from the platform and two from the phenolate moieties. Six-coordination, to give the preferred octahedral geometrical arrangement, is achieved by coordination of the nitrogen atom of the amine and by two solvent molecules (Fig. 9a, left).

On the other hand, if a stoichiometric amount of $Fe(ClO_4)_2$ is added to a solution of **11** containing collidine, the Fe^{2+} center looks for the coordination of the three nitrogen atoms, one from the amine and two from the pyridine moieties, while the phenolate oxygen atom of the platform and two solvent molecules complete six-coordination (Fig. 9a, right). These data provide the bases for the occurrence of a redox-driven translocation of the iron center between the two compartments, which share the central phenolate oxygen atom. Indeed, translocation was carried out electrochemically and was investigated by means of cyclic voltammetric experiments carried out in acetonitrile solution. The electrochemical behavior can be accounted for on the basis of the square scheme shown in Figure 9b that illustrates the pendular motion of the iron center driven by the Fe(III)/Fe(II) redox couple.

Voltammetric studies performed at high scan rates indicate that the time constant of the iron translocation, processes (ii) and (iv) of Figure 9b, is lower than 10 ms. The high translocation rate can be ascribed to the beneficial assistance of the central phenolate oxygen atom, which keeps the iron center coordinated over the course of the direct and reverse motion, thus reducing the energy of the transition state. A similar system in which one compartment is based on three salicylamide groups and the other on three bipyridine fragments has been also reported (291).

Figure 10 illustrates the translocation of a copper ion between the two coordination sites of the octadentate ligand **12** (11). The compartment that consists of four secondary amine groups is suitable for coordination of Cu^{2+}, whereas that consisting of two bipyridine moieties is more suitable for coordination of Cu^{+}. The ligand is flexible enough to fulfil the stereochemistry requirements of each metal oxidation state (square coordination for Cu^{2+} and tetrahedral for Cu^{+}). The translocation process is rapid and reversible and occurs on addition of ascorbic acid for the species containing Cu^{2+} and on addition of H_2O_2 for the species containing Cu^{+}.

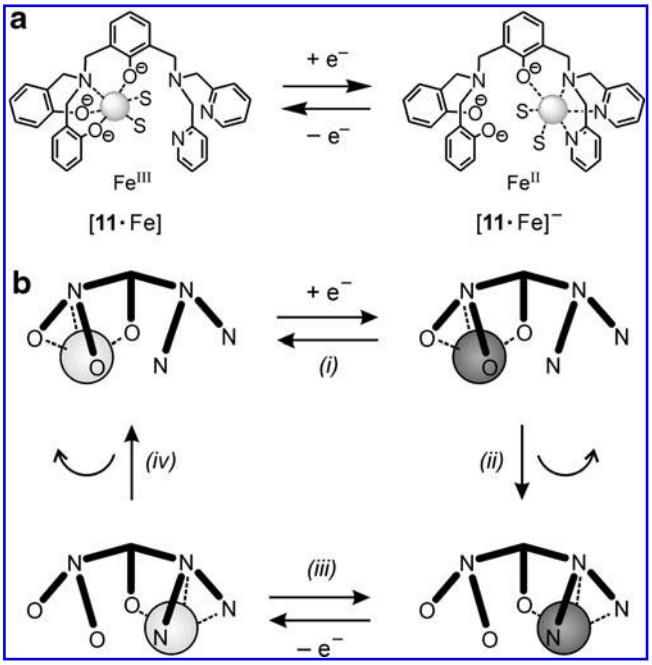

FIG. 9. Redox induced metal ion translocation in a ligand with two compartments. (a) Ligand **11** provides two donor set compartments capable of hosting a Fe^{3+} cation (left compartment) and a Fe^{2+} cation (right compartment); **(b)** a square scheme illustrating the pendular motion of the iron center between the two compartments of ligand **11**, driven by the Fe(II)/Fe(III) redox couple.

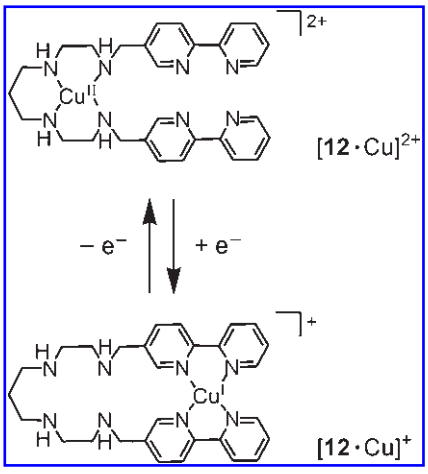

FIG. 10. Redox-driven translocation of a copper metal ion within the ditopic ligand 12.

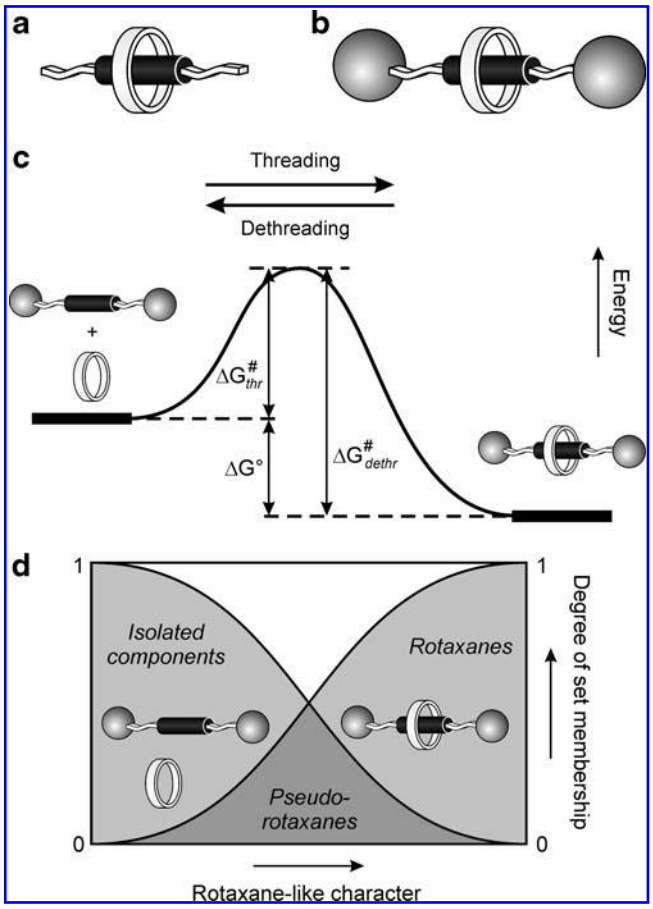

FIG. 11. The difference between pseudorotaxanes and rotaxanes. (a) Schematic representation of a pseudorotaxane structure; **(b)** schematic representation of a rotaxane structure; **(c)** self-assembly of rotaxane-like entities by slippage of a macrocyclic through relatively bulky stoppers; **(d)** schematic illustration showing that pseudorotaxanes belong to the fuzzy domain between isolated components and rotaxane structures.

In recent years, great attention has also been devoted to anion receptors and anion translocation (7).

C. Threading–dethreading molecular movements

As far as molecular machines are concerned, the most interesting host–guest systems are certainly the pseudorotaxanes (4, 87, 99, 143, 146, 166, 187, 245, 258) structures that can be defined (44) as interwoven inclusion complexes in which a molecular thread is encircled by one (Fig. 11a) or more beads (*i.e.*, macrorings) so that the extremities of the thread are directed away from the center of the bead.

The constituents of the assembly, like any complex, are at liberty to dissociate into separate molecular species. If two bulky substituents (stoppers) are placed at the ends of the thread, a pseudorotaxane is converted into a rotaxane (section "IV. Systems Based on Rotaxanes"), a structure that does not allow dethreading, because of the presence of the two stoppers (Fig. 11b). However, if the thread has relatively bulky substituents since the beginning, the ring can slip through them, a process that requires overcoming of a quite high activation barrier (Fig. 11c) (26). For such systems dethreading of the ring is not impossible, but requires overcoming of an even higher activation barrier, so that under appropriate conditions (*e.g.*, low temperature) they behave as rotaxanes. This shows that pseudorotaxanes can have some rotaxane-like character. From another viewpoint we can say that pseudorotaxanes belong to the fuzzy domain between the two extremes (Fig. 11d) corresponding to either the two isolated components or the assembled rotaxane structure (42). This is indeed a good example of fuzzy logic in chemistry, a concept that is now proving its value for a great variety of industrial chemical processes (248–250).

Some of the molecular motions that can be obtained with pseudorotaxanes are represented pictorially in Figure 12. Dethreading–rethreading of the thread and ring components is reminiscent of the movement of a piston in a cylinder. Starting from this simple motion (Fig. 12a), more complex processes can be devised. In a chemical system comprising a macrocycle and two thread-like species one can select, by means of a suitable input, which thread enters the ring's cavity (Fig. 12b). Analogously, a suitable stimulus can be used to choose which of the two macrocycles surrounds a particular thread-like species (Fig. 12c). The processes shown schematically in Figure 12 can also be taken as a basis for binary logic operations and for the design of logic gates (64).

The external stimulus used to power such rudimentary molecular machines must be able to weaken the noncovalent bonding forces that stabilize the initial supramolecular complex and depends on the nature of such forces.

In this section we will illustrate some examples of pseudorotaxanes in which the interactions responsible for complexation are donor–acceptor in nature. Such kind of interactions

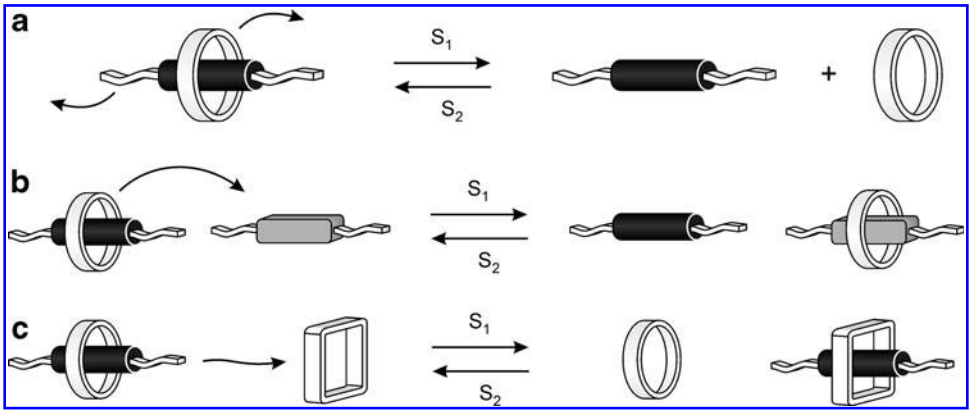

FIG. 12. (a) The dissociation of a pseudorotaxane and the interchange of (b) a macrocycle between two threads and (c) a thread between two macrocycles. S_1 and S_2 are appropriate external stimuli. Copyright Wiley-VCH Verlag GmbH & Co. KGaA. Reproduced with permission from Balzani *et al.* (64).

can be weakened by oxidation of the electron-donor unit or by reduction of the electron-acceptor one. The reduction of the electron-acceptor unit also weakens the [C–H···O] hydrogen bonds that accompany the donor–acceptor interactions in most of these supramolecular complexes. The donor–acceptor interaction can usually be restored by means of the reverse redox process. Of course, the oxidation and reduction processes needed to dissociate–associate a pseudorotaxane can be achieved by chemical, electrochemical, or photochemical inputs (50, 64, 69) and in the following some paradigmatic examples divided according to the nature of the energy inputs are reported.

1. Chemically driven movements. The assembly of complexes based on electron- donor–acceptor interactions can be controlled by means of redox stimuli that can be provided by the addition of oxidants and reductants. The inclusion complex formed between the electron-acceptor cyclophane $\mathbf{4}^{4+}$ and the well-known electron donor TTF (Fig. 4), and pseudorotaxanes composed of $\mathbf{4}^{4+}$ and thread-like species containing a TTF unit, can be disassembled (27, 29, 68) into their free components by oxidation of the TTF unit to its radical cation with one equivalent of $Fe(ClO_4)_3$ in acetonitrile or aqueous solution. The one-electron oxidized form of the TTF unit is stable under such conditions and can be reduced back to its neutral form by adding a stoichiometric amount of ascorbic acid. The reduction results in the insertion of the TTF unit into the tetracationic cyclophane. Dethreading can also be achieved by adding *o*-chloranil, which forms an adduct with the TTF unit; on addition of $Na_2S_2O_5$ in the presence of water, *o*-chloranil is reduced, affording the original pseudorotaxane (68). Such dethreading–rethreading processes can be easily monitored by ultraviolet–visible absorption spectroscopy, because

- the complex has a broad absorption band with a maximum ~ 850 nm, ascribed to the charge–transfer (CT) interaction between the electron-rich TTF unit and the electron-poor bipyridinium units of $\mathbf{4}^{4+}$;
- the neutral and cationic forms of the TTF unit have very different absorption features.

A system of this kind can, moreover, serve as a basis for the construction of a supramolecular device in which it is possible, by means of chemical stimuli, to select which of two guests enters the cavity of a macrocycle, and to interchange the two guests reversibly (Fig. 13) (118). Addition of the thread-like compound **13**, which contains a π-electron-rich dioxynaphthalene (DON) unit, to an aqueous solution of the $[\mathbf{4}\bullet TTF]^{4+}$ complex affects neither the CT absorption band characteristic of the complex nor the strong fluorescence band of the DON-based thread **13**, indicating that this thread does not displace TTF from inside the macrocyclic host.

On addition of a stoichiometric amount (with regard to TTF) of $Fe(ClO_4)_3$ the absorption bands of the radical cation TTF^+ are formed, the CT band of $[\mathbf{4}\bullet TTF]^{4+}$ disappears, and the fluorescence band of the DON-based species **13** is substantially quenched. These results show that oxidation causes expulsion of TTF^+ from $\mathbf{4}^{4+}$ and its replacement by the DON-based thread. On subsequent addition of ascorbic acid the system returns to its initial state.

2. Electrochemically driven movements. Electrochemical methods have been used extensively to control molecular recognition (25, 66, 69, 71, 85, 100, 133, 179, 182, 229, 285). As discussed in section "B. Energy supply," electrochemical techniques can be used not only to induce chemical or conformational changes in supramolecular systems, but also to probe their superstructures and organization. In other words, electrochemistry provides a handle on both the input stimuli and the readout signals that are necessary for monitoring the operation of molecular machines.

Key features of the systems that can be electrochemically controlled are

- the presence in one component of an electro-active unit characterized by reversible redox processes;
- the effect of the other component on the electrochemical behavior of the component containing the electro-active unit.

This second property enables investigation of the complexation–decomplexation process by, for example, voltammetric techniques.

CD (46, 112, 247) are a class of hosts that are inactive electrochemically yet can form stable pseudorotaxanes with a variety of electro-active guests (85, 157, 178, 179, 207, 275). It has been found, for example, that, whereas compounds containing bipyridinium (usually called viologen) in the dicationic forms (*e.g.*, $\mathbf{14}^{2+}$, Fig. 14) are not bound by β-CD, when reduced to their monocationic forms they interact weakly with the cavity of this host and give fairly stable pseudorotaxane complexes with β-CD when they are finally reduced to their uncharged forms (216, 217).

Similar results have been found for cobaltocenium derivatives, which do not interact with CD yet become good guests for inclusion in β-CD upon one-electron reduction to yield the neutral cobaltocene (290). Ferrocene and its derivatives (114, 147, 277, 300), and TTF (262, 308), behave in the opposite manner; that is, they are strongly bound in their most stable oxidation states, which correspond to uncharged species, but when they are oxidized they are not bound. These features have been exploited to construct dendrimers that contain up to 16 ferrocene units (94) or up to 32 cobaltocenium units (148), on their peripheries and therefore exhibit redox-controllable multisite complexation of β-CD. Such dendrimers

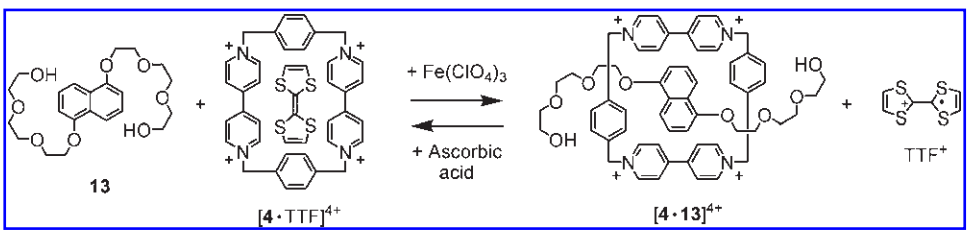

FIG. 13. The chemically redox-induced interchange of guests TTF and 13 into the cavity of cyclophane $\mathbf{4}^{4+}$.

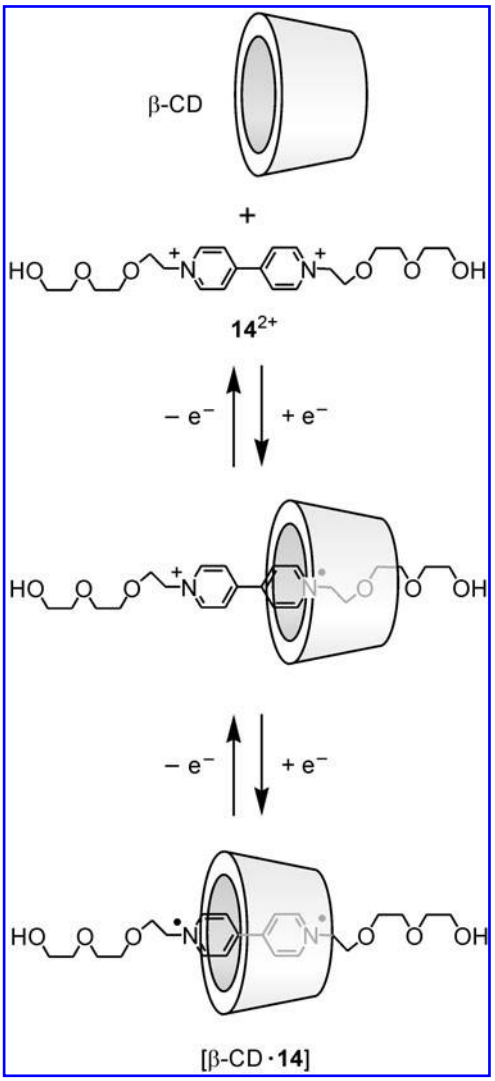

FIG. 14. The electrochemically induced threading–dethreading processes of the thread 14^{2+} into the cavity of *β*-CD. CD, cyclodextrin.

form very large supramolecular architectures that can be either broken apart, or assembled, on oxidation of the ferrocene units or on reduction of the cobaltocenium units, respectively. Ferrocene has also been used as the core of water-soluble dendrimers containing glucopyranosyl residues in the branches. In these compounds, the ferrocene unit is indeed complexed by *β*-CD, provided that only one of its two cyclopentadienyl rings bears a dendritic substituent (39).

Similar investigations have been performed on calixarenes, another important class of electroinactive receptors (81, 289, 307). In CH_2Cl_2 solution the tris(*N*-phenylureido)calix[6]arene **15** can complex the molecular thread 1,1′-dioctyl-4,4′-bipyridinium dication $\mathbf{16}^{2+}$ in a pseudorotaxane-type fashion (Fig. 15) with an association constant exceeding 10^6 L mol^{-1} (21). The pseudorotaxane species are stabilized by [$\pi\cdots\pi$] stacking, [C–H$\cdots$O] hydrogen bonding, [C–H$\cdots\pi$] interactions, and, interestingly, by hydrogen-bonding interactions between the counteranions of the dicationic guest and the N–H ureido groups of the host. Thread $\mathbf{16}^{2+}$ exhibits the two monoelectronic and reversible reduction processes typical of the viologen-based compounds (218, 276). When it is threaded within **15**, a large shift of its first reduction potential toward more negative values; the second reduction process, however, occurs at the same potential as for the free thread, indicating that one-electron reduction of the thread promotes dethreading (Fig. 15) (117). Oxidation of the radical cation $\mathbf{16}^{+}$ back to the dication leads to rethreading.

Cyclic voltammetric studies and stopped-flow absorption experiments showed that for this species, the (re)threading process is relatively slow ($k_{thr} \sim 3\times10^5$ l mol^{-1} s^{-1} at 298 K), and ^{1}H nuclear magnetic resonance (NMR) studies (20) indicated that in nonpolar solvents the insertion of $\mathbf{16}^{2+}$ into the cavity of **15** occurs exclusively through the rim bearing the ureido groups. The latter observation suggests the possibility of designing pseudorotaxanes with unidirectional threading–dethreading motions (117).

Another family of redox-inactive receptors capable of giving redox switchable pseudorotaxanes with viologen guest is that of the cucurbit[*n*]urils (186, 187, 197). The position of cucurbit[*7*]uril on a thread containing ferrocene as end groups is switched upon ferrocene oxidation (270, 288). Cucurbit[*8*]uril and 1,1′-dimethyl-4,4′-bipyridinium dication (also called methyl viologen, MV^{2+}) form a 1:1 inclusion complex that can be reversibly converted into a 1:2 complex by one electron reduction of the guest. This process has been exploited to obtain the reversible formation of a molecular loop when hexamethylene-bridged bis-viologen is used as a guest (171). A similar loop was also obtained starting from a thread containing a naphthalene-2-yloxy and a viologen linked by a flexible tether because of formation of a CT complex within the cucurbit[*8*]uril cavity (170). This loop can be open by reduction in the presence of added MV^{2+}. In aqueous solution the first stable π-dimer of a TTF cation radical encapsulated in the cavity of suitable cages has also been evidenced (304, 309).

One of the most extensively studied receptors in recent years has been the cyclophane $\mathbf{4}^{4+}$ (Fig. 4), which is a very efficient host for a wide variety of π-electron donating guests (4). Because it is redox active (17) its binding capacity can be subjected to electrochemical control. Two bielectronic reduction processes are observed for the tetracationic cyclophane $\mathbf{4}^{4+}$, the first corresponding to the uptake of the first electron by each of the equivalent bipyridinium units and the second to the subsequent reduction of the radical cations to neutral units. When an electron-donor unit is located inside the cavity of the cyclophane the potential associated with the first reduction process is shifted to more negative values, as a consequence of the CT interactions that stabilize the complex (113, 126, 285). The second reduction process at more negative potentials of this cyclophane is very important because, as already pointed out for the viologen-based thread $\mathbf{16}^{2+}$, it can be used to monitor the occurrence of decomplexation induced by the first two-electron reduction (178, 285). For example, in the presence of excess of a thread-like compound composed of a polyether chain that bears a 1,4-dioxybenzene unit in the middle, the potential value for the first bielectronic reduction of $\mathbf{4}^{4+}$ is shifted cathodically, whereas the second reduction process is almost unaffected (17). This observation is consistent with formation of a pseudorotaxane between the cyclophane and the thread, and dethreading of the pseudorotaxane upon two-electron reduction of the $\mathbf{4}^{4+}$ host, so that the second two-electron reduction process reflects that of the free

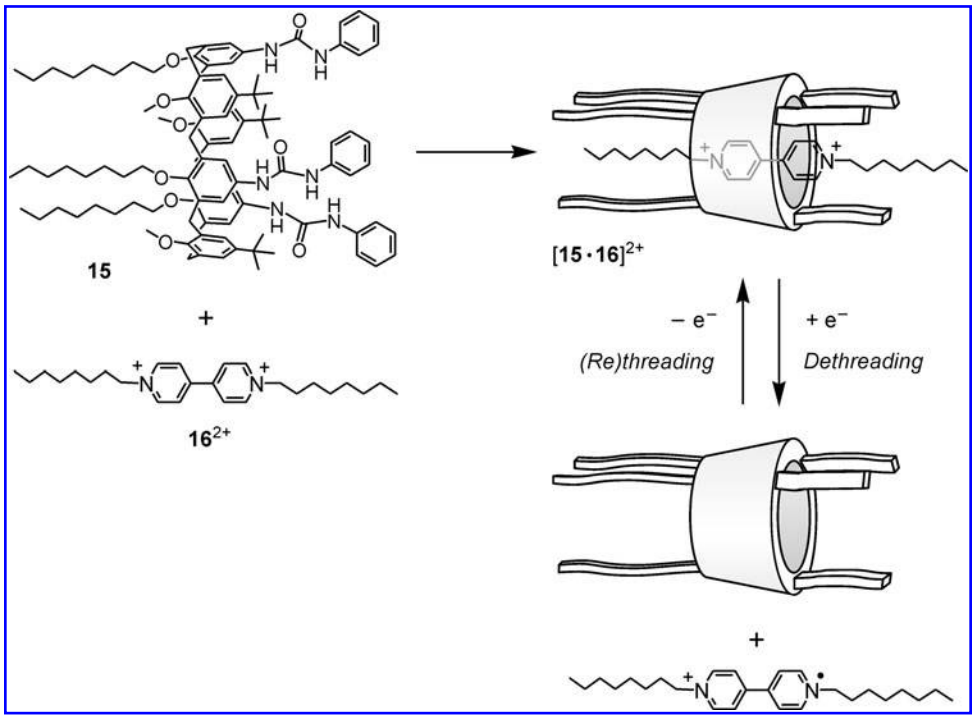

FIG. 15. The electrochemically induced dethreading–rethreading processes associated with the pseudorotaxane [15•16]$^{2+}$.

host. The occurrence of the dethreading reaction is not surprising, because reduction of the electron-acceptor component weakens the CT interaction that helps to hold together the components of the supramolecular architecture. Because all these processes are reversible, oxidation of **4** back to the tetracationic form affords the original pseudorotaxane. It should, in principle, also be possible to obtain useful information about the occurrence of dethreading–rethreading processes from the electrochemical behavior of the guest; the poor reversibility of the oxidation process associated with a 1,4-dioxybenzene unit, however, prevents the use of this type of control.

More interesting are pseudorotaxanes wherein both the cyclophane and thread components are characterized by chemically reversible redox processes; one example is the complex of TTF with **4**$^{4+}$ (Fig. 13) (29, 126) and related pseudorotaxanes (27, 68). This improvement in design not only enables monitoring the formation of the supramolecular species by studying both the reduction of the electron-acceptor component and the oxidation of the electron-donor species, but also provides a dual mode (reductive and oxidative) of control on the dethreading–rethreading process. The molecular thread **17**, obtained by attaching two polyether chains to a TTF unit (Fig. 16), forms a very stable pseudorotaxane with **4**$^{4+}$(29). Reversible dethreading–rethreading cycles of the pseudorotaxane [**4**•**17**]$^{4+}$ (and of [**4**•TTF]$^{4+}$, Fig. 13) can be performed either by oxidation and successive reduction of the electron-donating thread or by reduction and successive oxidation of the electron-accepting cyclophane (29). Such processes are accompanied by pronounced spectral differences that can be followed easily by the naked eye. This unique behavior makes the system appealing for the construction of electrochromic display devices and, because its input (electrochemical)-output (color) characteristics correspond to those of the XNOR (eXclusive Not OR) logic operation, for the design of molecular-level logic gates.

In suitably designed compounds CT interactions can give rise to intramolecular pseudorotaxane structures (33, 43, 227, 228). Electrochemically controlled threading–dethreading of a ring-in-ring self-complexed system has also been reported (57).

3. Photochemically driven movements. Stimulation by light is the most interesting way to power molecular-level machines (section "B. Energy supply"). Photons, like electrons, can be exploited both for causing the changes (writing) in chemical systems and for monitoring (reading) their states (54, 55, 62, 63, 65–67, 69, 70–72, 120, 182, 184, 256). In general, systems of this type that have been reported so far can be subdivided into those relying on photoinduced electron-transfer processes, and those based on photoisomerizations. In this context only the systems based on photoinduced electron transfer will be discussed.

Complexes such as [**4**•TTF]$^{4+}$ and [**13**•**4**]$^{4+}$ (Fig. 13) are primarily stabilized by π-electron donor–acceptor interactions. These interactions usually introduce new energy levels that cause the appearance of CT absorption bands, often in the visible region of the spectrum (17, 27, 29, 33, 68). Excitation in these bands leads formally to the transfer of an electron from the donor to the acceptor component and is, therefore, expected to destabilize the CT interaction responsible for self-assembly.

Occasionally, photoinduced electron transfer leads to the formation of charges of the same sign that repel each other and so contribute to forcing the molecular components apart. This simple approach to dethreading is, however, precluded, because back-electron transfer, that is, the deactivation of the CT excited state to the ground state, is much faster than the separation of the molecular components, a process that requires extended nuclear motions and solvation processes (53, 78, 122, 196, 263). In some particular instances (79, 80), laser flash photolysis experiments have been interpreted

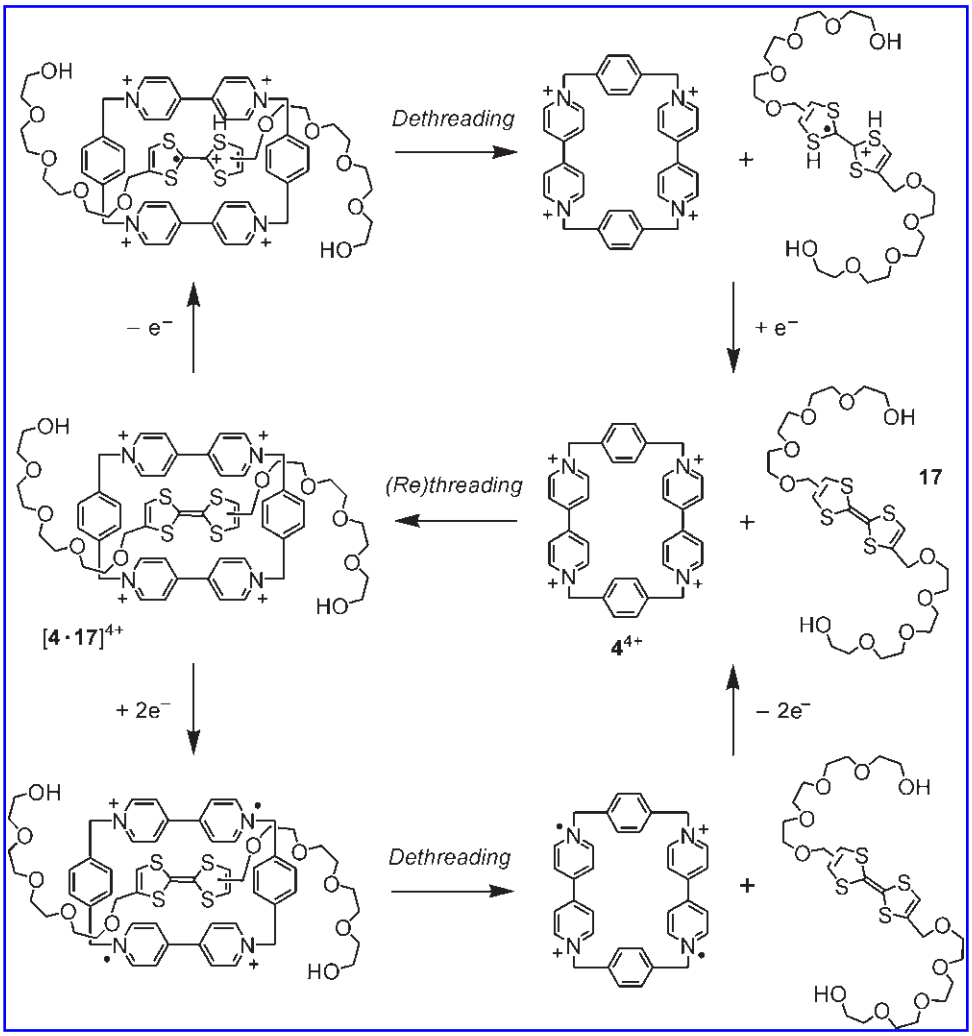

FIG. 16. The dual-mode electrochemically induced dethreading–rethreading processes associated with the pseudorotaxane $[4•17]^{4+}$.

as indicating dissociation of a small fraction of the irradiated complex.

To achieve light-induced dethreading of the $[13•4]^{4+}$ complex, a different approach was devised (33, 53) that was based on the use of an electron-transfer photosensitizer (P), separated from or linked to one of the components [either to the macrocycle (41) or to the thread (34, 40, 183, 214, 252, 266, 302, 303); see, for example, 18^{4+} in Fig. 17], and a reductant scavenger (Red) species. Good candidates for the role of photosensitizer are 9-anthracenecarboxylic acid (175) and metal complexes (177) such as $[Ru(bpy)_3]^{2+}$ (Fig. 17), whereas efficient reductant scavengers are triethanolamine and polycarboxylate anions, for example, oxalate anions (15). The photosensitizer must be able to absorb light efficiently, and have a sufficiently long-lived and reductant excited state, so that its light irradiation (process 1) will lead (process 2) to the transfer of an electron to the bipyridinium unit of the thread (Fig. 17).

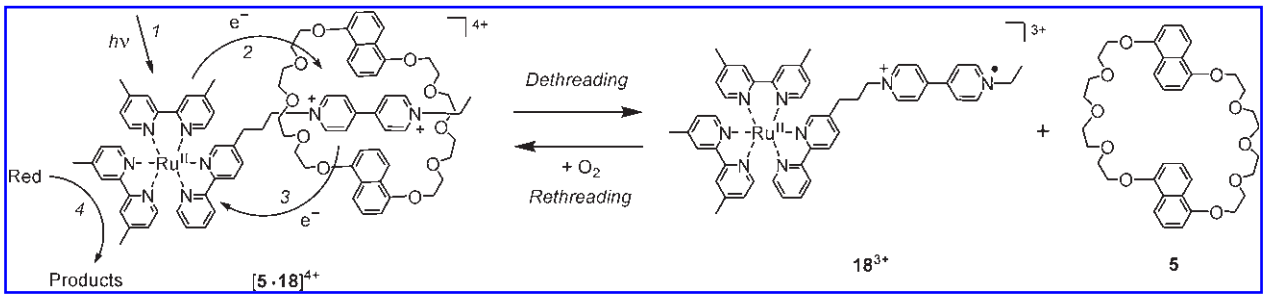

FIG. 17. Photocontrollable second-generation molecular machines based on pseudorotaxanes. In $[5•18]^{4+}$ the light-fueled motor (*i.e.*, the photosensitizer) is part of the acyclic component. Red (triethanolamine) is the reductant scavenger. Conditions: ethanol solution, 298 K.

The relatively fast back-electron transfer from the reduced bipyridinium unit of the thread to the oxidized photosensitizer (process 3) is prevented by the reductant, which, if present in a sufficient amount ($>10^{-3}$ *M*), regenerates (process 4) the original photosensitizer. Under these conditions, the persistent reduction of the bipyridinium unit of $\mathbf{18}^{4+}$ is achieved and the pseudorotaxane dethreads, as evidenced by the emission spectrum of the crown ether **5**. Oxygenation of the solution, from which O_2 was initially removed, reoxidizes the bipyridinium unit of the thread, thereby promoting rethreading with **5**.

The construction of these integrated pseudorotaxanes is not an easy task, so careful design is of paramount importance before embarking on time-consuming and demanding synthetic work. The successful operation of such a molecular machine is the result of the appropriate choice of the functional units, and their covalent linking into the thread and ring components to achieve the correct integration of functions and sequence of processes, and lack of interference between the units. The most important readout signal is the intensity of the 1,5-DON fluorescence associated with the free macrocycle **5**. By means of a repeated sequence of deoxygenation and irradiation followed by oxygenation, many dethreading–rethreading cycles can be performed on the same solution without any appreciable loss of signal until most of the reductant scavenger is consumed.

Systems that rely on this photosensitizer–scavenger strategy produce waste species resulting from the decomposition of the chemical reductant and oxidant.

In this regard, the search for efficient molecular machines exploiting clean, reversible photochemical reactions (in other words, machines that use only light as an energy supply) is of fundamental importance (50, 51, 54, 72, 120).

IV. Systems Based on Rotaxanes

Rotaxanes, the name of which derives from the Latin words *rota* and *axis* for wheel and axle, are topologically intriguing chemical species that are currently the object of much interest. They (258) are minimally composed (Fig. 11b) of a macrocyclic compound (the ring) threaded by a dumbbell-shaped molecule terminated by bulky groups (stoppers) that prevent disassembly. Important features of these systems derive from noncovalent interactions between components that contain complementary recognition sites. Such interactions, which are also responsible for the efficient template-directed syntheses (22, 260) of rotaxanes, include electron donor–acceptor ability, hydrogen bonding, hydrophobic–hydrophylic character, π-π stacking, electrostatic forces, and, on the side of the strong interaction limit, metal–ligand bonding. Rotaxanes have, therefore, both molecular and supramolecular character: molecular because the components are held together mechanically and can be unlinked only by breaking strong covalent bonds; supramolecular because of the presence of weak noncovalent interactions. As it will be shown later the most interesting features of these systems derive from the intercomponent noncovalent interactions, that is, from their supramolecular nature.

In a rotaxane the ring component can rotate around or shuttle along the axis component (Fig. 18).

Rotation of the wheel component is generally a spontaneous process; rotary movements based on rotaxanes are briefly

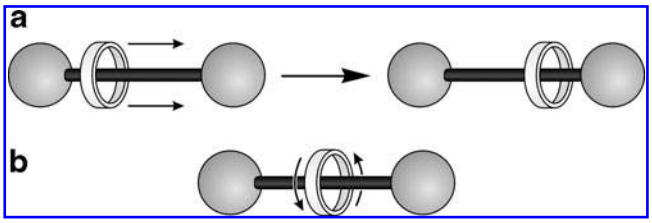

FIG. 18. Schematic representation of the linear (a) and rotary (b) movements that can occur in a rotaxane. Copyright Wiley-VCH Verlag GmbH & Co. KGaA. Reproduced with permission from Balzani *et al.* (64).

discussed in section "C. Ring pirouetting motion." If, during the template-directed synthesis of a rotaxane, location of two identical recognition sites within its dumbbell component can be arranged, the result is a degenerate, conformational equilibrium state in which the macrocyclic component spontaneously shuttles back and forth along the linear portion of the dumbbell (16, 18, 45). Compound $\mathbf{19}^{4+}$ (Fig. 19a) is an example of rotaxane that behaves as degenerate molecular shuttle (18). Several structural, kinetic, and theoretical studies have been devoted to examination of the deslipping process (1, 159, 163, 201, 246, 259).

When the two recognition sites in the dumbbell component differ in their constitutions (Fig. 19b), a rotaxane can exist as two different equilibrating conformations the populations of which reflect their relative free energies as determined primarily by the strengths of the two different sets of noncovalent bonding interactions. In the schematic representation shown in Figure 19b it has been assumed that the molecular shuttle resides preferentially in State 0 until a stimulus is applied that switches off the stronger of the two recognition sites, thus inducing the macrocycle to move to the second weaker recognition site, State 1. In appropriately designed rotaxanes this nondegenerate process can be controlled reversibly by use of chemical, electrochemical, or photochemical stimuli (50, 55, 62, 63, 69, 71, 100, 154, 178, 182, 184, 187, 194, 208, 256, 275). Protonation–deprotonation, oxidation–reduction, and other reversible processes can be exploited to alter reversibly the stereo-electronic properties of one of the two recognition sites, thus affecting their relative capacities to sustain noncovalent bonds. By switching off and on again the recognition properties of one of the two recognition sites, the relative proportions of the two species can be controlled reversibly. These kinds of controllable molecular shuttles can be self-assembled by use of one of a number of different template-directed synthetic strategies, which include threading–capping, slipping, and clipping procedures (4, 87, 99, 143, 146, 166, 187, 245, 258). The controlled shuttling movement is interesting not only mechanically, but also for information processing (binary logic). In the following discussion we illustrate some selected examples of rotaxanes in which the ring shuttling is induced by redox processes. Because, as already noticed, the convenient energy inputs to cause such processes are electric energy and light, only electrochemically and photochemically driven rotaxanes are described.

A. Electrochemically driven shuttles

When a rotaxane contains two different recognition sites in its dumbbell component, it can behave as a controllable

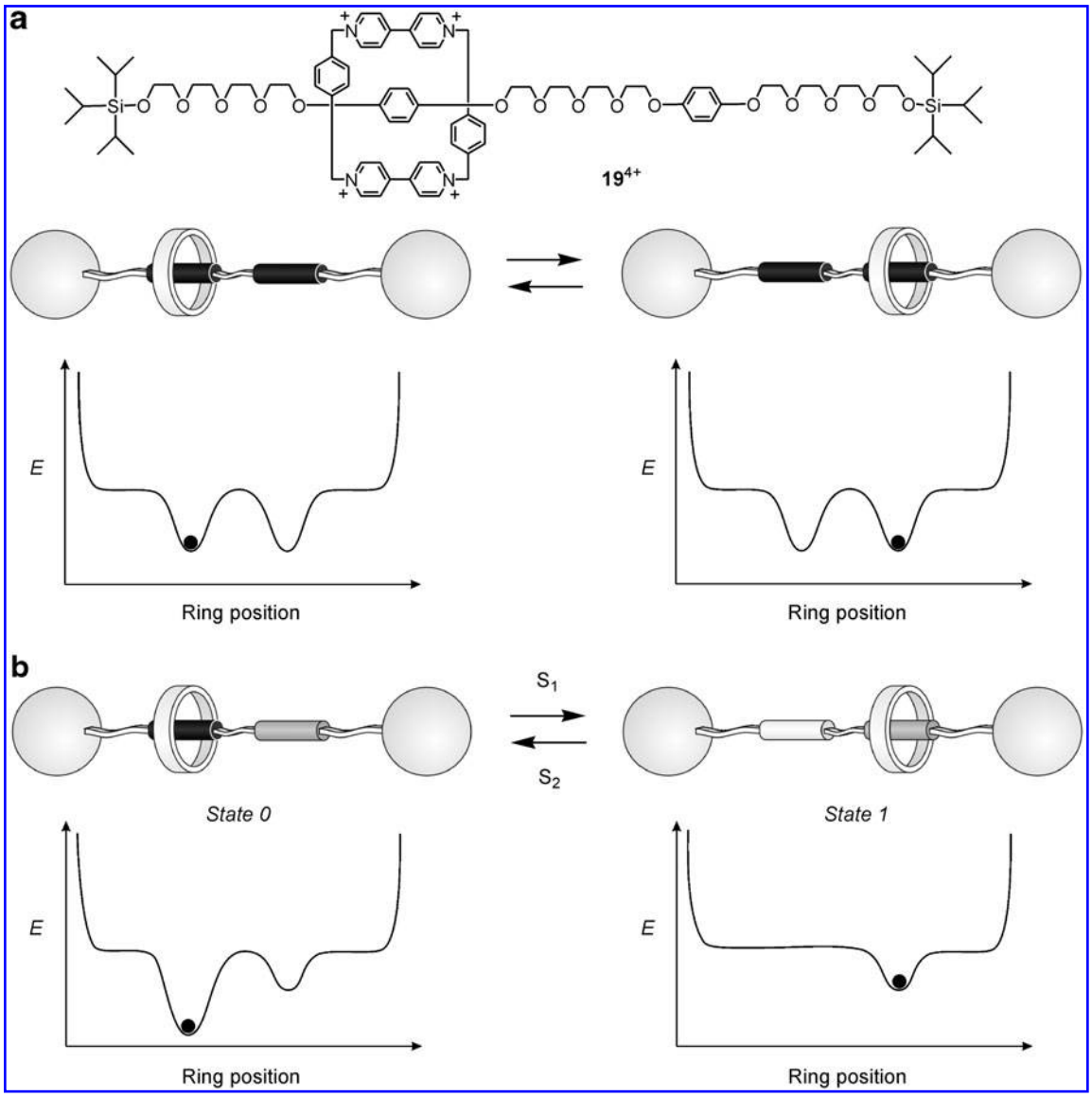

FIG. 19. Shuttling motion of the molecular ring component in rotaxanes. (a) Rotaxane $\mathbf{19}^{4+}$ behaves as a degenerate molecular shuttle; **(b)** operation of a rotaxane with two different recognition sites, in which ring shuttling can be controlled by external stimuli S_1 an S_2. The diagrams below each cartoon show an idealized representation of the potential energy of the system as a function of the position of the ring relative to the axle. The black circles indicate the potential energy corresponding to each of the structures shown in the cartoons. Copyright Wiley-VCH Verlag GmbH & Co. KGaA. Reproduced with permission from Balzani *et al.* (64).

molecular shuttle, and, if appropriately designed by incorporating suitable redox units, it can perform its machine-like operation by exploiting electrochemical energy inputs. Of course, in such cases electrons/holes, besides supplying the energy needed to make the machine work, can also be useful to read the state of the systems by means of the various electrochemical techniques.

The first example of electrochemically driven molecular shuttles is rotaxane $\mathbf{20}^{4+}$ (Fig. 20a) constituted by the electron-deficient cyclophane $\mathbf{4}^{4+}$ and a dumbbell-shaped component containing two different electron-donors, namely, a benzidine and a biphenol moieties, which represent two possible stations for the cyclophane (83). Because benzidine is a better recognition site for $\mathbf{4}^{4+}$ than biphenol, the prevalent isomer is that having the former unit inside the cyclophane. The rotaxane exhibits two one-electron oxidations, both assigned to the benzidine recognition site. A comparison of the halfwave potentials of $\mathbf{20}^{4+}$ with those of a model compound incorporating a benzidine unit not encircled by the tetracationic cyclophane shows that the potential for the first oxidation is more positive in the rotaxane, while that for the second oxidation is the same in both compounds. The shift of the first process indicates that the tetracationic cyclophane surrounds the benzidine station, making its first one-electron oxidation more difficult. The fact that the second oxidation is unaffected by the presence of the cyclophane can be explained by considering that, once the benzidine is oxidized to the corresponding radical cation, the tetracationic cyclophane moves away from it. Upon reduction of the benzidine unit back to its neutral state, the original equilibrium between the two conformations associated with the rotaxane is restored.

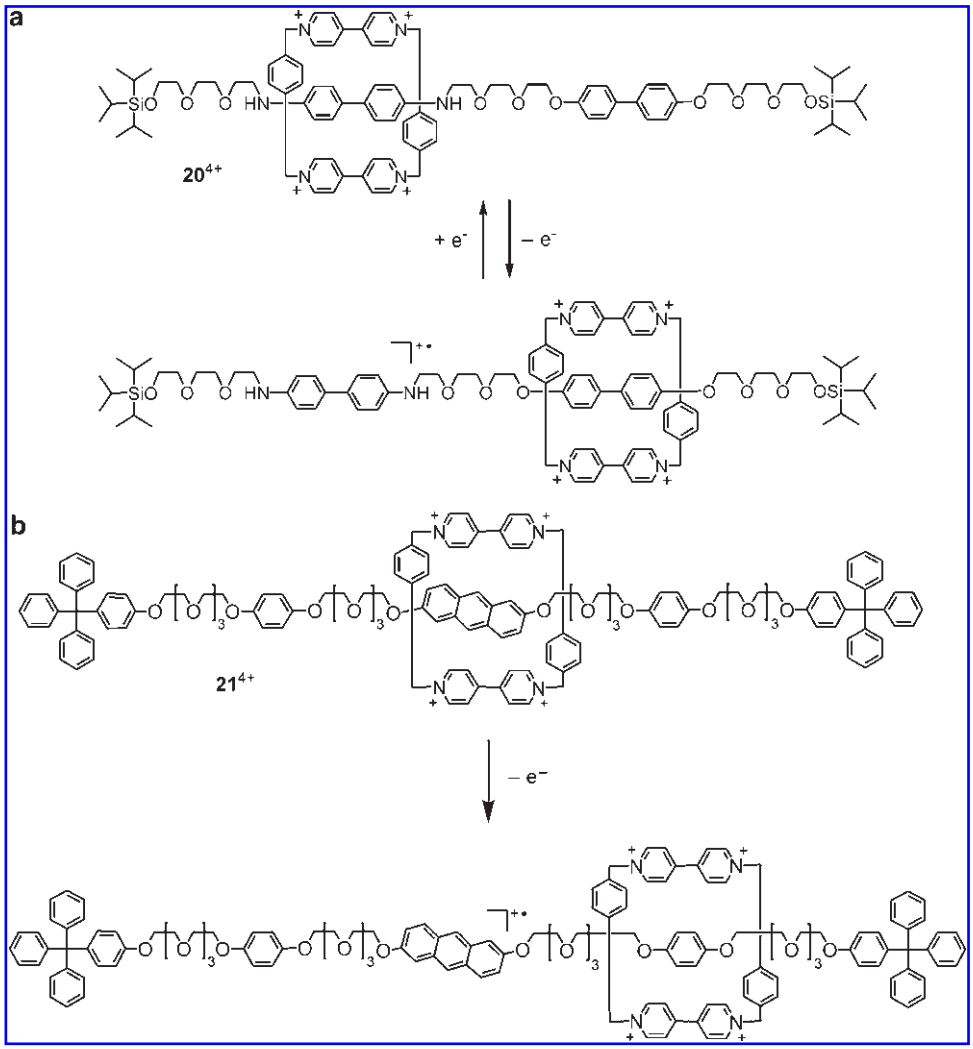

FIG. 20. Structure formulas of rotaxanes 20^{4+} (a) and 21^{4+} (b) and the electrochemically induced shuttling of the cyclophane along their dumbbell-shaped component.

After this first report, a remarkable number of electrochemically controllable molecular shuttles have been designed, constructed, and studied. Rotaxane $\mathbf{21}^{4+}$ (Fig. 20b), for instance, incorporates the same electron-deficient cyclophane $\mathbf{4}^{4+}$ of rotaxane $\mathbf{20}^{4+}$ and a dumbbell containing two kinds of electron-rich units, namely, one 2,6-dioxyanthracene and two 1,4-dioxybenzene (DOB) moieties (52). In solution, the rotaxane is present as the isomer with the 2,6-dioxyanthracene unit inside the cyclophane, owing to the fact that this unit is a better station in comparison with the DOB recognition sites.

The cyclic voltammogram of $\mathbf{21}^{4+}$ shows a first process that corresponds to the oxidation of the 2,6-dioxyanthracene recognition site. This oxidation occurs, however, at a potential that is more positive than that of a model compound incorporating this unit not surrounded by the ring. As far as the oxidation of the two DOB units is concerned, two distinct processes are observed: the first one occurs at a potential that is almost identical to that of a model compound incorporating only this unit, whereas the second one occurs at a potential that is almost identical to that of a model rotaxane incorporating this unit encircled by the tetracationic cyclophane. These observations indicate that (i) initially the tetracationic cyclophane resides around the 2,6-dioxyanthracene recognition site, making its oxidation more difficult, and (ii) once this recognition site is oxidized, the tetracationic cyclophane moves away from it and encircles one of the two DOB units (Fig. 20b) (52).

Another example is constituted by the pH-controllable rotaxane $\mathbf{22}H^{3+}$ (Fig. 21a),which is made of a crown ether containing two electron-donor DOB moieties and a dumbbell-shaped component that comprises in its rod section a secondary ammonium ion and the already seen electron-acceptor bipyridinium unit (32, 144). These units are two recognition centers, or in other words, two possible stations, for the ring component since it can establish hydrogen bonding interactions with the ammonium ion and CT interactions with the bipyridinium unit. For the employed macrocyclic component the hydrogen bonding interactions are much stronger than the CT ones, and therefore the stable structure of the rotaxane is that in which the macrocycle surrounds the ammonium station. Such a structure can be, however, destabilized upon addition of a suitable base that, by deprotonating the ammonium ion, causes the complete displacement of the ring to the bipyridinium station (Fig. 21a).

The occurrence of this shuttling process is evidenced by the fact that the first reduction of the bipyridinium unit occurs at a potential more negative than that found for the dumbbell component. This process exhibits a cyclic voltammetric

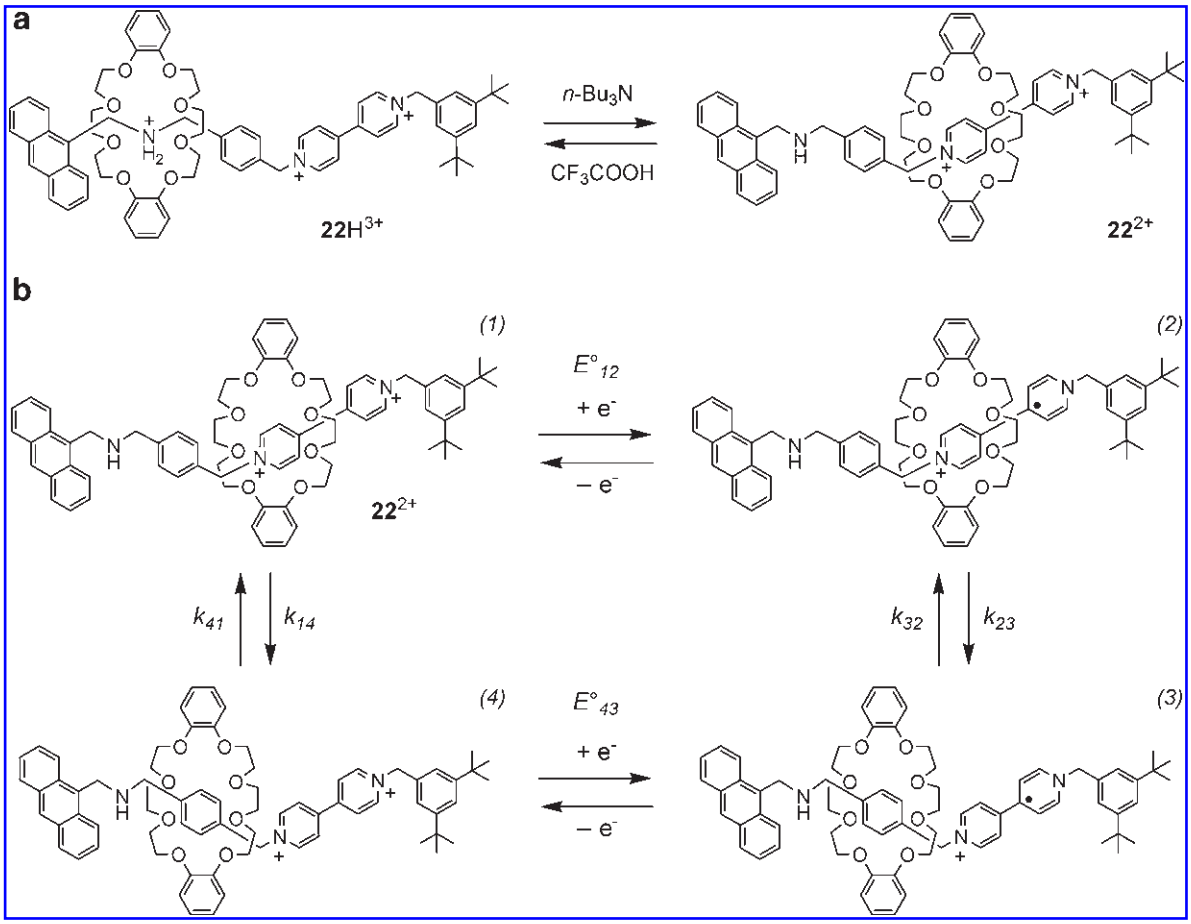

FIG. 21. Stimuli-controlled molecular shuttling in rotaxanes. (a) Structure formula of rotaxane $\mathbf{22}H^{3+}$ and representation of its operation as a pH controllable molecular shuttle; **(b)** dual-pathway square-scheme mechanism that accounts for the rearrangements induced by the monoelectronic reduction of deprotonated rotaxane $\mathbf{22}^{2+}$. The species 1 and 3 represent the stable structure of the deprotonated rotaxane and its monoreduced form, respectively, whereas 2 and 4 are metastable intermediates. Note that the exact position of the macrocycle along the axle in forms 3 and 4 is not known. From a simple digital simulation of the cyclic voltammetric patterns the following values have been obtained: $E^{\circ}_{12} = -0.59$ V, $E^{\circ}_{43} = -0.34$ V, $k_{14} \approx 0.15\,s^{-1}$, $k_{41} \leq 2.5\,s^{-1}$, $k_{23} \geq 100\,s^{-1}$, and $k_{32} \approx 1\,s^{-1}$.

pattern (a large and scan-rate dependent separation between the anodic and cathodic peak), which is typical of systems in which the redox process is followed by a molecular rearrangement taking place on the time scale of the electrochemical experiments. In the case of the examined rotaxane the nature of the occurring rearrangements can be elucidated by looking at the characteristics of the second reduction process, namely, a potential value that practically coincides with that of the protonated rotaxane (and the dumbbell-shaped component) and a behavior that is fully reversible. These two findings indicate that in the deprotonated rotaxane the monoreduced bipyridinium unit is no longer engaged in donor–acceptor interactions and that the system does not undergo any further rearrangement after one-electron reduction.

It can be concluded, as shown in the square scheme reported in Figure 21b, that in the deprotonated rotaxane (i) the first reduction of the bipyridinium weakens the CT interactions and promotes the displacement of the ring far from the monoreduced unit, and (ii) the reoxidation of such a unit, restoring its electron-acceptor power, causes the back movement of the ring.

From the electrochemical viewpoint this system is particularly interesting because, by changing its protonation state, electrons can play different roles: in protonated rotaxane $\mathbf{22}H^{3+}$ they are simply used to read the state of the system, whereas in deprotonated rotaxane $\mathbf{22}^{2+}$ they play the dual role of writing and reading the system.

Benzylic amide rotaxanes constitute another important class of interlocked compounds. Rotaxane **23**, for example, consists of a benzylic amide macrocycle that surrounds an axle featuring two hydrogen-bonding stations, namely, a succinamide and a naphthalimide units, separated by a long alkyl chain (Fig. 22) (3).

Initially, the macrocycle resides onto the succinamide station because the naphthalimide unit is a much poorer hydrogen-bonding recognition site. Electrochemical one-electron reduction of the naphthalimide unit causes, however, the shuttling of the macrocycle from the succinamide to the naphthalimide station (Fig. 23). Subsequent reoxidation of the naphthalimide site to the neutral state restores the original conformation. The thermodynamic and kinetic aspects of the shuttling motion were investigated in detail by a cyclic

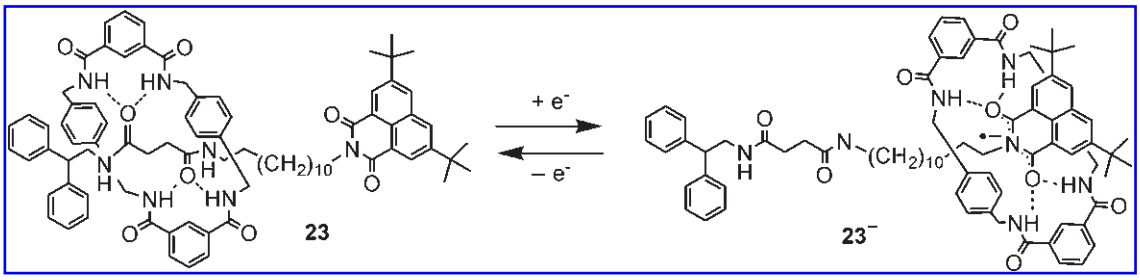

FIG. 22. The electrochemically induced shuttling in the benzylic amide rotaxane 23.

voltammetric analysis on changing scan rate, temperature, and solvent, aided by computer simulations (3). For example, in tetrahydrofuran at room temperature, it was found that the relative ring-binding affinities of the two stations can be switched by eight orders of magnitude and the redox-induced shuttling motion takes about 50 μs.

Rotaxane $\mathbf{24}^{6+}$ was specifically designed (35, 58) to achieve photoinduced ring shuttling in solution (88), but it behaves also as an electrochemically driven molecular shuttle. This compound has a modular structure: its ring component is the electron-donor macrocycle **25** containing two DOB units, whereas its dumbbell component, $\mathbf{26}^{6+}$, is made of several

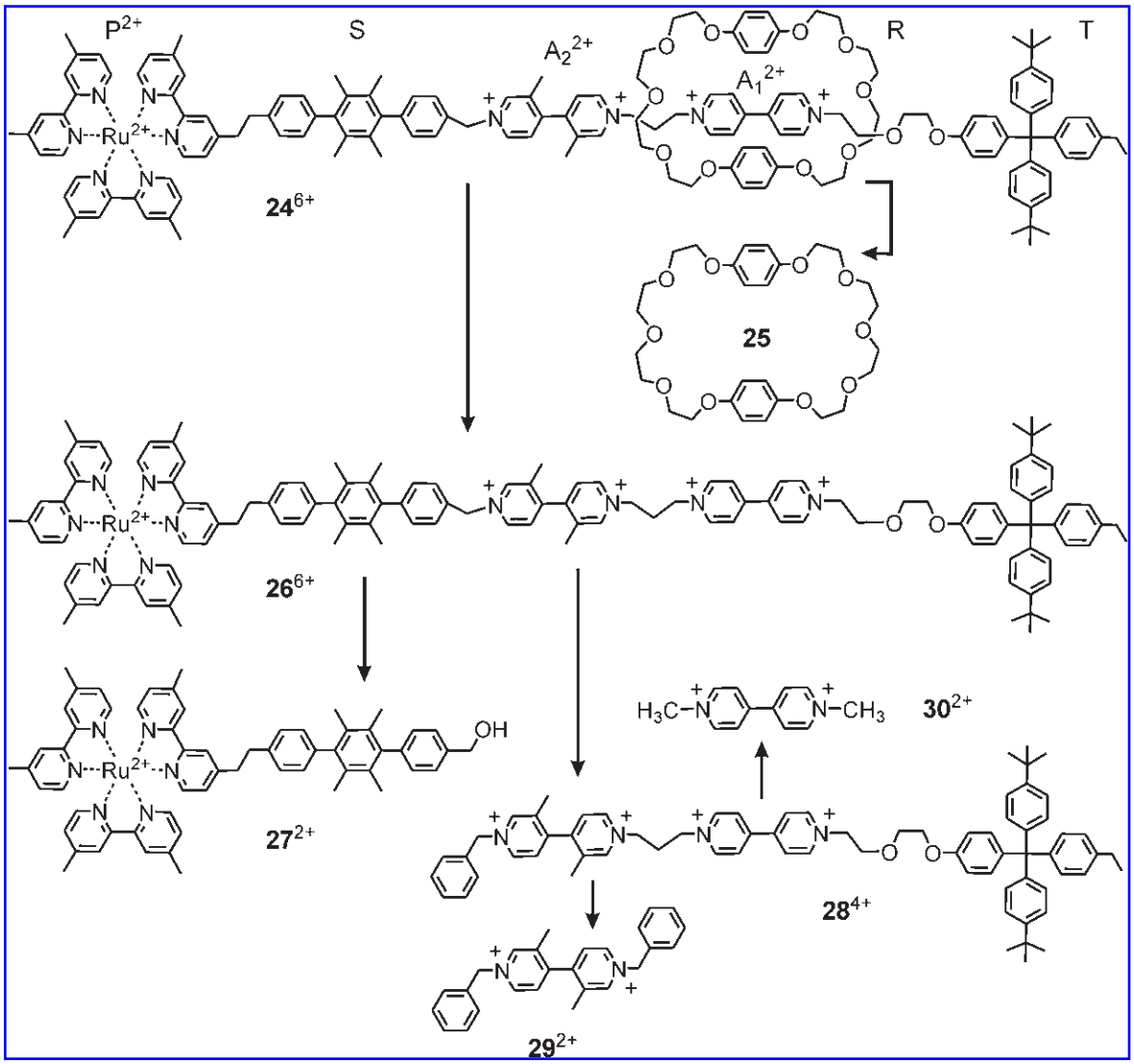

FIG. 23. Structure formulas of rotaxane $\mathbf{24}^{6+}$, of its ring and dumbbell-shaped components 25 and $\mathbf{26}^{6+}$, and model compounds $\mathbf{27}^{2+}$, $\mathbf{28}^{4+}$, $\mathbf{29}^{2+}$, and $\mathbf{30}^{2+}$ of the units present in the dumbbell.

covalently linked units. They are an Ru(II) polypyridine complex (P^{2+}), a *p*-terphenyl-type rigid spacer (S), a 3,3′-dimethyl-4,4′-bipyridinium (A_2^{2+}) and a 4,4′-bipyridinium (A_1^{2+}) electron-accepting stations, and a tetraarylmethane group as the terminal stopper (T) (Fig. 23).

Because of the presence of several redox-active units, the cyclic voltammogram of this rotaxane shows a complex redox pattern. However, the comparison with the electrochemical behavior of its molecular components and suitable model compounds (Fig. 23) enables to obtain useful information not only on its conformational features, but also, and most importantly, on its machine-like operation.

In dumbbell-shaped component $\mathbf{26}^{6+}$ all the redox processes of the incorporated units are present at almost the same potentials as in the separated units (Fig. 24a); this finding shows that there are no substantial intercomponent electronic interactions. On going from the dumbbell component to rotaxane $\mathbf{24}^{6+}$, some processes are affected, while others are not (Fig. 24a).

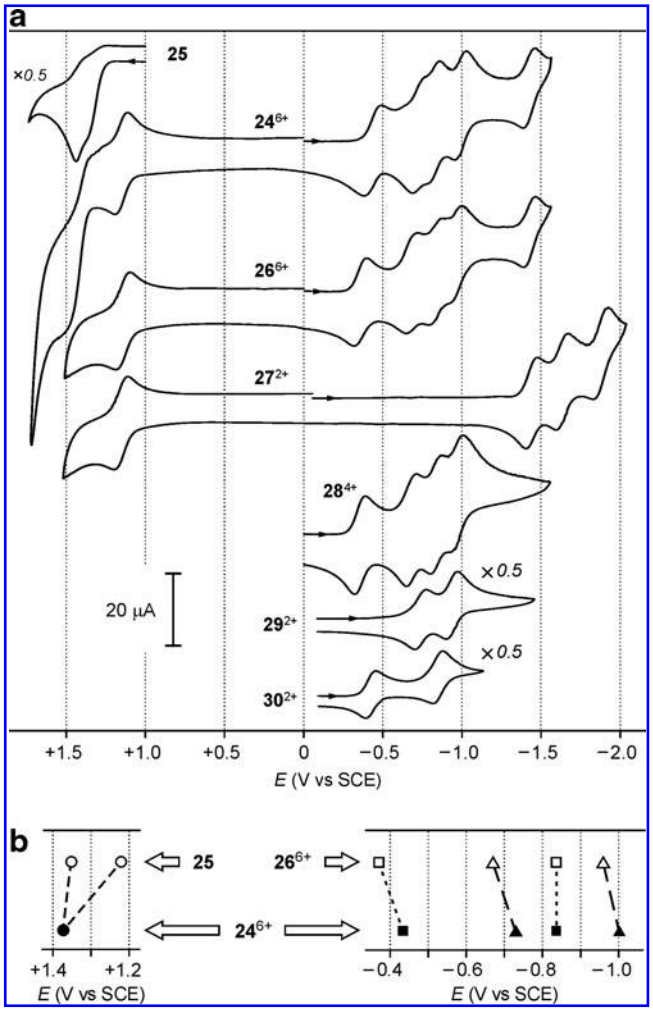

FIG. 24. Electrochemical properties of rotaxane $\mathbf{24}^{6+}$. (a) Cyclic voltammetric patterns for rotaxane $\mathbf{24}^{6+}$, its ring and dumbbell-shaped components **25** and $\mathbf{26}^{6+}$, and model compounds $\mathbf{27}^{2+}$, $\mathbf{28}^{4+}$, $\mathbf{29}^{2+}$, and $\mathbf{30}^{2+}$. **(b)** Potential shifts caused by the donor–acceptor interaction between ring **25** and dumbbell-shaped component $\mathbf{26}^{6+}$ when they are assembled in rotaxane $\mathbf{24}^{6+}$. Circles, squares, and triangles represent processes centered on dioxybenzene, A_1^{2+} and A_2^{2+} units, respectively. SCE, saturated calomel electrode.

All the processes related to the Ru-based unit, namely, the metal-localized oxidation and the ligand-localized reductions, do not show any appreciable changes. The first reduction of the A_1^{2+} unit is displaced noticeably toward more negative potential values, indicating that it is surrounded by the electron-donor macrocycle **25** (Fig. 24b). Accordingly, the oxidation of the two DOB units of the macrocycle is displaced toward more positive potential values and occurs simultaneously (Fig. 24b), as already observed for other rotaxanes containing ring **25** (5).

The fact that the ring encircles the A_1^{2+} station, as confirmed by the NMR spectrum, is an expected result on the basis of the reduction potentials of A_1^{2+} and A_2^{2+} in component $\mathbf{26}^{6+}$ (or of separated model compounds). The second process of $\mathbf{24}^{6+}$, which corresponds to the first reduction of the A_2^{2+} station, is also displaced toward more negative potential values (Fig. 24b), demonstrating that, at this stage, the A_2^{2+} unit is encircled by macrocycle **25**. A further proof of the ring displacement is given by the fact that the second reduction of the A_1^{2+} station occurs practically at the same potential of the dumbbell (Fig. 24b).This behavior confirms that, when the better station (A_1^{2+}) of the two has been deactivated upon reduction, the ring moves to the alternative A_2^{2+} station. Under these conditions, from the values of the first reduction potential of A_2^{2+} and the second reduction potential of A_1^{2+} in the dumbbell component, it can be estimated that the translational isomer with the ring surrounding A_2^{2+} is much more populated than that in which the ring encircles A_1^{+}. When also the A_2^{2+} station has been reduced, the position of the ring is no longer controlled by strong CT interactions; from the electrochemical results it seems that it resides close to A_2^{+}. The reversibility of the electrochemical processes involving the two stations shows that, after a two-electron reduction of rotaxane $\mathbf{24}^{6+}$, one-electron oxidation relocated the ring on the A_2^{2+} station and a successive one-electron oxidation entices it back again onto the A_1^{2+} station. The electrochemical reversibility of these processes also indicates that the rates of the electrochemically induced ring movements are fast.

The electrochemical and photophysical properties of a series of rotaxanes (*e.g.*, $\mathbf{31}^{4+}$, Fig. 25a), consisting of the $\mathbf{4}^{4+}$ electron-accepting cyclophane and a dumbbell containing a monopyrrolotetrathiafulvalene (TTFP) and a 1,5-DON units, have been investigated in acetonitrile solution (172). Both TTFP and DON are potential stations for the tetracationic cyclophane, because they can establish CT interactions with its electron-accepting bipyridinium units of the cyclophane. On the basis of the redox properties of the two stations, one might expect a strong preference of the tetracationic cyclophane for the TTFP station compared with the DON station. The interaction of the cyclophane with electron-donating units depends also on other factors, however, including the extension of the [$\pi\cdots\pi$] stacking and the formation of hydrogen bonds. Comparison with the behavior of suitable model compounds and of the free dumbbell components has provided evidence that two-station rotaxanes of this kind have complex electrochemical and spectral features that cannot simply be related to the presence of the two expected translational isomers. It seems that, owing to their length (~5–6 nm) and flexibility, such compounds can fold up in the solvent used to maximize the CT interactions. It seems also

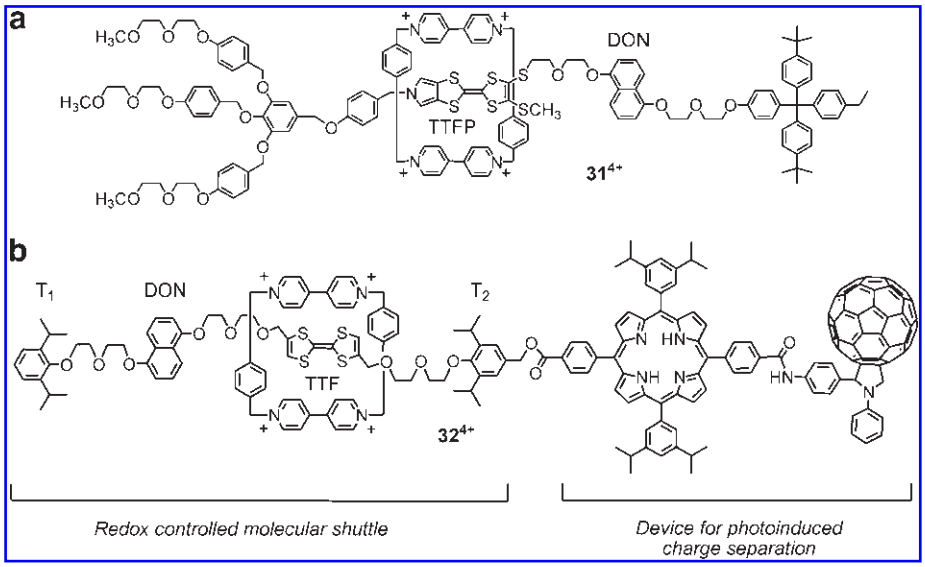

FIG. 25. Rotaxane-based molecular shuttles. (a) In rotaxanes such as $\mathbf{31}^{4+}$ there is an equilibrium between translational isomers: in the isomer represented in the figure, the tetracationic cyclophane moves away from the TTFP unit upon one-electron oxidation of this station; **(b)** structure formula of rotaxane $\mathbf{32}^{4+}$. DON, dioxynaphthalene; TTFP, monopyrrolotetrathiafulvalene.

that the two stoppers (in particular, the dendritic one) play a much more active role than that of simple bulky groups. Because of their not negligible electron-donating power, they presumably fold around the tetracationic cyclophane, thereby contributing to establishing its localization along the thread. The electrochemical results indicate that first oxidation of the TTFP unit surrounded by the cyclophane induces the displacement of the cyclophane. ^{1}H NMR studies have also furnished evidence that the presence of a bulky thiomethyl substituent on the TTFP unit, when situated in between the two stations as in the case of $\mathbf{31}^{4+}$, slows down the shuttling movement (173).

Folding in solution has also been evidenced for similar rotaxanes in which the TTFP station has been replaced by a TTF unit (280). Back-folding effects, however, are minimized on incorporation of a rigid spacer linking the two stations (233). As we will see in section "B. Molecule-based solid-state electronic circuits," rotaxanes of this type have been used to construct two dimensional molecular electronic circuits.

More recently, the second-generation molecular shuttle $\mathbf{32}^{4+}$ (Fig. 25b) was designed and constructed (253). The system is composed of two devices: a bistable redox-driven molecular shuttle, and a module for photoinduced charge separation. In the stable translational isomer the electron-accepting cyclophane $\mathbf{4}^{4+}$, which is confined in the region of the dumbbell delimited by the two stoppers T_1 and T_2, encircles the better electron-donor TTF station.

Voltammetric experiments revealed remarkable electronic interactions between the various units of $\mathbf{32}^{4+}$, pointing to the existence of folded conformations in solution (301). The TTF unit can be electrochemically oxidized only in a limited fraction of the rotaxane molecules; in these species, TTF oxidation causes the shuttling of the cyclophane $\mathbf{4}^{4+}$ away from this station. Most likely, $\mathbf{32}^{4+}$ occurs as conformations in which the electro-active TTF unit is buried inside a complex molecular structure and is, therefore, protected against oxidation performed by an electric potential applied externally. Such a behavior limits the efficiency for the operation of $\mathbf{32}^{4+}$ as a redox-driven molecular shuttle. The possibility of oxidizing TTF by an electric potential generated internally through intramolecular photoinduced electron transfer is currently under investigation.

In general terms, these results indicate that, as the structural complexity increases, the overall properties of the system cannot be easily rationalized solely on the basis of the type and sequence of the functional units incorporated in the molecular framework, that is, its primary structure. Higher-level conformational effects, which are reminiscent of those related to the secondary and tertiary structure of biomolecules (211), have to be taken into consideration. The comprehension of these effects constitutes a stimulating scientific problem, and a necessary step for the design of novel artificial molecular devices and machines.

An electrochemically driven shuttle stabilized by interactions completely different from those characteristic of the previously described systems is rotaxane $[\mathbf{33}\bullet\mathrm{Cu}]^+$ (Fig. 26), which contains a phenanthroline and a terpyridine unit in its dumbbell-shaped component (24, 110, 145). It also incorporates a Cu(I) center coordinated tetrahedrally by the phenanthroline ligand of the dumbbell together with the phenanthroline ligand of the macrocycle.

Oxidation of the tetracoordinated Cu(I) center of $[\mathbf{33}\bullet\mathrm{Cu}]^+$ to a tetracoordinated Cu(II) ion occurs on electrolysis (+1.0 V relative to the SCE) of a CH_3CN solution of the rotaxane. In response to the preference of Cu(II) for a pentacoordination geometry, the macrocycle shuttles away from the bidentate phenanthroline ligand of the dumbbell and encircles the terdentate terpyridine ligand instead. Consistently, the cyclic voltammogram shows the disappearance of the reversible wave (+0.68 V) associated with the tetracoordinated Cu(II)/Cu(I) redox couple and the concomitant appearance of a reversible wave (−0.03 V) corresponding to the pentacoordinated Cu(II)/Cu(I) redox couple. A second electrolysis at −0.03 V of the acetonitrile solution of the rotaxane reduces the pentacoordinated Cu(II) center back to a pentacoordinated Cu(I) ion. In response to the preference of Cu(I) for a tetracoordination geometry the macrocycle moves away from the terdentate terpyridine ligand and encircles the bidentate phenanthroline ligand. The cyclic voltammogram recorded after the second electrolysis shows the original redox wave

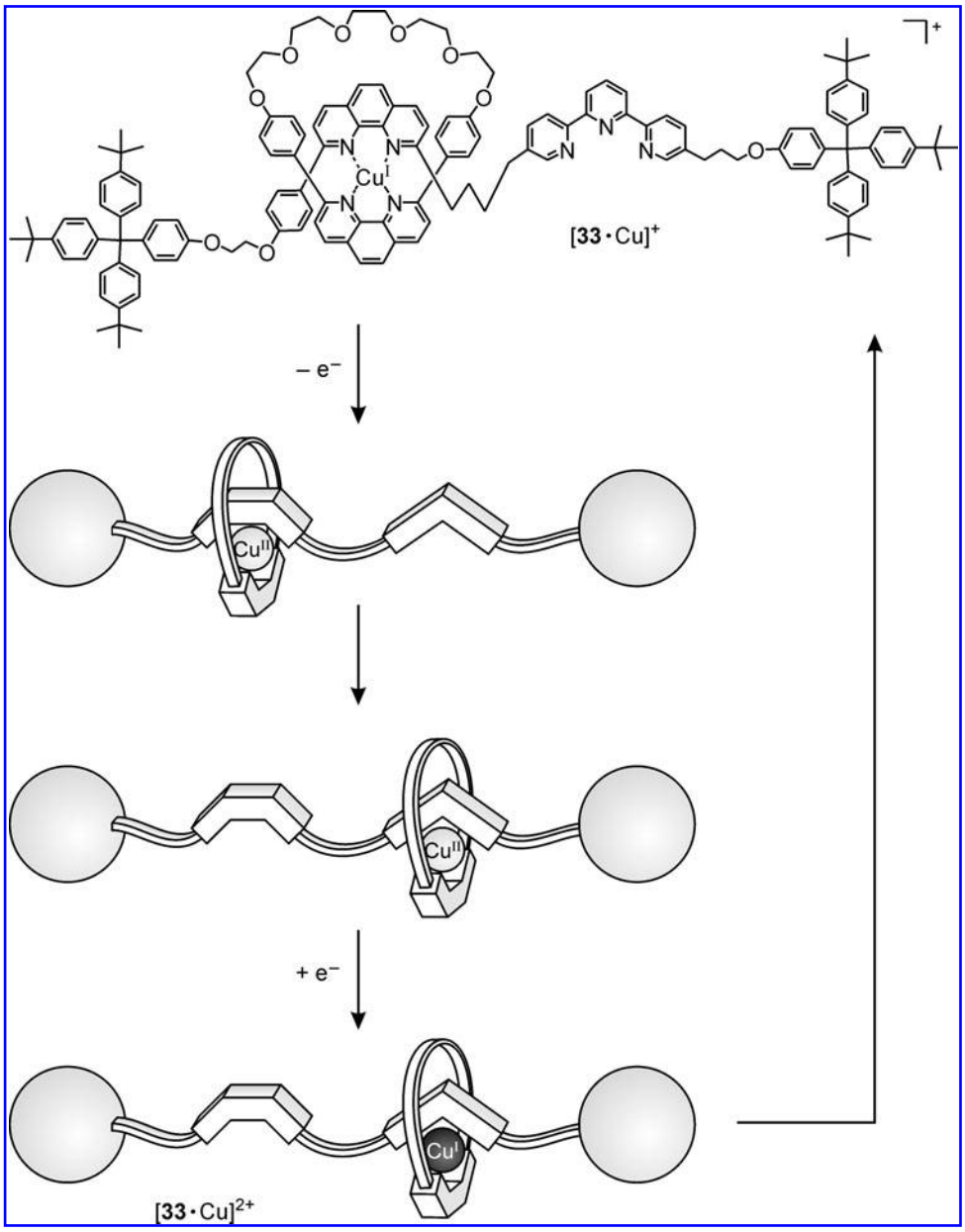

FIG. 26. Shuttling of the macrocyclic component of [33•Cu]$^{+}$ along its dumbbell-shaped component can be controlled electrochemically by oxidizing–reducing the metal center.

(+0.68 V) corresponding to the tetracoordinated Cu(II)/Cu(I) redox couple.

Very recently, this system has been improved by replacing the highly shielding and hindering phenathroline moiety contained in the ring with a nonhindering biisoquinoline unit (129). In the new rotaxane the electrochemically driven shuttling of the ring is, indeed, at least four orders of magnitude faster than in the previous phenanthroline-based system.

B. Photochemically driven shuttles

The shuttling of the macrocyclic component of rotaxane [**33**•Cu]$^{+}$ (Fig. 26) along the linear portion of its dumbbell-shaped component can be also induced photochemically (110). Irradiation (464 nm) of a acetonitrile solution of the rotaxane, in the presence of *p*-nitrobenzylbromide, leads the Cu(I)-based chromophoric unit to its metal-to-ligand CT excited state. Electron transfer from the photoexcited rotaxane to *p*-nitrobenzylbromide follows, generating a tetracoordinated Cu(II) center. In response to the preference of the Cu(II) ion for a pentacoordination geometry the macrocycle shuttles away from the bidentate phenanthroline ligand of the dumbbell and encircles the terdentate terpyridine ligand instead. On addition of ascorbic acid the pentacoordinated Cu(II) center is reduced to a pentacoordinated Cu(I) ion. In response to the preference of Cu(I) for a tetracoordination geometry the macrocycle moves away from the terdentate terpyridine ligand and encircles the bidentate phenanthroline ligand to restore the original conformation. Rotaxanes based on octahedral complexes have also been reported (84, 111).

As already pointed in section "A. Electrochemically driven shuttles," also rotaxane **24**$^{6+}$ (Fig. 23) can work by exploiting light energy inputs; it was indeed specifically designed to achieve photoinduced ring shuttling in solution (35, 58). Three strategies were devised to obtain the photoinduced

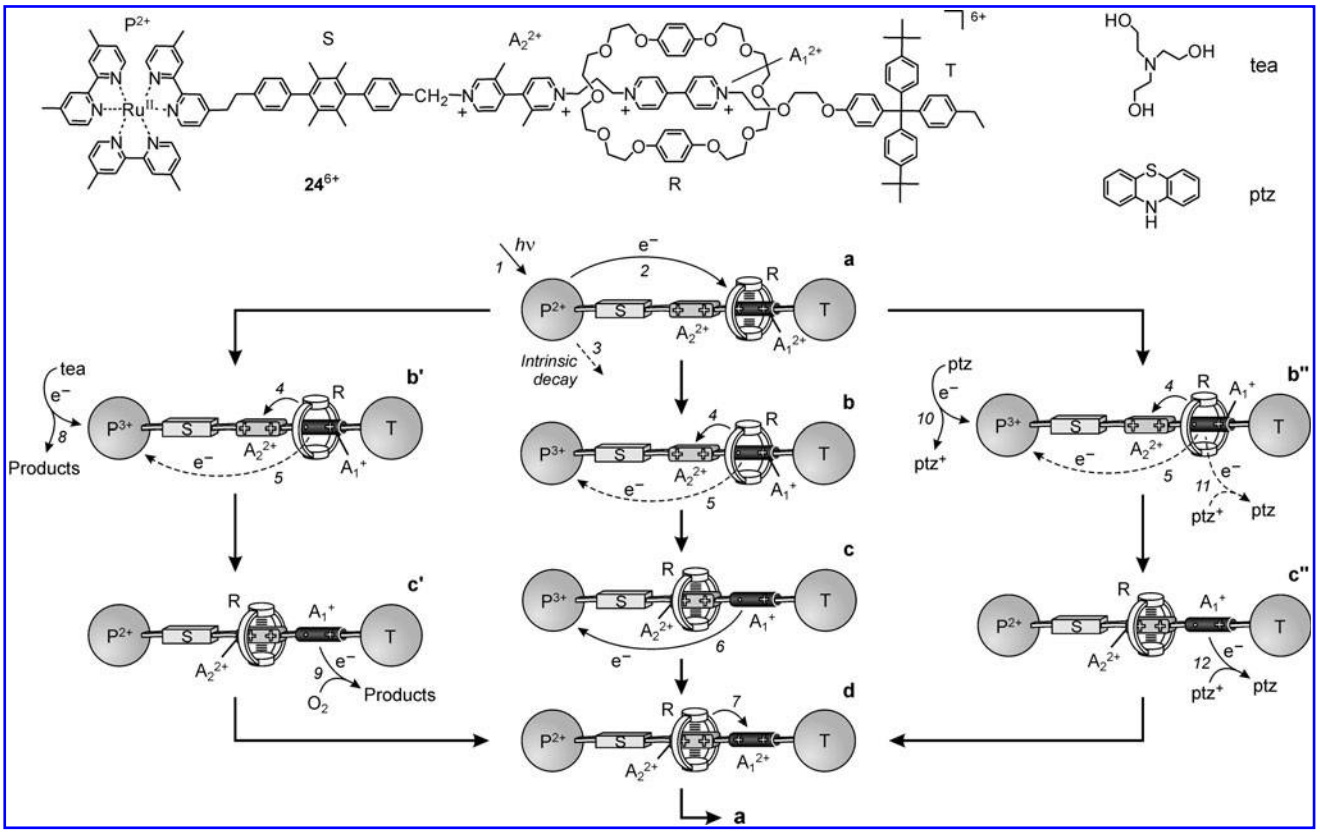

FIG. 27. Rotaxane 24^{6+} and schematic representation of the intramolecular (*center*), sacrificial (*left*), and relay (*right*) mechanisms for the photoinduced shuttling movement of macrocycle between the two stations, A_1^{2+} and A_2^{2+}.

abacus-like movement of the macrocycle between the two stations $\mathbf{A_1}^{2+}$ and $\mathbf{A_2}^{2+}$ (58).

1. intramolecular mechanism (Fig. 27, center), based on processes involving only the rotaxane component;
2. sacrificial mechanism (Fig. 27, left), which requires the help of external reactants that undergo decomposition;
3. relay mechanism (Fig. 27, right), which requires the assistance by an external species that undergoes a reversible redox process.

The intramolecular mechanism (Fig. 27, center) is based on the following four operations (35):

1. *Destabilization of the stable translational isomer*. Light excitation of the photo-active unit P^{2+} (step 1) is followed by transfer of an electron from the excited state to the A_1^{2+} station, which is encircled by the ring (step 2), with the consequent deactivation of this station; such a photoinduced electron-transfer process must compete with the intrinsic decay of the excited state of P^{2+} (step 3).
2. *Ring displacement*. The ring moves from the reduced station A_1^{+} to A_2^{2+} (step 4), a step that must compete with the back-electron-transfer process from A_1^{+} (still encircled by the ring) to the oxidized photo-active unit P^{3+} (step 5). This is the most difficult requirement to meet in the intramolecular mechanism.
3. *Electronic reset*. A back electron-transfer process from the free, reduced station A_1^{+} to P^{3+} (step 6) restores the electron-acceptor power to the A_1^{2+} station.
4. *Nuclear reset*. As a consequence of the electronic reset, back movement of the ring from A_2^{2+} to A_1^{2+} occurs (step 7).

Each absorbed photon could, in principle, cause the occurrence of a forward and back ring movement (*i.e.*, a full cycle) without generation of any waste product. In practice, the efficiency is very low, because 84% of the excited $*P^{2+}$ species undergoes deactivation (step 3) in competition with electron transfer (step 2), and 88% of the reduced A_1^{+} species undergoes back electron transfer (step 5) before ring displacement (step 4) can occur (inverting the positions of A_1^{2+} and A_2^{2+} increases the quantum yield of photoinduced electron transfer ($\Phi_2 = 0.50$) but prevents ring displacement because the back-electron-transfer reaction becomes exceedingly fast) (59). The somewhat disappointing quantum efficiency for ring shuttling (2%) is compensated by the fact the investigated system is a unique example of an artificial linear nanomotor, because it gathers together the following features:

1. it is powered by visible light (in other words, sunlight);
2. it exhibits autonomous behavior, like motor proteins;
3. it does not generate waste products;
4. its operation can rely only on intramolecular processes, allowing in principle operation at the single-molecule level;
5. it can be driven at a frequency of ~ 1 kHz;
6. it works in mild environmental conditions (*i.e.*, fluid solution at ambient temperature);
7. it is stable for at least 10^3 cycles.

Much higher efficiencies are obtained when the system operates by the sacrificial or relay mechanisms.

The sacrificial mechanism (35) is based on the use of external redox reactants (a reductant such as triethanoleamine, and an oxidant such as dioxygen) that operate as illustrated on the left of Figure 27. Destabilization of the stable translational isomer occurs as in the intramolecular mechanism. Because the solution contains a suitable reductant, a rapid reaction of this species with P^{3+} (step 8) competes successfully with the back electron-tranfer reaction (step 5); the originally occupied station thus remains in its reduced state A_1^{+}, and the displacement of the ring to A_2^{2+} (step 4), although slow, does occur. Restoration of the electron-acceptor power of the A_1^{2+} station is achieved by oxidizing A_1^{+} with a suitable oxidant such as dioxygen (step 9), and nuclear reset occurs as in the previous mechanism (step 7). Under these conditions, the efficiency of the photoinduced ring displacement is 0.16, which corresponds to the quantum yield of the photoinduced electron transfer (step 2). This mechanism is, of course, less appealing than the intramolecular mechanism, because it leads to the formation of waste products.

The relay mechanism (58) is based on the participation to the process of a species capable of undergoing a reversible redox reaction. After careful examination of the various aspects of the problem, phenothiazine (ptz) was chosen to play this role. When photoexcitation of $\mathbf{24}^{6+}$ is performed in the presence of ptz (Fig. 27, right), the photoinduced electron transfer (step 2) is followed by a diffusion controlled reaction between ptz and P^{3+} with formation of ptz^{+} and regeneration of P^{2+} (step 10). As a consequence, intramolecular back-electron transfer (step 5) can no longer occur and ring displacement (step 4) must only compete with the much slower intermolecular back-electron-transfer reaction between ptz^{+} and A_1^{+} (step 11). Under the experimental conditions used, ring displacement (step 4) occurs with 76% efficiency and both electron (steps 11 and/or 12) and nuclear (step 7) reset processes occur quantitatively. Therefore, $\mathbf{24}^{6+}$ behaves as an autonomous molecular motor that consumes only photons of visible light with an overall efficiency of 12%. The role played by ptz is that of an electron relay with a negative kinetic effect.

Another light-driven molecular shuttle that relies on an external electron relay has been reported (88) and concerns rotaxane **23** (Fig. 22). As already seen, it consists of a benzylic amide macrocycle that surrounds an axle featuring two hydrogen-bonding stations—a succinamide and a naphthalimide units—separated by a long alkyl chain. Initially, the macrocycle resides onto the succinamide station, because the naphthalimide unit is a much poorer hydrogen-bonding recognition site. Excitation with light at 355 nm (step 1 in Fig. 28) in acetonitrile at 298 K generates the singlet excited states of the naphthalimide unit, which then undergoes high-yield intersystem crossing to the triplet excited state.

Such a triplet state can be reduced in bimolecular encounters by an electron donor (1,4-diazabicyclo[2.2.2]octane) added to the solution in a sufficiently large amount (step 2). Because the back-electron-transfer process (step 3) is spin forbidden, and thus slow, the photogenerated ion pair can dissociate efficiently—as a matter of fact the naphthalimide radical anion survives for hundreds of microseconds before it decays by bimolecular charge recombination with a 1,4-diazabicyclo[2.2.2]octane radical cation. Because the naphthalimide anion is a much stronger hydrogen-bonding station compared with the succinamide, on reduction of the naphthalimide unit the macrocycle is expected to shuttle from the

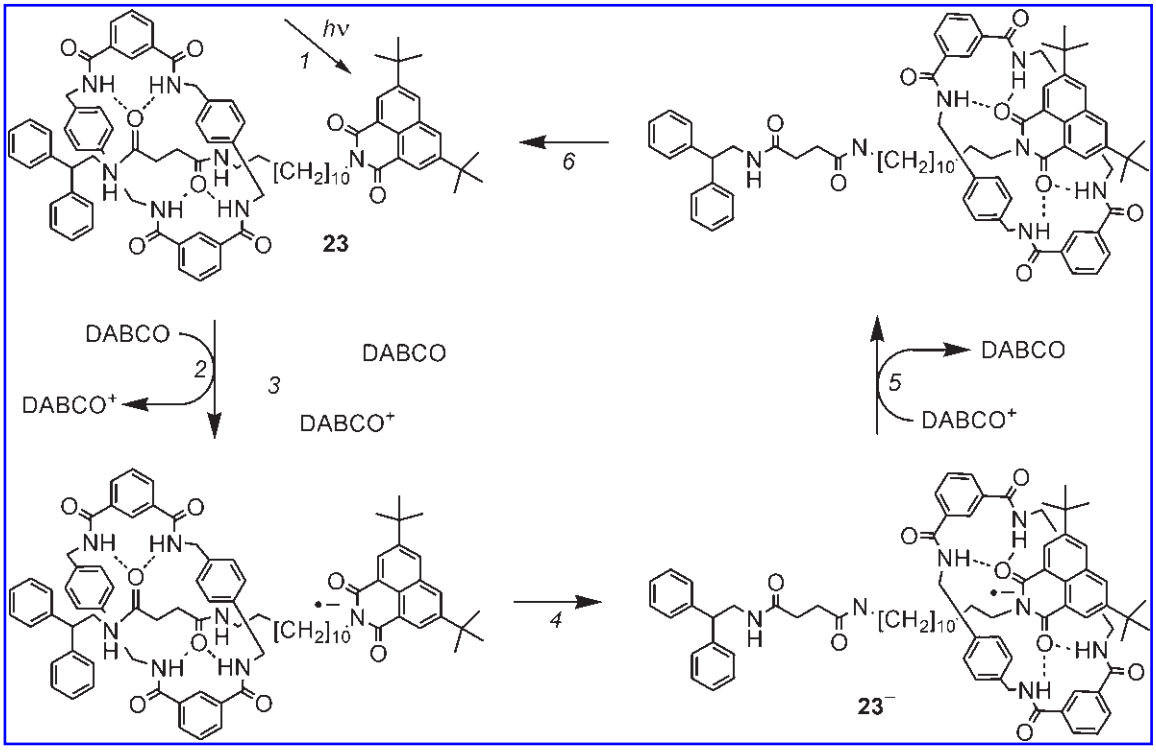

FIG. 28. Light-induced reversible shuttling of the macrocyclic component of the hydrogen-bonded rotaxane 23. The operation of this system relies on the use of DABCO as an electron relay. DABCO, 1,4-diazabicyclo[2.2.2]octane.

latter to the former station (step 4); this has been demonstrated by cyclic voltammetric experiments and confirmed by laser flash photolysis. The time required for ring shuttling ($\sim 1\ \mu s$) is much shorter than the lifetime of the naphthalimide radical anion ($\sim 100\ \mu s$). After charge recombination (step 5) the macrocycle moves back to its original position (step 6). The device can be cycled at a frequency depending on the charge recombination rate of the rotaxane radical anion. It can be estimated that if the shuttle is pumped by a laser at the frequency of its recovery stroke (step 5), that is, $10^4\ s^{-1}$, this molecular-level machine generates $\sim 10^{-15}$ W of mechanical power per molecule (88).

C. Ring pirouetting motion

In suitably designed rotaxanes the pirouetting-type movements of the ring around the axle can be electrochemically driven. Rotaxane [**34**•Cu]$^+$ has a structure (Fig. 29a) in which Cu(I) is coordinated tetrahedrically by the phenanthroline present in the axle and the phenanthroline contained in the ring (185, 243). Electrochemical oxidation of the Cu(I) center leads to a transient tetracoordinated Cu(II) species that, by the pirouetting of the ring around the axle, rearranges in tens of seconds to a structure in which the Cu(II) center reaches its most stable environment being pentacoordinated by the phenanthroline of the axle and the terpyridine of the ring ([**34**•Cu]$^{2+}$, Fig. 29a). On electrochemical reduction of Cu(II) a transient pentacoordinated Cu(I) species is obtained that rearranges in the millisecond time scale by means of a second pirouetting of the ring to the most stable structure with Cu(I) tetrahedrically coordinated (Fig. 29b). These results underline that the rearrangement rates from the less to the most stable geometries are drastically different for the two oxidation states of the metal.

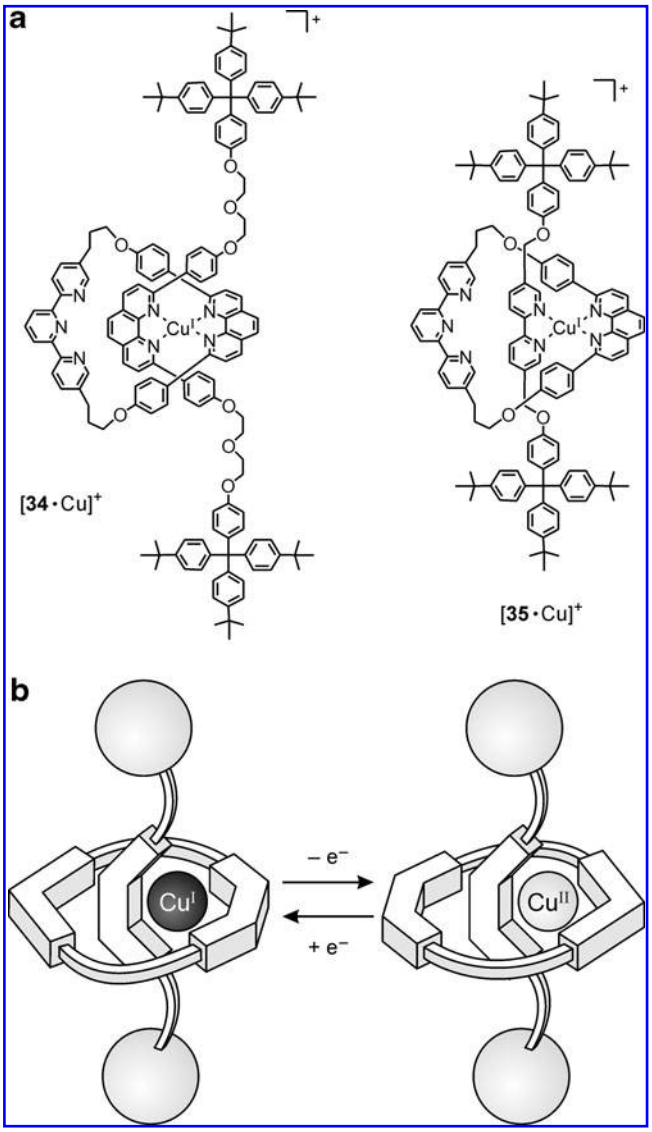

FIG. 29. (a) Structure of rotaxanes [34•Cu]$^+$ and [35•Cu]$^+$, and (b) schematic representation of the ring pirouetting induced by oxidation/reduction of the metal center.

To increase the rate of the ring pirouetting, the new rotaxane [**35**•Cu]$^+$ (Fig. 29a) was prepared (242) in which the metal center is more accessible because of the presence of a less hindered ligand compared to previous related systems. Ligand exchange within the coordination sphere of the metal is thus facilitated as much as possible. The molecular axle contains indeed a thin, 2,2′-bipyridine motif, which is less bulky than a 1,10-phenanthroline fragment and it is expected to spin more readily within the cavity of the ring as a consequence of Cu oxidation/reduction. Compared to [**34**•Cu]$^+$, in this rotaxane both the oxidation induced and the reduction induced ring pirouetting movements are more than three orders of magnitude faster. This example shows that subtle structural factors can have a very significant influence on the general behavior (rate of the movement, in particular) of copper(II/I)-based molecular machines.

Further improvement in the pirouetting rate has then been obtained by keeping the two stoppers of [**35**•Cu]$^+$ very remote from the copper center (202). The results obtained show that in this improved system the ring moves very fast around the axle (milliseconds) even at low temperature. As a consequence of the oxidation–reduction cycle, the ring of these rotaxanes does not necessarily perform a 360-degree rotation, but can only oscillate between the two positions on the threaded axle. To make real rotary motors it would be necessary to introduce directionality in the system by using, for example, a ring containing three different coordination sites and a well defined axle.

V. Systems Based on Catenanes

Catenanes, whose name derives from the Latin word catena for chain, are made of (at least) two interlocked macrocycles or rings (Fig. 30) (258). As rotaxanes, they are currently the object of much interest for their molecular and supramolecular character: (i) molecular because the components are held together mechanically and can be unlinked only by breaking strong covalent bonds; (ii) supramolecular because of the presence of weak noncovalent interactions between the components that contain complementary recognition sites (electron donor–acceptor ability, hydrogen bonding, hydrophobic–hydrophylic character, π-π stacking, electrostatic forces, and also metal–ligand bonding). Such intercomponent noncovalent interactions are also responsible for their efficient template-directed synthesis (22, 260). These important features make catenanes appealing systems for the

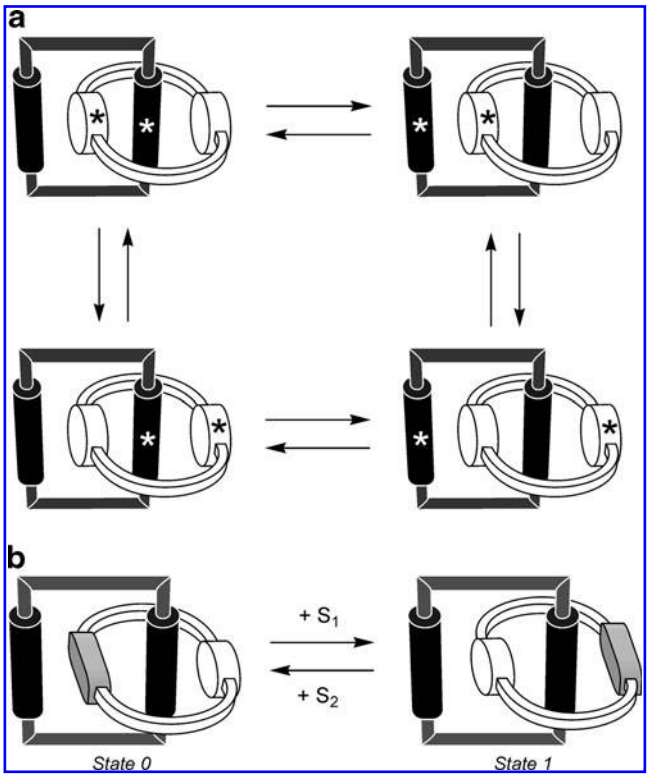

FIG. 30. Circumrotation motions of the molecular ring components in catenanes. (a) Dynamic processes associated with circumrotation of one ring in a catenane made of two different macrocycles each incorporating two identical recognition sites (asterisks are used to highlight the exchange of position of identical units); **(b)** the two coconformational isomers associated with a catenane incorporating two different recognition sites within one of its two macrocyclic components can be interchanged by appropriate stimuli (S_1 and S_2).

construction of molecular machines: (i) the mechanical bond allows a large variety of mutual arrangements of the molecular components, while conferring stability to the system; (ii) the interlocked architecture limits the amplitude of the intercomponent motion in the three directions; (iii) the stability of a specific arrangement (conformation) (143) is determined by the strength of the intercomponent interactions; and (iv) such interactions can be modulated by external stimulation. The large-amplitude motion that can be achieved with catenanes is the circumrotation of one ring with respect to the other, and when suitably designed they can be seen as simple prototypes of molecular rotors.

As already said, catenanes are minimally composed by two interlocked rings. If it is arranged during the template-directed synthesis to have two identical units, that is, recognition sites, located within two different macrocycles, then the resulting catenane undergoes degenerate conformational change. As illustrated in Figure 30a one of the macrocycles spontaneously circumrotates through the cavity of the other and *vice versa*. As each ring spends most of its time surrounding a recognition site of the other ring, each macrocycle has one site located inside and the other one positioned alongside with respect to the other macrocycle.

Much more appealing is, however, a catenane in which one of the two rings carries two different recognition sites, because in such a case there is the opportunity to control the dynamic processes (Fig. 30b). The two possible conformational isomers of such catenanes can be interchanged by appropriate stimuli. In a diagram of potential energy against rotation angle of the asymmetric macrocycle, the two conformations correspond to energy minima, provided by the intercomponent noncovalent bonding interactions. The initially populated coconformer is that associated with the most favorable energetic state (State 0). Stimulus S_1 has the effect of destabilizing such isomer and leads to the other one (State 1), a change that can simply be viewed as a circumrotation of the asymmetric macrocycle. An opposite stimulus S_2 restores the original situation. By switching off and on again the recognition properties of one of the two recognition sites of the asymmetric macrocycle, the relative populations of the two species can be controlled reversibly. Repeated switching between the two states does not need to occur through a full rotation. In fact, because of the intrinsic symmetry of the system, both the movement from State 0 to State 1 and that from State 1 to State 0 can take place, with equal probabilities, along a clockwise or anticlockwise direction. A full (360°) rotation movement can only occur in ratchet-type systems, that is, in the presence of asymmetry elements that can be structural or functional in nature. Mechanical movements in suitably designed catenanes can be induced by chemical, photochemical, or, as evidenced by the selected examples reported in the next section, by electrochemical stimulation (69, 74, 89, 100, 182, 191, 194, 211, 269).

A. Electrochemically driven motion

We have already said that when one of the two rings of a catenane carries two different recognition sites, the dynamic processes of one ring with respect to the other can be controlled. In particular, if redox units are incorporated in the catenane structure there is the possibility of controlling these processes upon electrochemical stimulation. Catenanes that exhibit such a behavior can be seen as electrochemically driven molecular rotors. An example is offered by catenane $\mathbf{36}^{4+}$ (Fig. 31a) that incorporates the previously seen macrocycle **25** and a tetracationic cyclophane comprising one bipyridinium and one *trans*-1,2-bis(4-pyridinium)ethylene unit (36, 37). In the major isomer, the bipyridinium unit is located inside the cavity of the macrocyclic polyether and the *trans*-bis(pyridinium)ethylene unit is positioned alongside, as confirmed by the electrochemical analysis. The cyclic voltammogram of the catenane shows four monoelectronic processes that, by a comparison with the data obtained for the free cyclophane, can be attributed as follows: the first and fourth processes to the first and second reductions of the bipyridinium unit, and the second and third ones to the first and second reductions of the *trans*-bis(pyridinium)ethylene unit. The comparison with the tetracationic cyclophane also reveals that all these reductions are shifted toward more negative potential values (Fig. 31b).

The discussion can be restricted to the first and second reduction processes that are of particular interest in this context. The shift of the bipyridinium-based process is in agreement with the catenane conformation in which the bipyridinium unit is located inside the cavity of the macrocyclic polyether (Fig. 31a); because of the CT interactions established with both the electron-donor units of the macrocycle, its reduction is more difficult than in the free tetracationic cyclophane. The shift of the *trans*-1,2-bis(4-pyridinium)ethylene-based

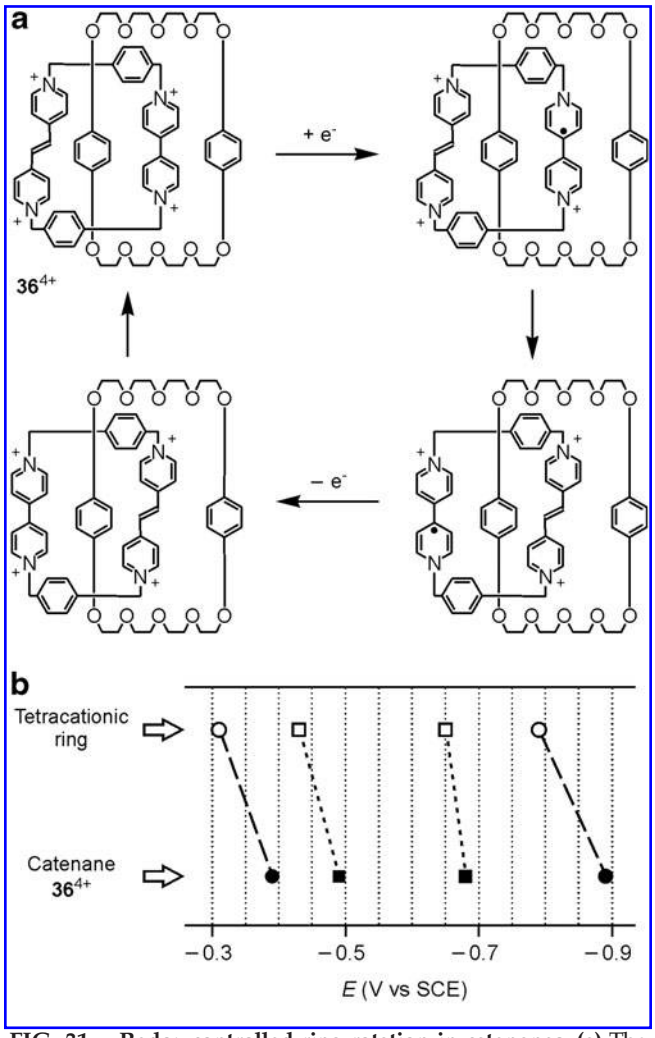

FIG. 31. Redox-controlled ring rotation in catenanes. (a) The circumrotation of the tetracationic cyclophane component of catenane $\mathbf{36}^{4+}$ can be controlled reversibly by reducing–oxidizing electrochemically its bipyridinium unit; **(b)** correlation between the halfwave reduction potentials of catenane $\mathbf{36}^{4+}$ and of its tetracationic ring component (circles and squares correspond to the reduction of bipyridinium and *trans*-bis(pyridinium) ethylene units, respectively). Copyright John Wiley & Sons. Reproduced with permission from Ceroni *et al.* (97).

reduction indicates that, once the bipyridinium unit is reduced, the CT interaction that stabilize the initial conformation are destroyed and, thereby, the tetracationic cyclophane circumrotates through the cavity of the macrocyclic polyether moving the *trans*-bis(pyridinium)ethylene unit inside, as shown by comparison of its reduction potential with that of a catenane model compound (36). The original equilibrium between the two conformations associated with catenane $\mathbf{36}^{4+}$ is restored upon oxidation of both units back to their dicationic states.

For a machine-like performance the presence of a desymmetrized ring is a necessary but not sufficient requirement. This statement is clearly demonstrated by the behavior of catenane $\mathbf{37}^{4+}$ made by the same tetracationic cyclophane of $\mathbf{36}^{4+}$ and a macrocycle containing two DON units (36, 37). As in the case of $\mathbf{36}^{4+}$ the major isomer is the one in which the bipyridinium unit is located inside the macrocycle. However, in contrast with the behavior of $\mathbf{36}^{4+}$, for which the first reduction process concerns the inside bipyridinium unit, the first reduction of $\mathbf{37}^{4+}$ involves the alongside *trans*-bis(pyridinium)ethylene unit. This process has been undoubtedly attributed to this unit by performing spectroelectrochemical experiments and comparing the spectrum of the monoreduced catenane with that of a model compound containing only the *trans*-bis(pyridinium)ethylene unit. The different behavior of the two catenanes, as far as the first reduction process is concerned, can be explained on the bases of the different strength of the CT interactions: in $\mathbf{37}^{4+}$ the bipyridinium unit is sandwiched between two DON moieties that are stronger electron donor than the DOB moieties of the macrocyclic component of catenane $\mathbf{36}^{4+}$. Because of these stronger interactions the reduction of such a unit becomes so difficult that it occurs at a potential more negative than that of the *trans*-bis(pyridinium)ethylene unit (Fig. 32).

As a consequence of the fact that in $\mathbf{37}^{4+}$ the first reduction concerns the alongside unit, the CT interactions responsible of the initial conformation are practically unaffected and no mechanical movement occurs in the monoreduced catenane.

Catenanes $\mathbf{38}^{4+}$ and $\mathbf{39}^{4+}$ (Fig. 33) are other examples of systems in which the conformational motion can be controlled electrochemically (28, 68). They are made of the symmetric tetracationic cyclophane $\mathbf{4}^{4+}$ and a desymmetrized ring comprising two different electron donor units, namely, a TTF and a DOB ($\mathbf{38}^{4+}$) or a DON ($\mathbf{39}^{4+}$) units. Because the TTF moiety is a better electron donor than the dioxyarene units, as witnessed by the potentials values for their oxidation, the thermodynamically stable conformation of these catenanes is that in which the symmetric ring encircles the TTF unit of the desymmetrized one (Fig. 33a, State 0).

The cyclic voltammogram of the free macrocycle shows a reversible process attributed to the monoelectronic oxidation of the TTF unit. In the catenanes, such a process occurs at more positive potentials, in agreement with the fact that the TTF unit is located inside the cavity of the tetracationic cyclophane and, therefore, engaged in strong CT interactions. In such

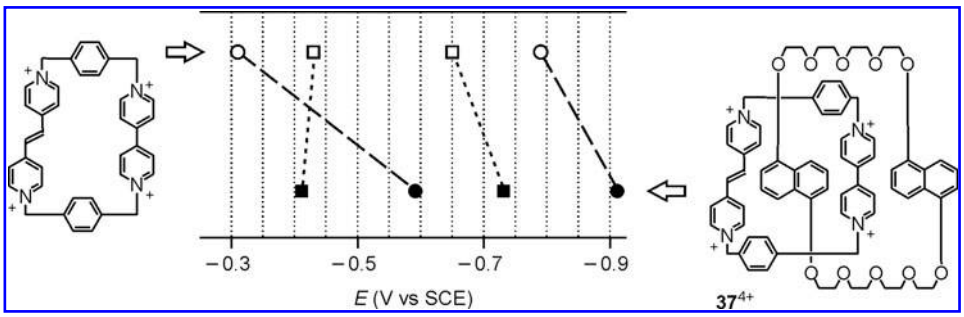

FIG. 32. Correlation between the halfwave reduction potentials of catenane $\mathbf{37}^{4+}$ and of its tetracationic ring component. Circles and squares correspond to the reduction of bipyridinium and *trans*-bis(pyridinium)ethylene units, respectively. Copyright John Wiley & Sons. Reproduced with permission from Ceroni *et al.* (97).

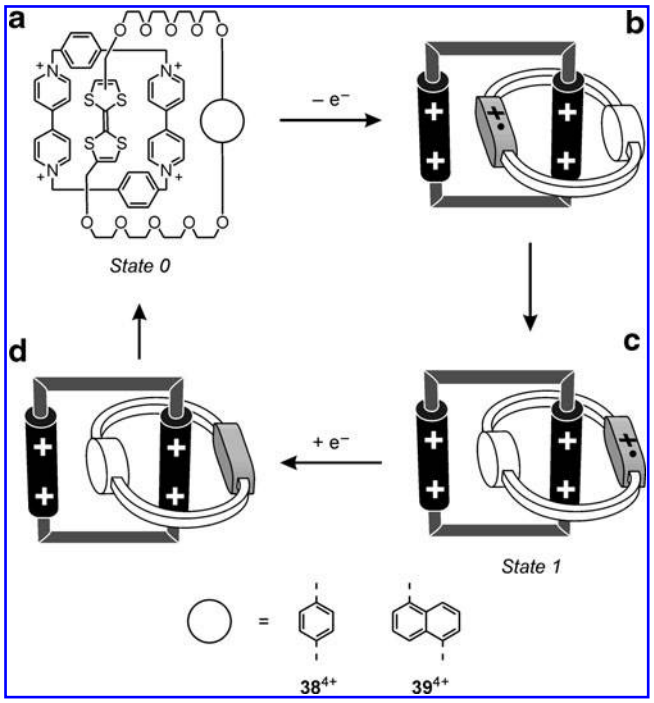

FIG. 33. Redox-controlled ring rotation in solution for catenanes 38^{4+} and 39^{4+}, which contain the symmetric electron-acceptor cyclophane 4^{4+} and a desymmetrized electron-donor ring.

catenanes this oxidation process is characterized by a large separation between the anodic and cathodic peaks, which varies as the scan rate is changed. Upon increasing the scan rate, the anodic peak moves to more positive potentials, whereas the cathodic one shifts to less positive values. These observations indicate that the oxidation–reduction of the TTF unit is accompanied by the circumrotation of the desymmetrized ring through the cavity of the tetracationic cyclophane and that this change is occurring on the time scale of the electrochemical experiment. Indeed, after oxidation, the newly formed monocationic TTF unit (Fig. 33b) loses its electron-donor power; as a consequence, it is expelled from the cavity of the tetracationic cyclophane and is replaced by the neutral dioxyarene unit (Fig. 33c, State 1). After reduction, the original conformation is restored as the neutral TTF unit replaces the dioxyarene unit inside the cavity of the tetracationic cyclophane. Ring rotation in these catenanes can also be obtained chemically. The tendency of *o*-chloranil to stack against TTF has been indeed exploited (28, 68) to lock this unit alongside the cavity of the tetracationic cyclophane. On addition of a mixture of $Na_2S_2O_5$ and NH_4PF_6 in H_2O, the adduct formed between the TTF unit and *o*-chloranil is destroyed, and the original conformation with TTF inside the cavity of the tetracationic cyclophane is then restored.

As we will see in section "B. Molecule-based solid-state electronic circuits," catenane $\mathbf{39}^{4+}$ was also incorporated in a solid state device that could be used for random access memory storage (107, 210). Additionally, this compound could be employed for the construction of electrochromic systems, because its various redox states are characterized by different colors (28, 68, 273).

By an appropriate choice of the functional units that are incorporated in the catenane components, more complex functions can be obtained. An example is represented by catenane $\mathbf{40}H^{5+}$ (Fig. 34), composed of a symmetric crown ether and a cyclophane ring containing two bipyridinium and one ammonium recognition sites (31). The electrochemical properties, as well as the absorption spectra, show that the crown ether surrounds a bipyridinium unit of the other ring both in

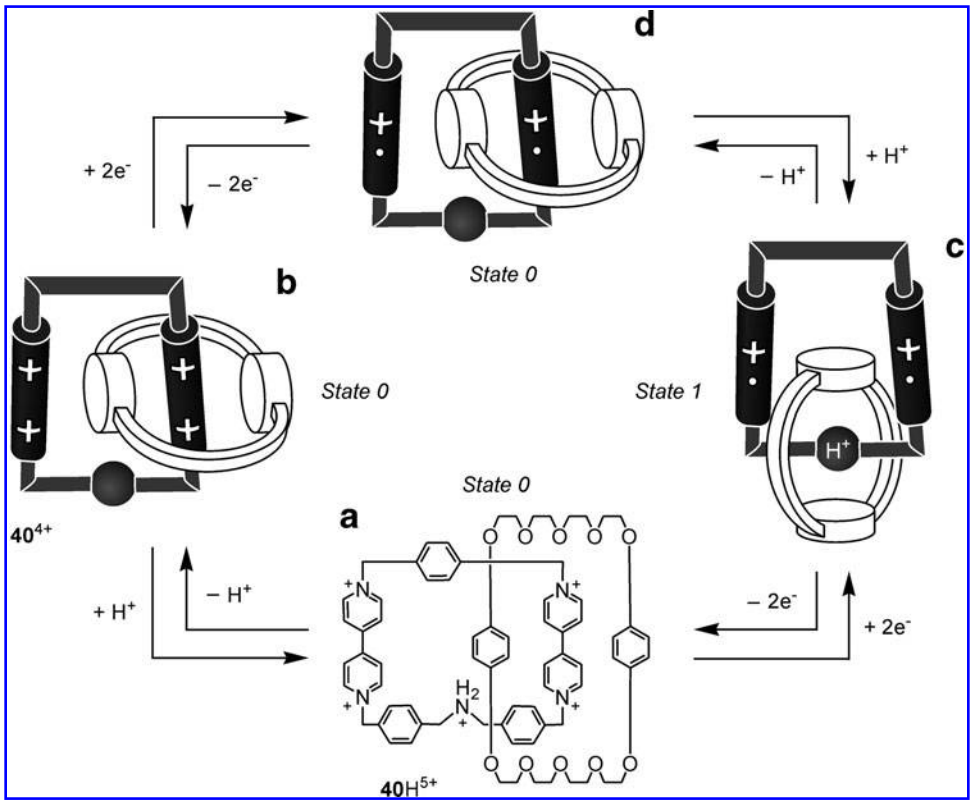

FIG. 34. Switching processes of catenane $40H^{5+}$ in solution. Starting from the deprotonated catenane $\mathbf{40}^{4+}$, the position of the ring switches under acid–base and redox inputs according to AND logic. Copyright John Wiley & Sons. Reproduced with permission from Ceroni *et al*. (97).

$\mathbf{40}H^{5+}$ (Fig. 34a) and in its deprotonated form $\mathbf{40}^{4+}$ (Fig. 34b), indicating that deprotonation–protonation of the ammonium unit does not cause any displacement of the ring (State 0).

Electrochemical measurements also show that, after one-electron reduction of both the bipyridinium units of $\mathbf{40}H^{5+}$ the ring is displaced on the ammonium function (Fig. 34c, State 1), which means that an electrochemically induced conformational switching does occur. Further, upon deprotonation of the two-electron reduced form of the catenane (Fig. 34d), the crown ether moves to one of the monoreduced bipyridinium units (State 0). Therefore, to achieve the motion of the ring in the deprotonated catenane $\mathbf{40}^{4+}$, it is necessary both to reduce (switch off) the bipyridinium units and protonate (switch on) the amine function. The mechanical motion in such a catenane occurs according to an AND logic (61), a function associated with two energy inputs of different nature.

Controlled rotation of the molecular rings has been achieved also in catenanes composed of three interlocked macrocycles. For example, catenane $\mathbf{41}H_2^{6+}$ (Fig. 35) is made up of two identical DOB-based macrocycles **25** interlocked with a cyclophane containing two bipyridinium and two ammonium units (31).

Because of the type of the macrocycles used, the stable conformation of $\mathbf{41}H_2^{6+}$ is that in which the two rings surround the bipyridinium units (Fig. 35a, State 0). Upon addition of one electron in each of the bipyridinium units, the two macrocycles move on the ammonium stations (Fig. 35b, State 1), and move back to the original position when the bipyridinium units are reoxidized.

Very recently, it has been reported the synthesis and characterization of the six desymmetrized donor–acceptor catenanes $\mathbf{42}^{2+}$–$\mathbf{47}^{2+}$ (Fig. 36), where different donor and acceptor units are assembled within a confined catenated geometry (91).

They are formed by (i) a desymmetrized electron acceptor ring containing two different units, namely, a 4,4′-bipyridinium dication (BPY^{2+}) and a neutral naphthalene diimide (NDI) or pyromellitic imide (PMI) moieties, and (ii) an electron donor ring that can be symmetric for the presence of two identical DOB or DON units, or desymmetrized by the presence of two different donors, that is, a TTF and a DON moieties. The two $\mathbf{44}^{2+}$ and $\mathbf{47}^{2+}$ catenanes, containing four

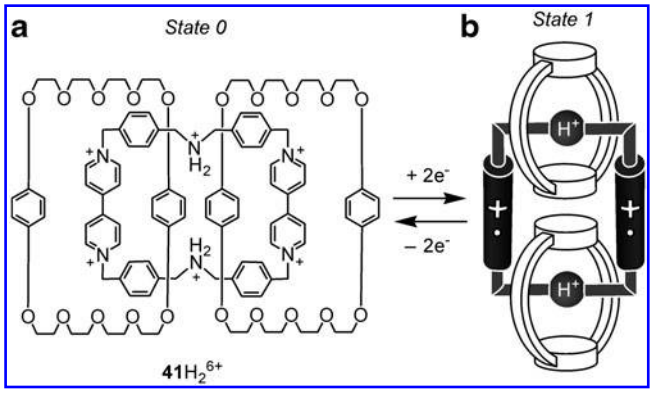

FIG. 35. Redox-controlled movements of the ring components in catenane $\mathbf{41}H_2^{6+}$, composed of three interlocked macrocycles. These motions are obtained upon reduction–oxidation of the bipyridinium units of the cyclophane. Copyright John Wiley & Sons. Reproduced with permission from Ceroni *et al*. (97).

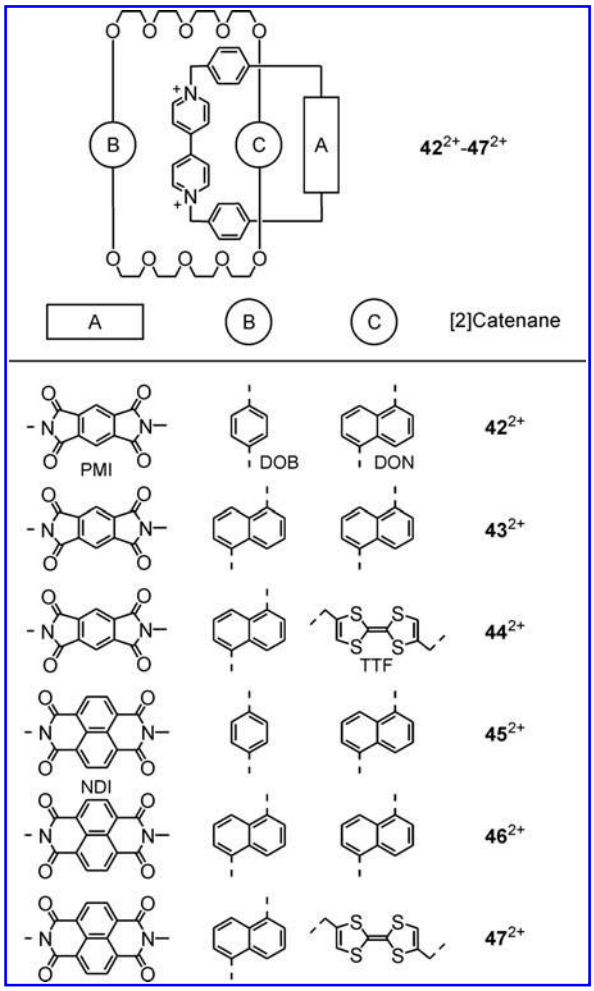

FIG. 36. General structure and component units of the desymmetrized catenanes $\mathbf{42}^{2+}$–$\mathbf{47}^{2+}$.

different donor and acceptor units, are fully desymmetrized. In all the catenanes the electron donor ring surrounds the better electron acceptor BPY^{2+} unit, and in the case of catenanes $\mathbf{44}^{2+}$ and $\mathbf{47}^{2+}$ the better electron donor TTF unit is located inside the electron acceptor ring. Such conformations can be switched altering the redox state of the donors and acceptors incorporated in the structure as evidenced by the rich and complex electrochemical patterns exhibited by these catenanes.

On the reduction side, the cyclic voltammogram of $\mathbf{42}^{2+}$ reveals four reversible monoelectronic processes. Spectroelectrochemical experiments and comparison with suitable model compounds (36, 156) indicate that (i) the first process is consistent with the reduction of a BPY^{2+} unit engaged in CT interactions inside the cavity of the donor ring; (ii) the second reduction concerns the monoreduced BPY^{+} unit, likely still inside the cavity of the donor ring; (iii) the third process corresponds to the reduction of the inside PMI unit (the translocation probably occurs upon reduction of the BPY^{+} unit to its neutral form); and finally (iv) the fourth reduction involves PMI^{-}, on the position of which relatively to the donor ring there is little information.

In catenanes $\mathbf{43}^{2+}$ and $\mathbf{44}^{2+}$, because of the stronger electron donating power of the crown ethers comprised in the

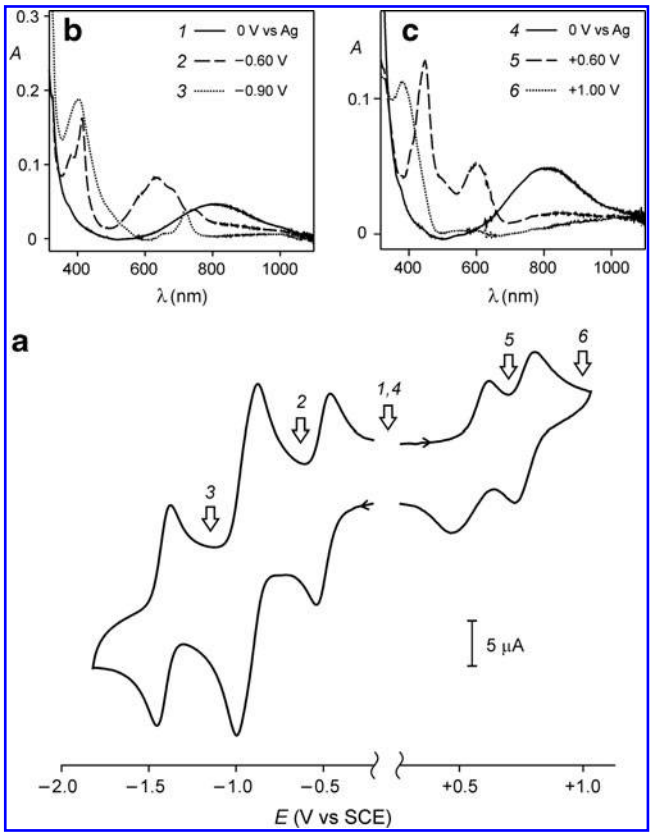

FIG. 37. Voltammetric and spectroelectrochemical response of catenane 44^{2+} in CH_3CN at room temperature. (a) Cyclic voltammetric curve (conditions: 0.49 m*M*, tetraethylammonium hexafluorophosphate 73 m*M* as supporting electrolyte, 200 mV/s, glassy carbon working electrode). **(b)** Absorption spectra observed before (full line) and after exhaustive reduction at −0.60 V (dashed line) and −0.90 V (dotted line) *versus* an Ag pseudoreference electrode. **(c)** Absorption spectra observed before (full line) and after exhaustive oxidation at +0.60 V (dashed line) and +1.00 V (dotted line) *versus* an Ag pseudoreference electrode. The numbered arrows in **(a)** mark the potential values at which the corresponding curves in **(b)** and **(c)** were recorded in the spectroelectrochemical experiments.

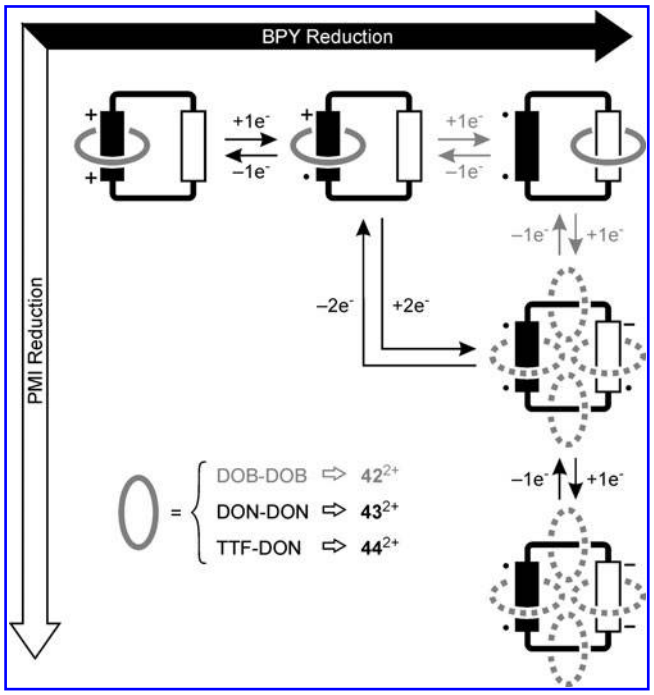

FIG. 38. The conformation changes associated with the four reduction processes for catenanes 42^{2+}–44^{2+}. Horizontal and vertical processes represent the BPY-centered and PMI-centered reductions, respectively. In the *upper right part* of the scheme, *gray arrows* refer to the behavior of 42^{2+}, while *black arrows* describe the behavior of 43^{2+} and 44^{2+}. The dotted ellipses indicate that the interactions are turned off and there is little information about the donor ring location. BPY, 4,4′-bipyridinium dication. PMI, pyromellitic imide.

structure, the BPY^{2+} unit becomes more difficult to be reduced than in catenane 42^{2+} so that its second reduction overlaps to the first reduction of the PMI unit. The reduction pattern of 43^{2+} and 44^{2+} (Fig. 37a) consists therefore of three reversible waves: (i) spectroelectrochemical experiments (for 44^{2+}, Fig. 37b) confirm that the first process concerns the monoelectronic reduction of the BPY^{2+} unit located inside the donor ring; (ii) the second process, which involves the exchange of two electrons, can be unambiguously assigned to the overlapping reduction of the inside BPY^{+} and the alongside PMI (150); and (iii) the third process, which is monoelectronic, corresponds to the $PMI^{-/2-}$reduction.

The conformation changes coupled with the four-electron reduction processes for the 42^{2+}–44^{2+} PMI-containing catenanes are summarized in Figure 38.

In the case of three 45^{2+}–47^{2+} NDI-based catenanes the reduction pattern comprises four reversible monoelectronic processes regardless of the nature of the donor rings. This behavior can be explain considering that the NDI unit is easier to be reduced than PMI. As a consequence the processes observed can be assigned to $BPY^{2+/+}$, $NDI^{0/-}$, $BPY^{+/0}$, and $NDI^{-/2-}$, respectively, in the order of increasing reduction potential. The proposed conformational changes coupled with these four one-electron reduction processes are as follows (Fig. 39): (i) the electron-donor ring remains around the BPY^{+} radical cation after the first reduction; (ii) the second reduction is indicated by spectroelectrochemical experiment to be the $NDI^{0/-}$ process (150), and the potential value, more consistent with the reduction of the NDI moiety in the alongside position, suggests that the donor ring still encircles the monoreduced BPY^{+} unit; (iii) the remarkably negative potential value found for the third process, assigned to the $BPY^{+/0}$ reduction, is in agreement with the assumption that no translocation of the donor component has occurred; and (iv) the fourth process is attributed to the reduction of the NDI^{-} unit, on the position of which relatively to the donor ring there is little information, as noted previously for the PMI-based catenanes.

On the oxidation side, we discuss only the behavior of the fully desymmetrized catenanes 44^{2+} and 47^{2+} because they are particularly interesting from the viewpoint of molecular machines. Their electrochemical patterns are very similar and consist of three oxidative processes (for 44^{2+}, Fig. 37a): the first two (Fig. 37c) are assigned to the two consecutive monoelectronic TTF oxidations (38), while the third one is ascribed to the oxidation of the DON unit. The first and second TTF oxidations exhibit the same features observed for catenane 39^{4+}

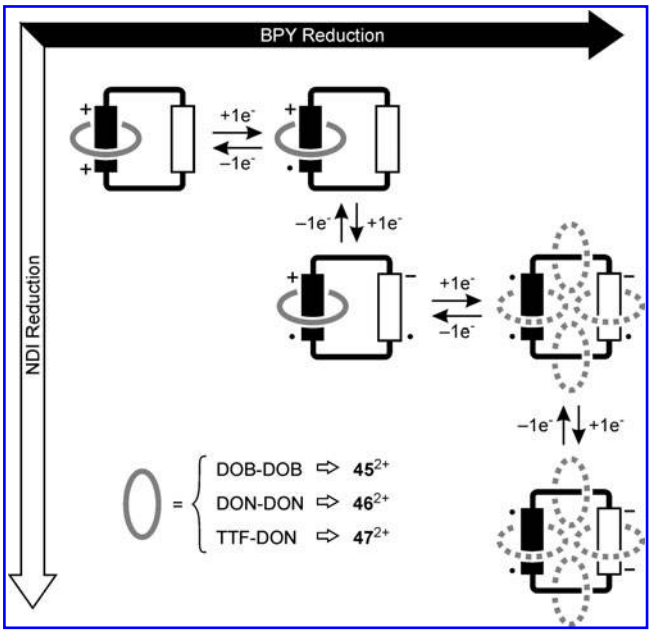

FIG. 39. The conformational changes associated with the four reduction processes for catenanes 45^{2+}–47^{2+}. Horizontal and vertical processes represent the BPY-centered and NDI-centered reductions, respectively. The dotted ellipses indicate that the interactions are turned off and there is little information about the donor ring location. NDI, naphthalene diimide.

and therefore can be interpreted in the same way: after the $TTF^{0/+}$ oxidation, the electron donor ring circumrotates with respect to the electron accepting ring, delivering the DON unit into its cavity.

This electrochemical study evidences that in the desymmetrized $\mathbf{42}^{2+}$ -$\mathbf{47}^{2+}$ catenanes the inside/alongside topological preference, dominated by the intercomponent CT interactions, can be modulated reversibly upon reduction of the electron acceptors, or oxidation of the electron donors in the cases of fully desymmetrized $\mathbf{44}^{2+}$ and $\mathbf{47}^{2+}$ catenanes. Such a feature makes these catenanes appealing structures for the construction of molecular machines and, in a perspective, rotary motors. Upon electrochemical stimulation in a relatively narrow and easily accessible potential window these interlocked molecules can be reversibly switched among several (six and seven for $\mathbf{44}^{2+}$ and $\mathbf{47}^{2}$, respectively) states, all characterized by distinct electronic and optical properties. Such a possibility could open interesting routes for the development of molecular electronic devices that go beyond binary logic.

A catenane composed of two identical benzylic amide macrocycles was also investigated by cyclic voltammetry (98). Computer simulation of the voltammetric data, together with quantum chemical calculations, suggest that reduction of the macrocycles is followed by their irreversible chemical soldering, owing to the formation of a C–C bond between two reduced carbonyl groups. Hence, the electrochemical stimulus can be used to prevent the mutual rotation of the two rings, although the irreversibility of the reaction limits further developments.

Other examples of electrochemically driven switching processes concern metal-based catenanes (75, 92, 100, 109, 205, 206), including heterodinuclear bis-macrociclic transition-metal complexes (193).

A representative case is catenane $[\mathbf{48}\bullet Cu]^{+}$ (Fig. 40), which incorporates two identical macrocyclic components comprising terpyridine and phenanthroline ligands.

The Cu(I) ion is coordinated tetrahedrally by the two phenathroline ligands, whereas the two terpyridine ligands are located well away from each other (92). The cyclic voltammogram of $[\mathbf{48}\bullet Cu]^{+}$ contains a reversible wave (+0.63 V relative to the SCE) associated with the tetracoordinated Cu(II)/Cu(I) redox couple. The visible absorption spectrum of the catenane contains a metal-to-ligand CT band at 439 nm for the tetracoordinated Cu(I) chromophore. On electrochemical oxidation of $[\mathbf{48}\bullet Cu]^{+}$ or on treatment with $NOBF_4$ the tetracoordinated Cu(I) center is converted into a tetracoordinated Cu(II) ion, which has an absorption band at 670 nm. The intensity of this band decreases with time, however. Indeed, in response to the preference of the Cu(II) ion for a coordination number higher than four, one of the two macrocycles circumrotates through the cavity of the other, affording a pentacoordinated Cu(II) ion. Subsequently the other macrocycle undergoes a similar circumrotational process, yielding a hexacoordinated Cu(II) ion, which gives, instead, a weak absorption band at 687 nm. Electrolysis (−1.0 V) of the acetonitrile solution of the catenane reduces the hexacoordinated Cu(II) center back to a hexacoordinated Cu(I) ion. In response to the preference of Cu(I) for a tetracoordinated geometry the two macrocycles circumrotate through the cavity of each other in turn, affording the original conformation quantitatively.

VI. Heterogeneous Systems

The design, synthesis, and operation of multicomponent molecular systems capable of performing specific, directional mechanical movements under the action of a defined energy input—namely, molecular machines—constitute a fascinating challenge in the field of nanoscience. Owing to the progress made in several branches of chemistry, physics, biology, and materials science, various types of artificial molecular machines have been developed and some selected examples have been reported in the previous sections.

Most of the studies on molecular machines have been performed in solution. Under such conditions, the investigated systems contain a huge number of molecules that behave independently from one another because they cannot be addressed individually and hence controlled. In spite of this limitation, the described systems illustrate a number of very interesting concepts concerning molecular-level movements controlled by external inputs. Incoherence, however, remains a major impediment to designing and realizing systems capable of performing useful functions. It seems therefore reasonable that for several real applications the molecular machines have to be interfaced with the macroscopic world by ordering them in some way at interfaces or on surfaces (2). The problem of obtaining ordered arrays of molecular devices (76, 82, 104, 125, 135, 237, 251, 267) can be addressed by a variety of techniques.

Realizing the summation of motion at the molecular level to achieve macroscopic motion, for instance mimicking the operation of miosyn/actin-driven movement of muscles, is a real challenge. The approaches taken include changes in surface

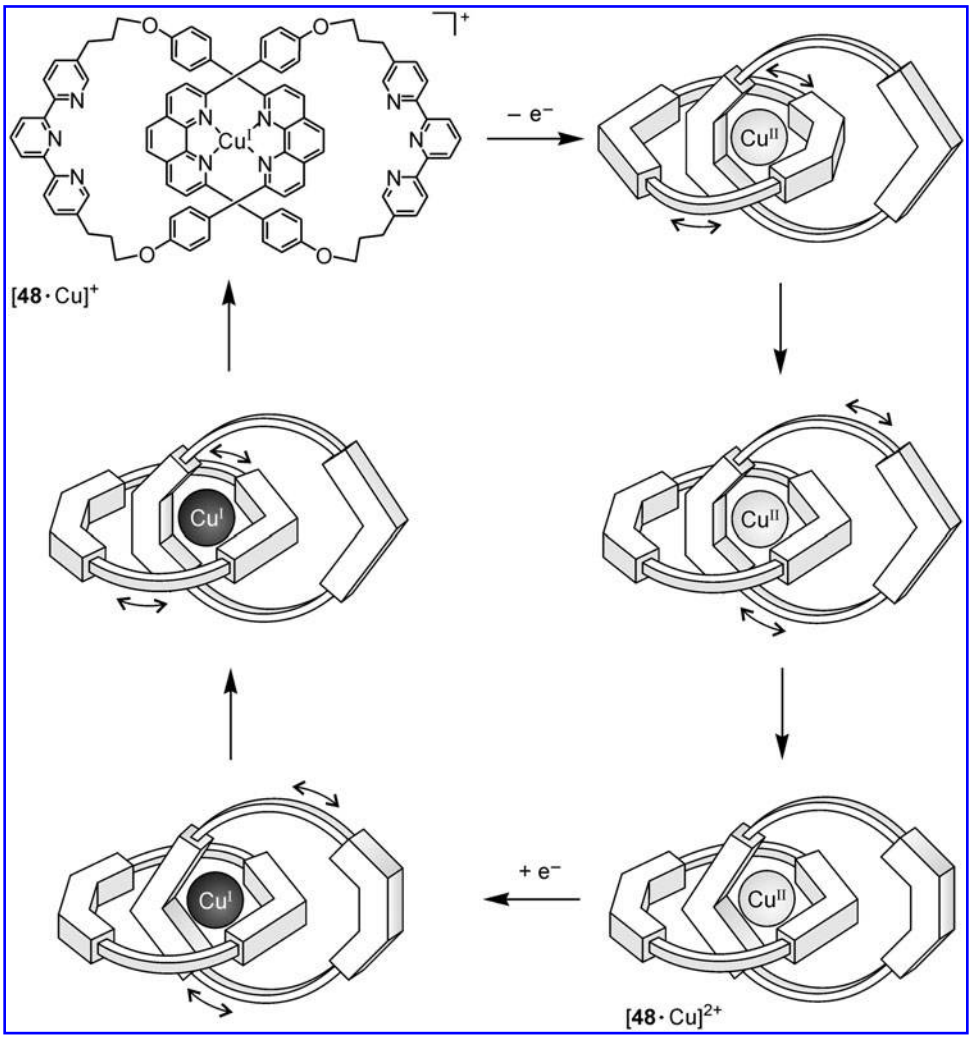

FIG. 40. Circumrotation of the macrocyclic components of catenate [48•Cu]$^{+}$ can be controlled reversibly by oxidizing or reducing the metal center. Copyright Wiley-VCH Verlag GmbH & Co. KGaA. Reproduced with permission from Balzani *et al*. (64).

properties (*e.g.*, surface tension), direct translation of molecular to macroscopic motion, and signal collection by suitably designed architectures.

In the last few years, the development of scanning probe techniques (73, 153, 203, 255, 271) has enabled direct observation and manipulation of single molecules on surfaces. Techniques of this kind have opened novel directions to the study of molecular machines and have also contributed to better understand the differences between movement at the macroscopic and at the molecular level.

Studies on molecular machines on surfaces and at interfaces have been recently carried out by several research groups. We will briefly describe here only a small number of paradigmatic examples.

A. Molecular machines working on surfaces and at interfaces

The Langmuir-Blodgett (LB) technique constitutes an efficient means of transferring organized monolayers from the air–water interface onto a solid substrate (239). A series of investigations (30, 104) showed that cationic catenanes and rotaxanes such as **22**H^{3+} (Fig. 21) can be used to obtain ordered films on the air–water interface when the PF_6^- counterions are replaced by amphiphilic counterions such as the dihexadecylphosphate anion (104).

These anions align in a parallel manner at the interface, with the phosphate portion pointing toward the aqueous substrate. To balance this high negative charge density, a layer of cationic rotaxanes associates near the surface as an ordered, reproducible monolayer, possibly stabilized by stacking interactions between adjacent molecules. For instance, the **22**H^{3+}-dihexadecylphosphate films were transferred onto indium tin oxide supports for spectroscopic and electrochemical investigations. Reversible switching of the potential values for the reduction processes of the bipyridinium unit of **22**H^{3+} upon cyclic exposure of the films to vapors of HCl and NH_3 was observed (104). A comparison of the behavior of the rotaxane-containing films with that of films containing its dumbbell-shaped component suggested that the switching process is mainly related to a rearrangement of the multilayer upon protonation–deprotonation of the ammonium centre. However, the occurrence of a ring shuttling motion in the case of the rotaxane-containing films could not be excluded. Nonetheless, the examined thin films may be useful for sensing purposes because they provide a reversible electrical output signal in response to acid–base input stimuli.

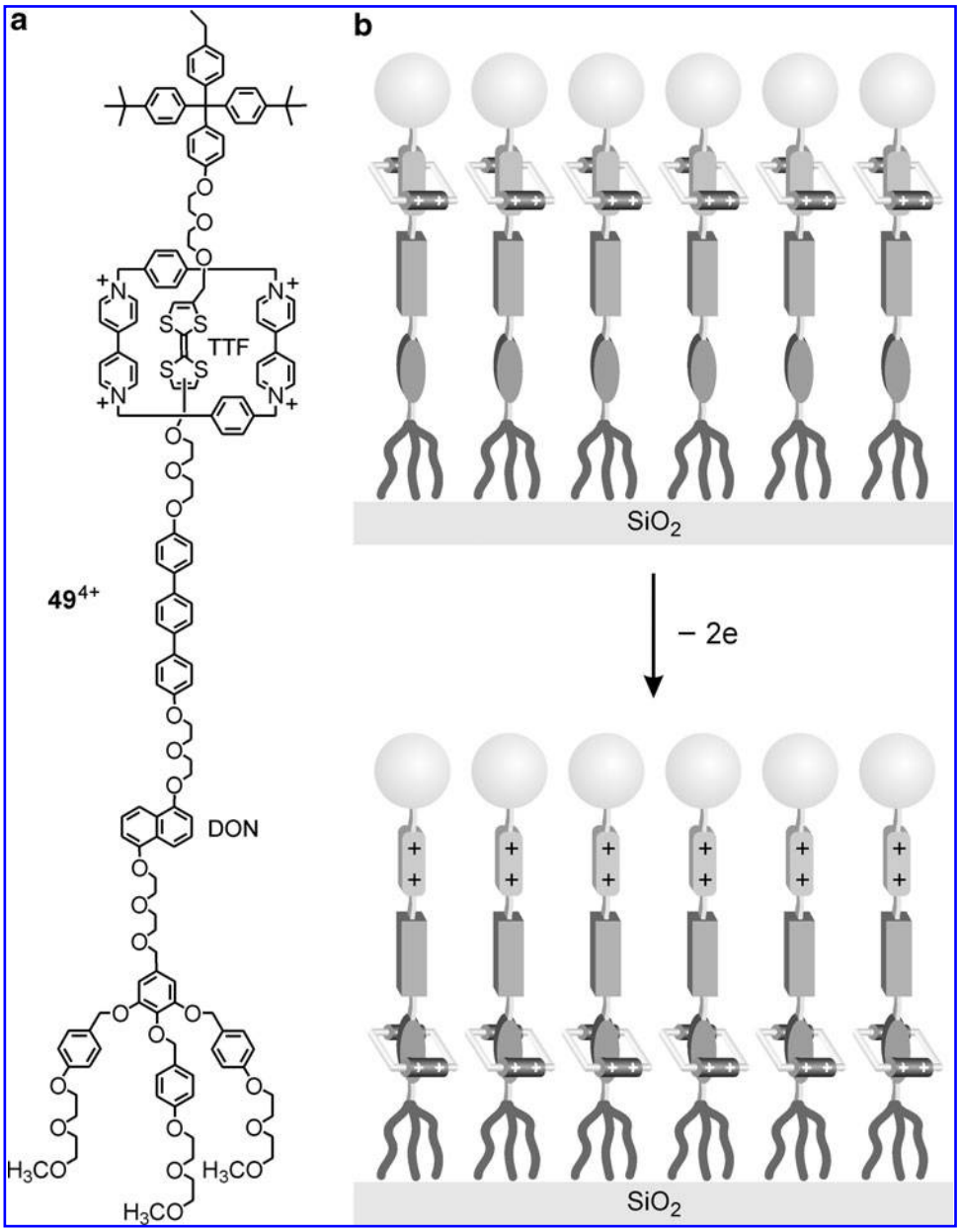

FIG. 41. (a) Structure formula of the amphiphilic TTF-DON rotaxane 49^{4+} and (b) scheme of the redox switching of its Langmuir-Blodgett monolayer. Reproduced by permission of the Royal Society of Chemistry from Silvi *et al.* (268).

Amphiphilic bistable TTF-DON rotaxanes such as $\mathbf{49}^{4+}$ (Fig. 41a) were synthesized and investigated (280) to obtain stable and well organized LB films (155, 162, 167).

The occurrence of ring shuttling in $\mathbf{49}^{4+}$ embedded in closely packed LB films on solid substrates, induced by chemical oxidation of the TTF station, was observed using X-ray photoelectron spectroscopy (XPS) (162). In XPS, the photoemission intensity of each element attenuates exponentially with the depth at which the electron is emitted. The switching behavior was monitored by using XPS to track nitrogen, which is present solely in the moving macrocyclic component of the rotaxane. Upon oxidation of the rotaxane molecules in a silica-supported monolayer, the photoemission intensity for the nitrogen 1s electrons was significantly decreased with respect to the starting state. This observation, together with the results of quantitative data analyses and independent control experiments, confirmed that in the film the ring components move from the upper station (TTF) to the lower one (DON) upon oxidation of the former (Fig. 41b) (155, 162, 167).

The formation of self-assembled monolayers (SAMs) on metallic gold is an effective yet simple method to attach molecules to surfaces (209, 282). Rotaxanes with suitable functionalization have been extensively employed to prepare Au-SAMs (168, 230, 281, 292, 295). The first studies on mechanical shuttling in a SAM, however, were carried out on systems in which the molecular components became mechanically interlocked as a consequence of surface immobilization (180, 181, 296). In this setting the metal surface plays the dual role of a stopper and an interface (electrode).

A monolayer of the rotaxane $\mathbf{50}^{4+}$ (Fig. 42), consisting of the electron accepting cyclophane $\mathbf{4}^{4+}$ threaded on a molecular axle that includes an electron donating diiminobenzene unit and is stoppered by an adamantane moiety, was assembled on a gold electrode (181).

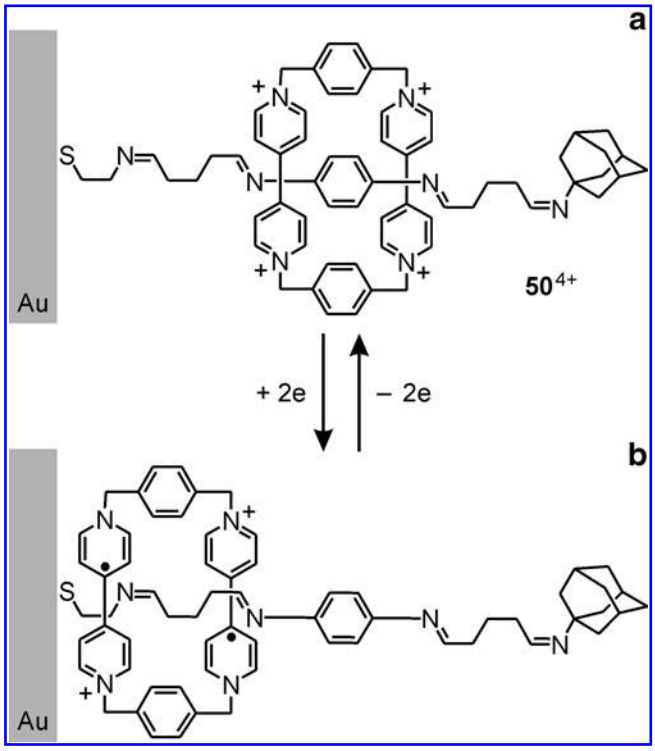

FIG. 42. The electrochemically driven ring shuttling of rotaxane 50^{4+} incorporated into a self-assembled monolayer on a gold electrode. Reproduced by permission of the Royal Society of Chemistry from Silvi *et al*. (268).

The tetracationic ring, which is originally located on the diiminobenzene unit (Fig. 42a) by virtue of electron donor–acceptor interactions, is displaced toward the electrode upon one-electron reduction of its two bipyridinium units at −0.53 V relative to the SCE, owing to disruption of the donor–acceptor interactions and electrostatic attraction to the electrode (Fig. 42b). Reoxidation of the reduced cyclophane at −0.33 V causes ring shuttling to the original diiminobenzene site.

The position of the tetracationic and dicationic (reduced) cyclophane rings and the shuttling rate constants (80 and 320 s^{-1} at 298 K for reduction- and reoxidation-induced processes, respectively) were determined by chronoamperometry and impedance measurements. Investigation of the temperature dependence of the shuttling rates showed (180) that the reduction-induced shuttling is an energetically downhill process with no measurable activation barrier, whereas reoxidation-induced shuttling requires thermal activation. The lack of an energy barrier in the former case is in agreement with the fact that the shuttling is mainly driven by coulombic attraction of the still positively charged cyclophane toward the negatively polarized electrode. Therefore, ring shuttling does not need assistance by thermal energy, in contrast with the typical operation of molecular motors.

Another clever approach involves the immobilization of bistable molecular shuttles containing a pyridine residue in the macrocyclic component onto an Au-SAM of 11-mercaptoundecanoic acid (96, 139). The grafting is achieved because of the formation of hydrogen bonds between the pyridine unit of the rotaxane molecules and the carboxylic groups at the top of the SAM. Electrochemically driven shuttling in one of these systems was recently shown to occur on the millisecond time scale by chronoamperometry (139). The redox-controlled mechanical switching in SAMs of disulfide-functionalized bistable TTF-DON rotaxanes analogous to 49^{4+} (Fig. 41a) was also extensively investigated (281, 292).

Surface-mounted molecular rotary motors are also extremely interesting from a basic viewpoint (194). They could also find applications in a variety of molecular-size devices and machines, for example, in the fields of nanoelectronic, nanophotonics and nanofluidics (287). Two different types of surface-mounted molecular rotors can be distinguished. In an azimuthal rotor (Fig. 43a), the axis of rotation is perpendicular to the surface, whereas in an altitudinal rotor (Fig. 43b), it is parallel to the surface.

A family of molecular rotors (*e.g.*, compound **51** in Fig. 44a) has been designed to perform rotation under electrochemical stimulation (93, 244, 286). The molecules have a piano-stool structure with a stator meant to be grafted on an oxide surface and a rotor bearing redox-active groups, so that addressing the molecule with nano-electrodes would trigger rotation (Fig. 44b). To avoid intramolecular electron transfer between two electro-active units, which would compete with rotation, insulating spacers based on platinum acetylide units were inserted into the structure, but several difficulties remain to be overcome.

In the frame of these studies on molecular machines working on surfaces and at interfaces, the development of systems capable of mimicking at molecular level the function of a macroscopic valve (section "1. Nanovalves") and the possibility of obtaining an amplification of the molecular motion at larger scale (section "2. Microcantilever bending by molecular muscles").

1. Nanovalves. A macroscopic valve is a machine constructed by combining a controllable component that regulates the flow of gases or liquids with a reservoir that can also serve as a supporting platform for the movable element.

Construction of such a device at the molecular scale requires the integration of a stable and inert nanocontainer with an appropriate moving part that can act as a gatekeeper to regulate the molecular transport in to and out of the container. The construction of functioning nanovalves (19, 192) can be useful for controlling drug delivery, signal transduction, nanofluidic systems, and sensors.

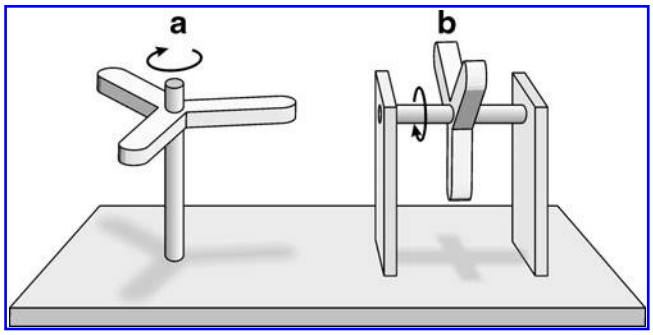

FIG. 43. Azimuthal (a) and altitudinal (b) surface-mounted molecular rotors. Copyright Wiley-VCH Verlag GmbH & Co. KGaA. Reproduced with permission from Balzani *et al*. (64).

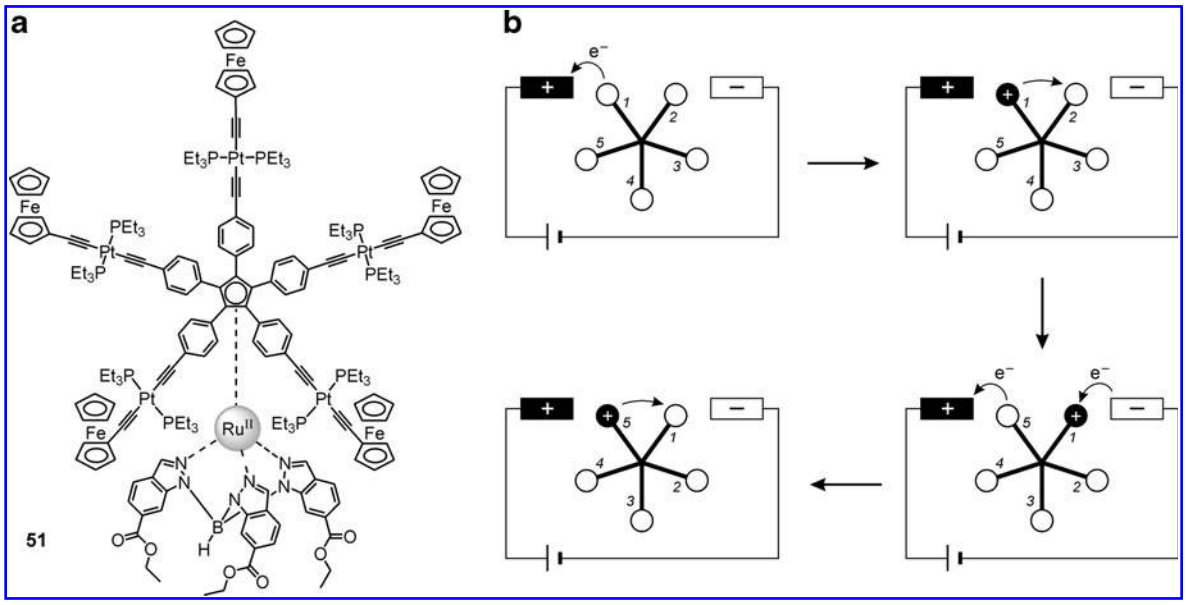

FIG. 44. A molecular rotor designed to perform rotation under electrochemical stimulation in a nanoelectrode junction. (a) Structural formula of molecular rotor **51**. **(b)** Schematic representation of the proposed operation mechanism. A potential difference applied across the nanojunction results in oxidation of the ferrocene group nearest the anode, which is then electrostatically repelled away towards the cathode. The oxidized unit close to the cathode is reduced while a new ferrocene unit is oxidized at the anode. Overall, the passage of each electron across the nanojunction results in the clockwise rotation of the upper part of the molecule by one-fifth of a turn. Copyright Wiley-VCH Verlag GmbH & Co. KGaA. Reproduced with permission from Balzani *et al.* (64).

A recently investigated approach is based on the use of the mechanical motion of molecular shuttles to regulate the access to nanocontainers (224–226, 235, 254). A redox switchable TTF-DON bistable rotaxane structurally similar to $\mathbf{49}^{4+}$ (Fig. 41a) was covalently attached to mesoporous silica nanoparticles. As shown schematically in Figure 45, the silica nanopores can be closed and opened by moving the mechanically interlocked ring component of the rotaxane closer to and away from the pores' orifices, respectively (226). When the ring sits on the preferred TTF station, access to the interior of the nanoparticles is unrestricted and diffusion of the solute (a luminescent iridium complex) from the surrounding solution can occur.

Chemically induced oxidation of the TTF unit results in a shuttling of the ring closer to the solid surface, thereby blocking the access to the pores and trapping any solute molecule inside. Back reduction of the TTF unit reverses the mechanical motion, thus releasing the guest molecules and returning the system to its initial state.

More recently, it has been shown that the properties of these rotaxane-based valves can be fine tuned by changing the length of the linkers between the surface and the rotaxane molecules and the location of the movable components on the nanoparticles (225).

pH-Driven (224) and enzyme-responsive (235) nanovalves have also been constructed.

2. Microcantilever bending by molecular muscles. An exciting development in the field of molecular machines has been the construction of molecular muscles based on rotaxane dimer topology that can undergo contraction and stretching movements in solution (123, 174, 299). Cumulative nanoscale movements within surface-bound molecular muscles based on rotaxanes have been harnessed to perfom large-scale mechanical work.

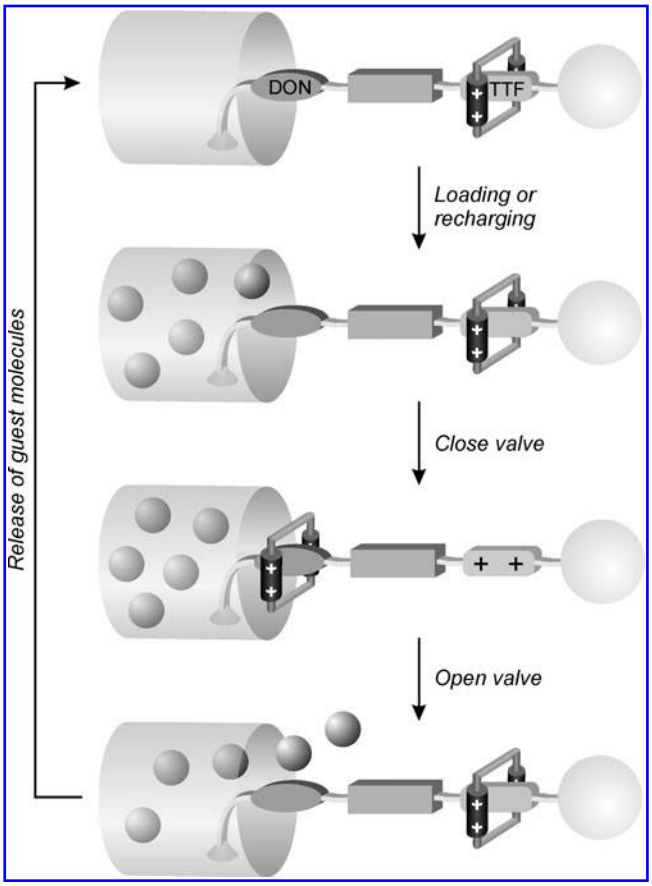

FIG. 45. Operation scheme of a molecular valve based on redox-switchable rotaxanes attached to silica nanopores. Reproduced by permission of the Royal Society of Chemistry from Silvi *et al.* (268).

The investigated system (161, 204) consists of the palindromic bistable rotaxane **52**$^{8+}$ with two rings and four stations, namely, two TTF and two oxynaphthalene moieties (Fig. 46). Tethers attached to each ring anchor the whole rotaxane system as a SAM to a gold surface deposited on silicon microcantilever beams.

Each microcantilever ($500\times100\times1\ \mu$m) is covered with approximately 6 billions of randomly oriented rotaxane molecules. The setup was then inserted into a fluid cell.

Oxidation of the ring-preferred TTF station with iron(III) perchlorate results in shuttling of the two rings onto the oxynaphthalene stations, significantly shortening the interring separation (from 4.2 to 1.4 nm). This change in the interring distance induces a tensile stress on the gold surface of the microcantilever, which causes an upward bending of the beam by about 35 nm. Under the same conditions a monolayer of the dumbbell alone is inactive. Back reduction of the TTF station with ascorbic acid returns the cantilever to its original position. The process can be repeated over several cycles, though with gradually decreasing amplitude. Indeed, this important experiment demonstrates the possibility of harnessing cumulative nanoscale movements within surface-bound molecular shuttles to perform larger-scale mechanical work (131, 137, 238).

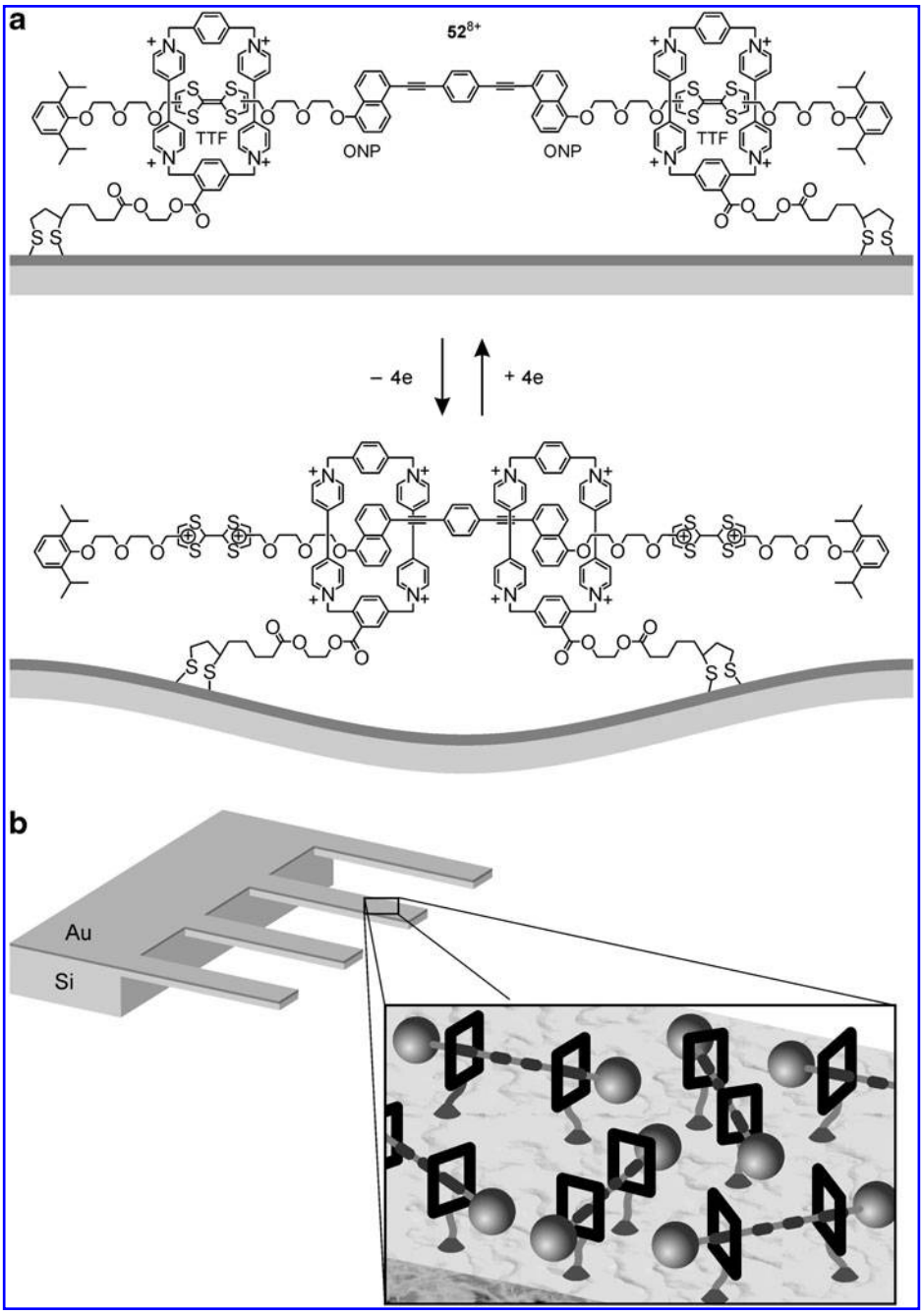

FIG. 46. (a) A molecular muscle based on a self-assembled monolayer of the palindromic rotaxane 52^{8+} (b) anchored on the gold-covered surface of silicon microcantilever beams. Reproduced by permission of the Royal Society of Chemistry from Silvi *et al*. (268).

B. Molecule-based solid-state electronic circuits

The results reported above encouraged attempts to incorporate rotaxanes and catenanes in electrically addressable solid-state devices. In a first study (108, 298), the V-shaped rotaxanes $\mathbf{53}^{4+}$ and $\mathbf{54}^{4+}$ (Fig. 47) were used in the form of molecular monolayers sandwiched between lithographically fabricated metal wires. The switches were read by monitoring current flow at reducing voltages. In the closed state, current flow was dominated by resonant tunneling through the electronic states of the molecules. The switches were irreversibly opened by applying an oxidizing voltage across the device. The V-shaped dumbbell component of the rotaxanes exhibits similar properties. The results obtained showed that these systems behave as singly configurable logic gates.

More interesting observations were made on incorporation of the bistable catenane $\mathbf{39}^{4+}$ (Figs. 33 and 48) into a solid-state device (106, 107). A monolayer of the catenane (Fig. 48b) was transferred onto a photolithographically patterned polycrystalline silicon electrode. The patterning was such that the Langmuir film was deposited along several parallel lines of poly-Si on the electrode. A second set of orthogonally oriented wires was then deposited on top of the first set such that a crossbar architecture is obtained. This second set of electrodes consisted of a 5-nm thick layer of Ti, followed by a 100-nm thick layer of Al. The bottom poly-Si electrode of the molecular sandwich was 7 μm wide and the top Ti/Al electrode 10 μm wide. By this approach, an array of junctions, each one addressable individually, was constructed (Fig. 48c).

The mechanism for conduction is by electron tunneling through the single-molecule thick layer between the junction electrodes. Thus, any change in the electronic characteristics of the interelectrode medium is expected to affect the tunneling efficiency and change the resistance of the junction. Such devices are conductors, not capacitors. Experiments were carried out by applying a series of voltage pulses (between +2.0 and −2.0 V) and reading, after each pulse, current through the device at 200 mV, a potential that does not affect switching (Fig. 49a). The current(read)–voltage(write) curve displays a highly histeretic profile (Fig. 49b), making the catenane junction device interesting for potential use in random access memory storage.

The current–voltage curve was interpreted on the basis of the mechanism illustrated in Figure 50a, which is derived from the behavior of the same catenane $\mathbf{39}^{4+}$ in solution (28, 68, 95). Conformation I is the switch open state and conformation IV the switch closed state of the device. When $\mathbf{39}^{4+}$ is oxidized (+2 V), the TTF unit is ionized in state II and experiences a coulombic repulsion inside the tetracationic cyclophane component, resulting in circumrotation of the crown ether and formation of conformation III; note that in solution at +2 V TTF undergoes two-electron oxidation and the DON unit is also oxidized (28, 68).

When the voltage is reduced to near-zero bias, a metastable conformation IV is obtained, which, however, does not return to conformation I. The initial conformation can in fact be restored only *via* states V and VI in which the bipyridinium units of the cyclophane component are reduced; note that in solution, at the potential value used, −2 V, the bipyridinium units undergo two-electron reduction (28). Most likely, the reduction of the bipyridinium units weakens the CT interaction with the DON unit, thereby decreasing the barrier for its escape from the cyclophane cavity. The same behavior was

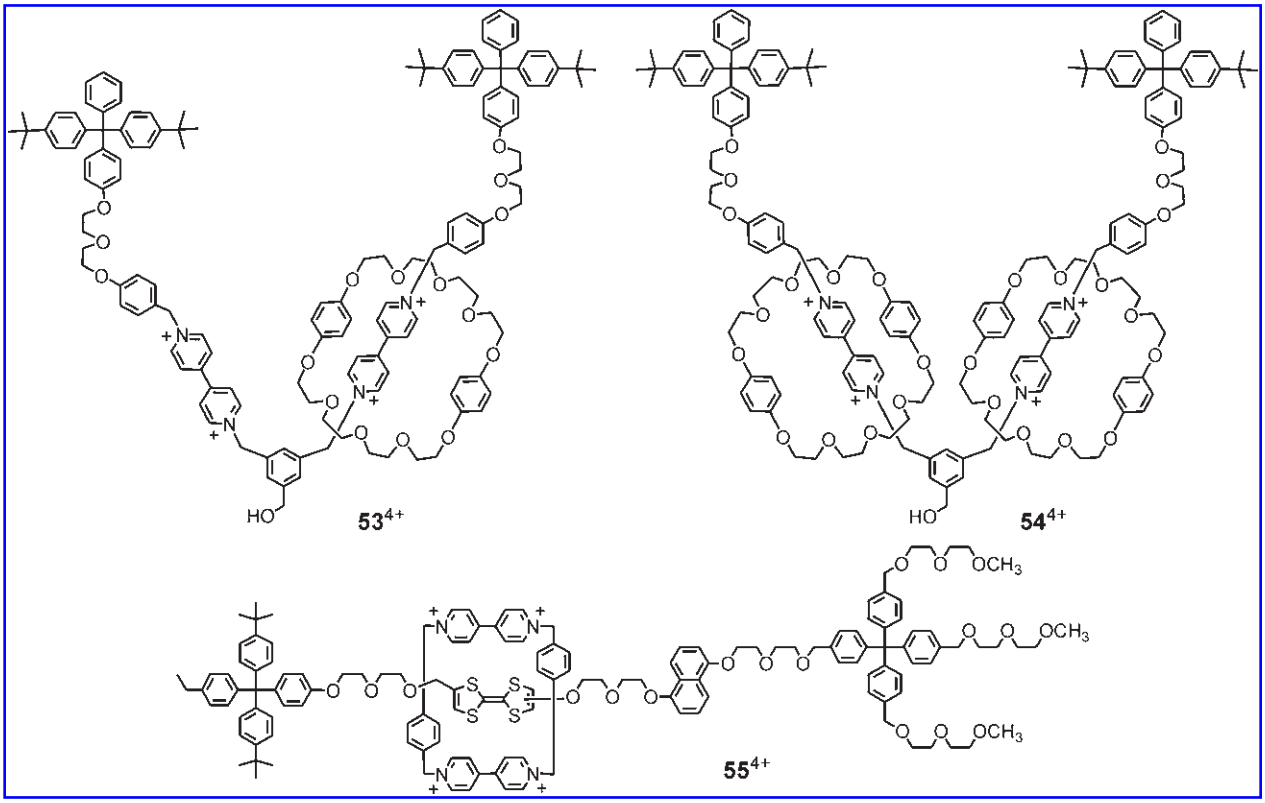

FIG. 47. Structure formulas of V-shaped rotaxanes $\mathbf{53}^{4+}$ and $\mathbf{54}^{4+}$, and bistable rotaxane $\mathbf{55}^{4+}$, used to construct switchable electronic junctions for memory and logic function purposes.

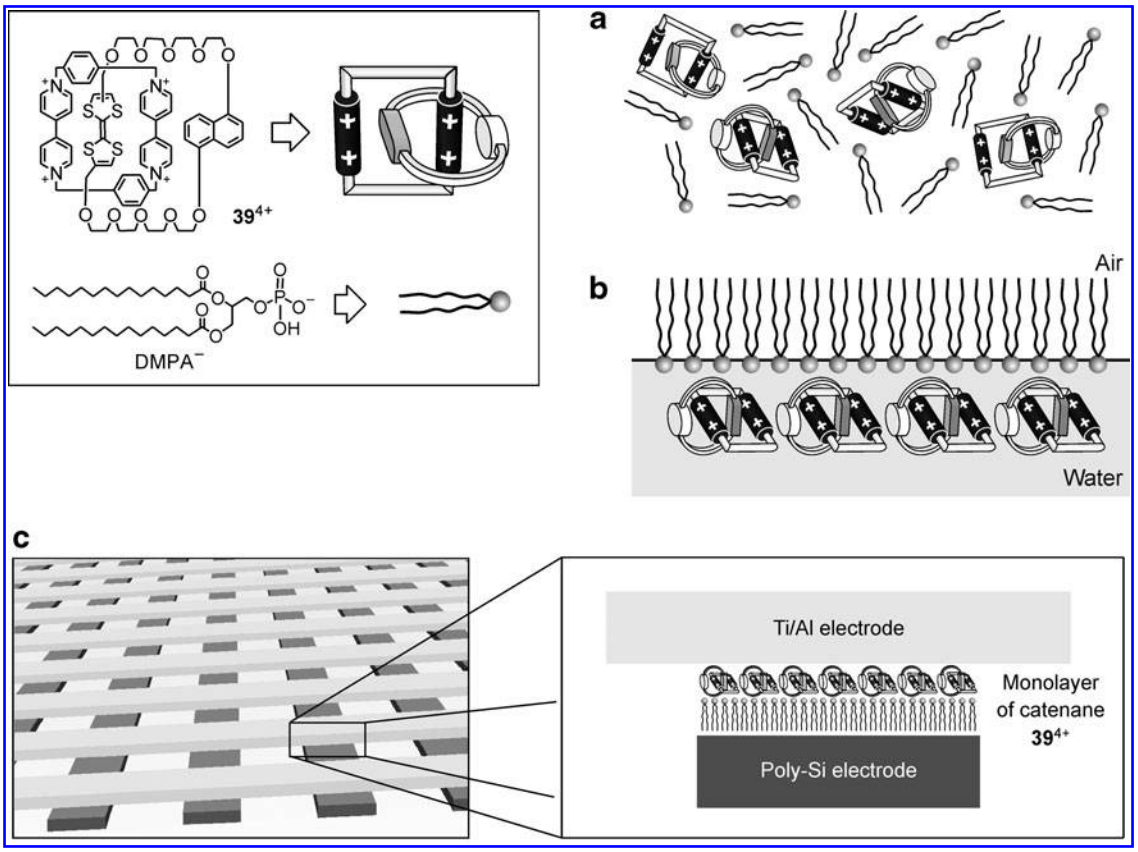

FIG. 48. Introduction of functional catenanes into solid-state devices. (a) Disordered state in solution and **(b)** ordered monolayer of catenane $[\mathbf{39}^{4+}][\text{DMPA}^-]_4$ ($\text{DMPA}^- =$ dimyristoylphosphatidyl anion). **(c)** Schematic representation of a solid-state device based on junctions consisting of the monolayer of catenane $[\mathbf{17}^{4+}][\text{DMPA}^-]_4$ sandwiched between polysilicon and Ti/Al electrodes in a crossbar arrangement.

observed for solid-state devices containing TTF-based bistable rotaxanes such as $\mathbf{49}^{4+}$ and $\mathbf{55}^{4+}$ (Figs. 41a and 47, respectively) (102, 210, 236, 237, 274), and interpreted on the basis of an analogous mechanism (Fig. 50b).

Because these results and their interpretation gave rise to some controversy (101, 158, 264, 265, 293), intensive efforts were undertaken to characterize the mechanical rearrangement associated with redox switching in bistable catenanes like $\mathbf{39}^{4+}$ and related bistable rotaxanes (164, 172, 233, 279, 280), as well as their structural organization in monolayers (125, 167, 168, 231) and the molecule–electrode interface (125, 127, 305). The metastable state corresponding to conformation IV (Fig. 50) was in fact observed for a number of different bistable rotaxanes and catenanes in a variety of environments (solution, SAM, solid-state polymer matrix) (103, 140, 232, 292). The conductance switching in these systems was also extensively investigated by theoretical calculations (169, 188–190). Further, the color change associated with the redox-driven switching of TTF-based bistable catenanes and rotaxanes in a polymer matrix can be exploited to make solid-state electrochromic devices (273).

Recently, by use of the same paradigms described above, a molecular electronic memory with an amazingly high density of 10^{11} bits cm^{-2} was constructed by sandwiching

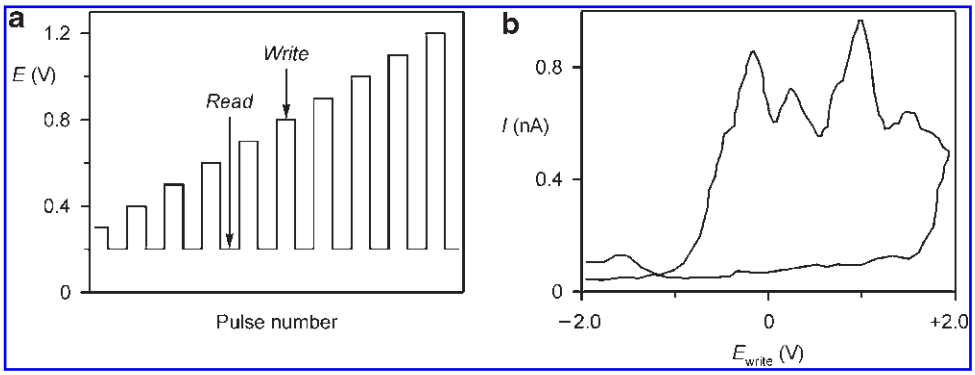

FIG. 49. Current-potential characteristics of the catenane-based solid-state devices. (**a**) A perturbing (write) potential is applied across the device, the state of which is then observed by measuring the current flow at the (read) potential of 200 mV. (**b**) Plot of the read current as a function of the write voltage for the device based on catenane $\mathbf{39}^{4+}$. Copyright Wiley-VCH Verlag GmbH & Co. KGaA. Reproduced with permission from Balzani *et al.* (64).

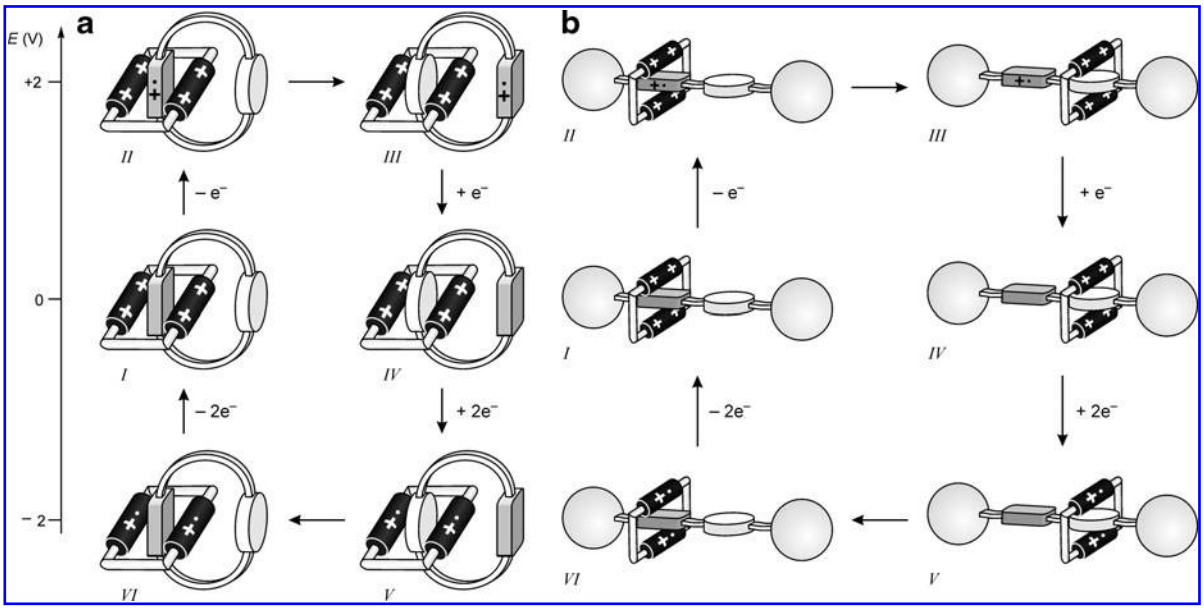

FIG. 50. Proposed molecular-level mechanism for the operation of solid-state electronic devices based on (a) catenanes like 39^{4+} and (b) rotaxanes like 49^{4+} (Fig. 41a) and 55^{4+} (Fig. 47). Copyright Wiley-VCH Verlag GmbH & Co. KGaA. Reproduced with permission from Balzani *et al*. (64).

a monolayer of the bistable rotaxane $\mathbf{49}^{4+}$ (Fig. 41a) between arrays of nanoelectrodes in a crossbar arrangement (152). The realization of this device relies on a novel method for producing ultra-dense, highly aligned arrays and crossbars of metal or semiconductor nanowires with high aspect ratios (215). It was estimated that each junction acting as a memory element consists of ~100 rotaxane molecules. For practical reasons, only 128 (16×8 contacts) of the 160,000 memory cells (400×400 nanowires) contained in the circuit were tested (152). The measurements showed that 25% of the tested cells displayed good and reproducible switching, whereas 35% failed because of bad contacts or shorts, and the remaining 40% showed poor switching. This work is a compelling demonstration that the combination of top-down and bottom-up nanofabrication methods can lead to outstanding technological achievements. However, several aspects—such as stability, reliability, and ease of fabrication—need to be optimized before these systems can find real industrial applications (48).

VII. Conclusions and Perspectives

The results described show that molecular devices and machines can be obtained by utilizing careful incremental design strategies, the tools of modern synthetic chemistry, and the paradigms of supramolecular chemistry, together with some inspiration from natural systems. They also show that the redox-driven machines and the redox switchable devices, like those illustrated in this section, exhibit peculiar and interesting feature. They can indeed work by exploiting light (through photoinduced electron-transfer processes) and electrical energy (through electrochemically induced redox processes) that offer several advantages in comparison with chemical energy inputs. In particular, photons and electrons power molecular devices and machines without formation of waste products and photochemical and electrochemical techniques are also useful to read the state of the system monitoring in this way its operation.

For such systems, and in general for molecular devices and machines, it is possible to devise future developments, which are under investigation in our and other laboratories, namely, (i) the design and construction of more sophisticated artificial molecular motors and machines, showing complex motions and better performances in terms of stability, speed, switching, and so forth; (ii) the use of such systems to do molecular-level tasks such as uptake-release, transportation, catalysis, and mechanical gating of molecular channels; and (iii) the possibility of exploiting their logic behavior for information processing. In this regard, a chemical approach to molecular logic gives the opportunity of implementing even complex logic operations with one molecule or supramolecular species. It is difficult, at the present stage, to predict which one of these two strategies will have the greater technological impact, if any. These and other questions regarding the advent of molecular computers (*e.g.*, serial or parallel architectures, solid-state, or soft matter) represent one of the big challenges of nanotechnology.

The results described in the section also evidence that, although investigations of molecular devices and machines in solution are of fundamental importance, for any kind of applications in the field of technology they have to be interfaced with the macroscopic world by ordering them in some way so that they can behave coherently and can be addressed in space. Viable possibilities include deposition on surfaces, incorporation into polymers, organization at interfaces, or immobilization into membranes or porous materials.

The recent achievements in this direction, some of which have been reviewed here, seem to indicate that useful materials and devices based on artificial molecular machines will see the light in a not too distant future. For example, the construction of artificial muscles based on polymeric materials capable of amplifying contraction–extension nanoscale motions is a task that can nowadays be undertaken. Molecular shuttles could also be employed for sensing and processing chemical information (200), and as components of electrochromic materials

(273). Other stimulating challenges involve the use of molecular machines for directing flows in microfluidic networks (47), operating drug delivery systems (19, 192, 254), transporting and sorting nanoobjects (284), and controlling chemical (240) and biochemical (294) processes. To this aim, collaborative efforts from experts in different disciplines such as chemistry, physics, materials science, and engineering—and possibly biology and medicine—are mandatory. Certainly, many problems related to the complex synthesis and operation of these systems, together with issues such as stability and reproducibility, remain to be solved (49).

Apart from foreseeable applications related to the development of nanotechnology (283), investigations on molecular machines in heterogeneous environments are important to increase the basic understanding of the processes that determine the behavior of nanoscale objects, as well as to develop reliable theoretical models. This research has also the important merit of stimulating the ingenuity of chemists. Looking at molecular and supramolecular species from the viewpoint of functions with references to devices of the macroscopic world is indeed a very interesting exercise that introduces novel concepts into Chemistry as a scientific discipline.

References

1. Affeld A, Hübner GM, Seel C, and Schalley CA. Rotaxane or pseudorotaxane? Effects of small structural variations on the deslipping kinetics of rotaxanes with stopper groups of intermediate size. *Eur J Org Chem*: 2877–2890, 2001.
2. Allara DL. A perspective on surfaces and interfaces. *Nature* 437: 638–639, 2005.
3. Altieri A, Gatti FG, Kay ER, Leigh DA, Martel D, Paolucci F, Slawin AMZ, and Wong JKY. Electrochemically switchable hydrogen-bonded molecular shuttles. *J Am Chem Soc* 125: 8644–8654, 2003.
4. Amabilino DB and Stoddart JF. Interlocked and intertwined structures and superstructures. *Chem Rev* 95: 2725–2828, 1995.
5. Amabilino DB, Asakawa M, Ashton PR, Ballardini R, Balzani V, Belohradsky M, Credi A, Highuci M, Raymo FM, Shimizu T, Stoddart JF, Venturi M, and Yase K. Aggregation of self-assembling branched [n]rotaxanes. *New J Chem* 22: 959–972, 1998.
6. Amendola V, Colasson B, Fabbrizzi L, and Rodriguez Douton MJ. Redox-driven intramolecular anion translocation between a metal centre and a hydrogen-bond-donating compartment. *Chem Eur J* 13: 4988–4997, 2007.
7. Amendola V, Esteban-Gomez D, Fabbrizzi L, and Licchelli M. What anions do to N-H-containing receptors. *Acc Chem Res* 39: 343–353, 2006.
8. Amendola V, Fabbrizzi L, and Pallavicini P. Controlling the assembling/disassembling process of metal-containing superstructures. *Coord Chem Rev* 216: 435–448, 2001.
9. Amendola V, Fabbrizzi L, Gianelli L, Maggi C, Mangano C, Pallavicini P, and Zema M. Electrochemical assembling/disassembling of helicates with hysteresis. *Inorg Chem* 40: 3579–3587, 2001.
10. Amendola V, Fabbrizzi L, Linati L, Mangano C, Pallavicini P, Pedrazzini V, and Zema M. Electrochemically controlled assembling/disassembling processes with a bis-imine bisquinoline ligand and the Cu-II/Cu-I couple. *Chem Eur J* 5: 3679–3688, 1999.
11. Amendola V, Fabbrizzi L, Mangano C, and Pallavicini P. Molecular machines based on metal ion translocation. *Acc Chem Res* 34: 488–493, 2001.
12. Amendola V, Fabbrizzi L, Mangano C, Pallavicini P, Roboli E, and Zema M. M and P double helical complexes of copper(I) with bis-imino bis-quinoline enantiomerically pure chiral ligands. *Inorg Chem* 39: 5803–5806, 2000.
13. Amendola V, Fabbrizzi L, Mundum E, and Pallavicini P. Formation of a dicopper(I) helicate by oxidative dehydrogenation of a monomeric copper(II) polyamine complex. *Dalton Trans*: 773–774, 2003.
14. Amendola V, Fabbrizzi L, Pallavicini P, Sartirana E, and Taglietti A. Monitoring the redox-driven assembly/disassembly of a dicopper(I) helicate with an auxiliary fluorescent probe. *Inorg Chem* 42: 1632–1636, 2003.
15. Amouyal E. Photochemical production of hydrogen and oxygen from water—A review and state-of-the-art. *Sol Energy Mater Sol Cells* 38: 249–276, 1995.
16. Anelli PL, Asakawa M, Ashton PR, Bissell RA, Clavier G, Górski R, Kaifer AE, Langford SJ, Mattersteig G, Menzer S, Philp D, Slawin AMZ, Spencer N, Stoddart JF, Tolley MS, and Williams DJ. Toward controllable molecular shuttles. *Chem Eur J* 3: 1113–1135, 1997.
17. Anelli PL, Ashton PR, Ballardini R, Balzani V, Delgado M, Gandolfi MT, Goodnow TT, Kaifer AE, Philp D, Pietraszkiewicz M, Prodi L, Reddington MV, Slawin AMZ, Spencer N, Stoddart JF, Vicent C, and Williams DJ. Molecular meccano. 1. [2]Rotaxanes and a [2]catenane made to order. *J Am Chem Soc* 114: 193–218, 1992.
18. Anelli PL, Spencer N, and Stoddart JF. A molecular shuttle. *J Am Chem Soc* 113: 5131–5133, 1991.
19. Angelos S, Choi E, Vögtle F, De Cola L, and Zink JI. Photodriven expulsion of molecules from mesostructured silica nanoparticles. *J Phys Chem C* 111: 6589–6592, 2007.
20. Arduini A, Calzavacca F, Pochini A, and Secchi A. Unidirectional threading of triphenylureidocalix[6]arene-based wheels: oriented pseudorotaxane synthesis. *Chem Eur J* 9: 793–799, 2003.
21. Arduini A, Ferdani R, Pochini A, Secchi A, and Ugozzoli F. Calix[6]arene as a wheel for rotaxane synthesis. *Angew Chem Int Ed* 39: 3453–3457, 2000.
22. Aricó F, Badjic JD, Cantrill SJ, Flood AH, Leung KCF, Liu Y, and Stoddart JF. Templated synthesis of interlocked molecules. *Top Curr Chem* 249: 203–259, 2005.
23. Armaroli N and Balzani V. The future of energy supply: challenges and opportunities. *Angew Chem Int Ed* 46: 52–66, 2007.
24. Armaroli N, Balzani V, Collin JP, Gaviña P, Sauvage JP, and Ventura B. Rotaxanes incorporating two different coordinating units in their thread: Synthesis and electrochemically and photochemically induced molecular motions. *J Am Chem Soc* 121: 4397–4408, 1999.
25. Armaroli N, Chambron JC, Collin JP, Dietrich-Buchecker CO, Flamigni L, Kern JM, and Sauvage JP. Electrochemically and photochemically driven ring motions in copper catenanes and rotaxanes. In: *Electron Transfer in Chemistry*, Volume 3, edited by Balzani V. Weinheim, Germany: Wiley-VCH, 2001, pp. 582–616.
26. Asakawa M, Ashton PR, Ballardini R, Balzani V, Belohradsky M, Gandolfi MT, Kocian O, Prodi L, Raymo FM, Stoddart JF, and Venturi M, The slipping approach to self-assembling [n]rotaxanes. *J Am Chem Soc* 119: 302–310, 1997.
27. Asakawa M, Ashton PR, Balzani V, Boyd SE, Credi A, Mattersteig G, Menzer S, Montalti M, Raymo FM, Ruffilli C,

Stoddart JF, Venturi M, and Williams DJ. Molecular meccano, 49- Pseudorotaxanes and catenanes containing a redox-active unit derived from tetrathiafulvalene. *Eur J Org Chem*: 985–994, 1999.
28. Asakawa M, Ashton PR, Balzani V, Credi A, Hamers C, Mattersteig G, Montalti M, Shipway AN, Spencer N, Stoddart JF, Tolley MS, Venturi M, White AJP, and Williams DJ. A chemically and electrochemically switchable [2]catenane incorporating a tetrathiafulvalene unit. *Angew Chem Int Ed* 37: 333–337, 1998.
29. Asakawa M, Ashton PR, Balzani V, Credi A, Mattersteig G, Matthews OA, Montalti M, Spencer N, Stoddart JF, and Venturi M. Electrochemically induced molecular motions in pseudorotaxanes: a case of dual-mode (oxidative and reductive) dethreading. *Chem Eur J* 3: 1992–1996, 1997.
30. Asakawa M, Higuchi M, Mattersteig G, Nakamura T, Pease AR, Raymo FM, Shimidzu T, and Stoddart JF. Current/voltage characteristics of monolayers of redox-switchable [2]catenanes on gold. *Adv Mater* 12: 1099–1102, 2000 and references therein.
31. Ashton PR, Baldoni V, Balzani V, Credi A, Hoffmann HDA, Martinez-Diaz MV, Raymo FM, Stoddart JF, and Venturi M. Dual-mode "co-conformational" switching in catenanes incorporating bipyridinium and dialkylammonium recognition sites. *Chem Eur J* 7: 3482–3493, 2001.
32. Ashton PR, Ballardini R, Balzani V, Baxter I, Credi A, Fyfe MCT, Gandolfi MT, Gómez-López M, Martínez-Díaz MV, Piersanti A, Spencer N, Stoddart JF, Venturi M, White AJP, and Williams DJ. Acid-base controllable molecular shuttles. *J Am Chem Soc* 120: 11932–11942, 1998.
33. Ashton PR, Ballardini R, Balzani V, Boyd SE, Credi A, Gandolfi MT, Gómez-López M, Iqbal S, Philp D, Preece JA, Prodi L, Ricketts HG, Stoddart JF, Tolley MS, Venturi M, White AJP, and Williams DJ. Simple mechanical molecular and supramolecular machines: photochemical and electrochemical control of switching processes. *Chem Eur J* 3: 152–170, 1997.
34. Ashton PR, Ballardini R, Balzani V, Constable EC, Credi A, Kocian O, Langford SJ, Preece JA, Prodi L, Schofield ER, Spencer N, Stoddart JF, and Wenger S. Ru-II polypyridine complexes covalently linked to electron acceptors as wires for light-driven pseudorotaxane-type molecular machines. *Chem Eur J* 4: 2413–2422, 1998.
35. Ashton PR, Ballardini R, Balzani V, Credi A, Dress R, Ishow E, Kleverlaan CJ, Kocian O, Preece JA, Spencer N, Stoddart JF, Venturi M, and Wenger S. A photochemically driven molecular-level abacus. *Chem Eur J* 6: 3558–3574, 2000.
36. Ashton PR, Ballardini R, Balzani V, Credi A, Gandolfi MT, Menzer S, Pérez-García L, Prodi L, Stoddart JF, Venturi M, White AJP, and Williams DJ. Molecular meccano.4. The self-assembly of [2]catenanes incorporating photoactive and electroactive pi-extended systems. *J Am Chem Soc* 117: 11171–11197, 1995.
37. Ashton PR, Ballardini R, Balzani V, Gandolfi MT, Marquis DJF, Pérez-García L, Prodi L, Stoddart JF, and Venturi M. The self-assembly of controllable [2]catenanes. *J Chem Soc Chem Commun*: 177–180, 1994.
38. Ashton PR, Balzani V, Becher J, Credi A, Fyfe MCT, Mattersteig G, Menzer S, Nielsen MB, Raymo FM, Stoddart JF, Venturi M, and Williams DJ. A three-pole supramolecular switch. *J Am Chem Soc* 121: 3951–3957, 1999.
39. Ashton PR, Balzani V, Clemente-León M, Colonna B, Credi A, Jayaraman N, Raymo FM, Stoddart JF, and Venturi M. Ferrocene-containing carbohydrate dendrimers. *Chem Eur J* 8: 673–684, 2002.
40. Ashton PR, Balzani V, Credi A, Kocian O, Pasini D, Prodi L, Spencer N, Stoddart JF, Tolley MS, White AJP, and Williams DJ. Cyclophanes and [2]catenanes as ligands for transition metal complexes: Synthesis, structure, absorption spectra, and excited state and electrochemical properties. *Chem Eur J* 4: 590–607, 1998.
41. Ashton PR, Balzani V, Kocian O, Prodi L, Spencer N, and Stoddart JF. A light-fueled "piston cylinder" molecular-level machine. *J Am Chem Soc* 120: 11190–11191, 1998.
42. Ashton PR, Baxter I, Fyfe MCT, Raymo FM, Spencer N, Stoddart JF, White AJP, and Williams DJ. Rotaxane or pseudorotaxane? That is the question! *J Am Chem Soc* 120: 2297–2307, 1998.
43. Ashton PR, Gómez-López M, Iqbal S, Preece JA, and Stoddart JF. A self-complexing macrocycle acting as a chromophoric receptor. *Tetrahedron Lett* 38: 3635–3638, 1997.
44. Ashton PR, Philp D, Spencer N, and Stoddart JF. The self-assembly of [n]pseudorotaxanes. *J Chem Soc Chem Commun*: 1677–1679, 1991.
45. Ashton PR, Philp D, Spencer N, and Stoddart JF. A new design strategy for the self-assembly of molecular shuttles. *J Chem Soc Chem Commun*: 1124–1128, 1992.
46. Atwood JL, Davies JED, Macnicol DD, and Vögtle F. (Eds). *Comprehensive Supramolecular Chemistry*, Volume 3. Oxford: Pergamon Press, 1996.
47. Bachand GD, Rivera SB, Carroll-Portillo A, Hess H, and Bachand M. Active capture and transport of virus particles using a biomolecular motor-driven, nanoscale antibody sandwich assay. *Small* 2: 381–385, 2006.
48. Ball P. A switch in time. *Nature* 445: 362–363, 2007.
49. Ball P. Welcome to the machine. *Chem World* 7: 56–60, 2010.
50. Ballardini R, Balzani V, Credi A, Gandolfi MT, and Venturi M. Artificial molecular-level machines: which energy to make them work? *Acc Chem Res* 34: 445–455, 2001.
51. Ballardini R, Balzani V, Credi A, Gandolfi MT, and Venturi M. Artificial molecular-level machines with [Ru(bpy)3]2 as a "light-fueled motor." *Int J Photoenergy* 3: 63–77, 2001.
52. Ballardini R, Balzani V, Dehaen W, Dell'Erba AE, Raymo FM, Stoddart JF, and Venturi M. Molecular meccano, 56-Anthracene-containing [2]rotaxanes: Synthesis, spectroscopic, and electrochemical properties. *Eur J Org Chem*: 591–602, 2000.
53. Ballardini R, Balzani V, Gandolfi MT, Prodi L, Venturi M, Philp D, Ricketts HG, and Stoddart JF. A photochemically driven molecular machine. *Angew Chem Int Ed Engl* 32: 1301–1303, 1993.
54. Ballardini R, Credi A, Gandolfi MT, Marchioni F, Silvi S, and Venturi M. Using light to induce energy and electron transfer or molecular motions in multicomponent systems. *Photochem Photobiol Sci* 6: 345–356, 2007.
55. Balzani V and Credi A. Artificial molecular-level machines. *Chem Rec* 1: 422–435, 2001.
56. Balzani V, Becher J, Credi A, Nielsen MB, Raymo FM, Stoddart JF, Talarico AM, and Venturi M. Molecular meccano—Part 58. The electrochemically-driven decomplexation/recomplexation of inclusion adducts of ferrocene derivatives with an electron-accepting receptor. *J Org Chem* 65: 1947–1956, 2000.
57. Balzani V, Ceroni P, Credi A, Gómez-Lopez M, Hamers C, Stoddart JF, and Wolf R. Controlled dethreading/rethreading of a scorpion-like pseudorotaxane and a

related macrobicyclic self-complexing system. *New J Chem* 25: 25–31, 2001.
58. Balzani V, Clemente-León M, Credi A, Ferrer B, Venturi M, Flood AH, and Stoddart JF. Autonomous artificial nanomotor powered by sunlight. *Proc Natl Acad Sci USA* 103: 1178–1183, 2006.
59. Balzani V, Clemente-Leon M, Credi A, Semeraro M, Venturi M, Tseng HR, Wegner S, Saha S, and Stoddart JF. A comparison of shuttling mechanisms in two constitutionally isomeric bistable rotaxane-based sunlight-powered nanomotors. *Aust J Chem* 59: 193–206, 2006.
60. Balzani V, Credi A, and Venturi M. Processing energy and signals by molecular and supramolecular systems. *Chem Eur J* 14: 26–39, 2008.
61. Balzani V, Credi A, and Venturi M. Molecular logic circuits. *Chem Phys Chem* 4: 49–59, 2003.
62. Balzani V, Credi A, and Venturi M. Molecular-level devices and machines. In: *Stimulating Concepts in Chemistry*, edited by Shibasaki M, Stoddart JF, and Vögtle F. Weinheim, Germany: Wiley-VCH, 2000, pp. 255–266.
63. Balzani V, Credi A, and Venturi M. Molecular-level devices. In: *Supramolecular Science: Where It Is and Where It Is Going*, edited by Ungaro R and Dalcanale E. Dordrecht, The Netherlands: Kluwer Academic Publishers, 1999, pp. 1–22.
64. Balzani V, Credi A, and Venturi M. *Molecular Devices and Machines—Concepts and Perspectives for the Nanoworld*. Weinheim, Germany: Wiley-VCH, 2008.
65. Balzani V, Credi A, and Venturi M. Molecular devices and machines. *Nanotoday* 2: 18–25, 2007.
66. Balzani V, Credi A, and Venturi M. Controlled disassembling of self-assembling systems: toward artificial molecular-level devices and machines. *Proc Natl Acad Sci USA* 99: 4814–4817, 2002.
67. Balzani V, Credi A, Ferrer B, Silvi S, and Venturi M. Artificial molecular motors and machines: design principles and prototype systems. *Top Curr Chem* 262: 1–27, 2005.
68. Balzani V, Credi A, Mattersteig G, Matthews OA, Raymo FM, Stoddart JF, Venturi M, White AJP, and Williams DJ. Switching of pseudorotaxanes and catenanes incorporating a tetrathiafulvalene unit by redox and chemical inputs. *J Org Chem* 65: 1924–1936, 2000.
69. Balzani V, Credi A, Raymo FM, and Stoddart JF. Artificial molecular machines. *Angew Chem Int Ed* 39: 3348–3391, 2000.
70. Balzani V, Credi A, Silvi S, and Venturi M. Artificial nanomachines based on interlocked molecular species: recent advances. *Chem Soc Rev* 35: 1135–1149, 2006.
71. Balzani V, Gómez-López M, and Stoddart JF. Molecular machines. *Acc Chem Res* 31: 405–414, 1998.
72. Balzani V. Photochemical molecular devices. *Photochem Photobiol Sci* 2: 459–476, 2003.
73. Barth JV, Costantini G, and Kern K. Engineering atomic and molecular nanostructures at surfaces. *Nature* 437: 671–679, 2005.
74. Bath J and Turberfield AJ. DNA Nanomachines. *Nat Nanotech* 2: 275–284, 2007.
75. Baumann F, Livoreil A, Kaim W, and Sauvage JP. Changeover in a multimodal copper(II) catenate as monitored by EPR spectroscopy. *Chem Commun*: 35–36, 1997.
76. Bayly SR, Gray TM, Chmielewski MJ, Davis JJ, and Beer PD. Anion templated surface assembly of a redox-active sensory rotaxane. *Chem Commun* 22: 2234–2236, 2007.
77. Belle C, Pierre JL, and Saint-Aman E. A molecular redox switch via iron translocation in a bicompartmental ligand. *New J Chem* 22: 1399–1402, 1998.
78. Benniston AC, Harriman A, and Lynch VM. Photoactive [2]rotaxanes—structure and photophysical properties of anthracene-stoppered and ferrocene-stoppered [2]rotaxanes. *J Am Chem Soc* 117: 5275–5291, 1995.
79. Benniston AC, Harriman A, and Yufit DS. Artificial phototropism: Reversible photoseparation of self-assembled interlocking conjugates. *Angew Chem Int Ed Engl* 36: 2356–2358, 1997.
80. Benniston AC, Harriman A, Philp D, and Stoddart JF. Charge recombination in cyclophane-derived, intimate radical-ion pairs. *J Am Chem Soc* 115: 5298–5299, 1993.
81. Bernardo AR, Lu T, Córdova E, Zhang L, Gokel GW, and Kaifer AE. Host-guest complexation at the electrode/solution interface—the inclusion of an amphiphilic viologen guest by an amphiphilic calix[6]arene host. *J Chem Soc Chem Commun*: 529–530, 1994.
82. Biscarini F, Cavallini M, Kshirsagar R, Bottari G, Leigh DA, Leon S, and Zerbetto F. Self-organization of nano-lines and dots triggered by a local mechanical stimulus. *Proc Natl Acad Sci USA* 103: 17650–17654, 2006.
83. Bissell RA, Córdova E, Kaifer AE, and Stoddart JF. A chemically and electrochemically switchable molecular shuttle. *Nature* 369: 133–137, 1994.
84. Bonnet S, Collin JP, Koizumi M, Mobian P, and Sauvage JP. Transition-metal-complexed molecular machine prototypes. *Adv Mater* 18: 1239–1250, 2006.
85. Boulas PL, Gómez-Kaifer M, and Echegoyen L. Electrochemistry of supramolecular systems. *Angew Chem Int Ed* 37: 216–247, 1998.
86. Bourgel C, Boyd ASF, Cooke G, Augier de Cremiers H, Duclairoir FMA, and Rotello VM. The first redox controlled hydrogen bonded three-pole switch. *Chem Commun* 19: 1954–1955, 2001.
87. Breault GA, Hunter CA, and Mayers PC. Supramolecular topology. *Tetrahedron* 55: 5265–5293, 1999.
88. Brouwer AM, Frochot C, Gatti FG, Leigh DA, Mottier L, Paolucci F, Roffia S, and Wurpel GWH. Photoinduction of fast, reversible translational motion in a hydrogen-bonded molecular shuttle. *Science* 291: 2124–2128, 2001.
89. Browne WR and Feringa BL. Making molecular machines work. *Nat Nanotech* 1: 25–35, 2006.
90. Bucher C, Moutet JC, Pécaut J, Royal G, Saint-Aman E, and Thomas F. Redox-triggered molecular movement in a multicomponent metal complex in solution and in the solid state. *Inorg Chem* 43: 3777–3779, 2004.
91. Cao D, Amelia M, Klivansky LM, Koshkakaryan G, Khan SI, Semeraro M, Silvi S, Venturi M, Credi A, and Liu Y. Probing donor-acceptor interactions and co-conformational changes in redox active desymmetrized [2]catenanes. *J Am Chem Soc* 132: 1110–1122, 2010.
92. Cárdenas DJ, Livoreil A, and Sauvage JP. Redox control of the ring-gliding motion in a Cu-complexed catenane: a process involving three distinct geometries. *J Am Chem Soc* 118: 11980–11981, 1996.
93. Carella A, Coudret C, Guirado G, Rapenne G, Vives G, and Launay JP. Electron-triggered motions in technomimetic molecules. *Dalton Trans* 2: 177–186, 2007.
94. Castro R, Cuadrado I, Alonso B, Casado CM, Móran M, and Kaifer AE. Multisite inclusion complexation of redox active dendrimer guests. *J Am Chem Soc* 119: 5760–5761, 1997.
95. Ceccarelli M, Mercuri F, Passerone D, and Parrinello M. The microscopic switching mechanism of a [2]catenane. *J Phys Chem B* 109: 17094–17099, 2005.

96. Cecchet F, Rudolf P, Rapino S, Margotti M, Paolucci F, Baggerman J, Brouwer AM, Kay ER, Wong JKY, and Leigh DA. Structural, electrochemical, and photophysical properties of a molecular shuttle attached to an acid-terminated self-assembled monolayer. *J Phys Chem B* 108: 15192–15199, 2004.
97. Ceroni P, Credi A, and Venturi M. (Eds). *Electrochemistry of Functional Supramolecular Systems*. Hoboken, NJ: Wiley. Copyright John Wiley & Sons, 2010.
98. Ceroni P, Leigh DA, Mottier L, Paolucci F, Roffia S, Tetard D, and Zerbetto F. Electrochemically induced dynamics of a benzylic amide [2]catenane. *J Phys Chem B* 103: 10171–10179, 1999.
99. Chambron JC, Dietrich-Buchecker CO, and Sauvage JP. From classical chirality to topologically chiral catenands and knots. *Top Curr Chem* 165: 131–162, 1993.
100. Champin B, Mobian P, and Sauvage JP. Transition metal complexes as molecular machine prototypes. *Chem Soc Rev* 36: 358–366, 2007.
101. Chandross EA. More on molecular electronics. *Science* 303: 1137–1137, 2004.
102. Chen Y, Ohlberg DAA, Li XM, Stewart DR, Williams RS, Jeppesen JO, Nielsen KA, Stoddart JF, Olynick DL, and Anderson E. Nanoscale molecular-switch devices fabricated by imprint lithography. *Appl Phys Lett* 82: 1610–1612, 2003.
103. Choi JW, Flood AH, Steuerman DW, Nygaard S, Braunschweig AB, Moonen NNP, Laursen BW, Luo Y, DeIonno E, Peters AJ, Jeppesen JO, Xu K, Stoddart JF, and Heath JR. Ground-state equilibrium thermodynamics and switching kinetics of bistable [2]rotaxanes switched in solution, polymer gels, and molecular electronic devices. *Chem Eur J* 12: 261–279, 2006.
104. Clemente-León M, Credi A, Martínez-Díaz MV, Mingotaud C, and Stoddart JF. Towards organization of molecular machines at interfaces: Langmuir films and Langmuir-Blodgett multilayers of an acid-base switchable rotaxane. *Adv Mater* 18: 1291–1296, 2006.
105. Coffey T and Krim J. C-60 molecular bearings and the phenomenon of nanomapping. *Phys Rev Lett* 96: art. n. 186104, 2006.
106. Collier CP, Jeppesen JO, Luo Y, Perkins J, Wong EW, Heath JR, and Stoddart JF. Molecular-based electronically switchable tunnel junction devices. *J Am Chem Soc* 123: 12632–12641, 2001.
107. Collier CP, Mattersteig G, Wong EW, Luo Y, Beverly K, Sampaio J, Raymo FM, Stoddart JF, and Heath JR. A [2]catenane-based solid state electronically reconfigurable switch. *Science* 289: 1172–1175, 2000.
108. Collier CP, Wong EW, Belohradsky M, Raymo FM, Stoddart JF, Kuekes PJ, Williams RS, and Heath JR. Electronically configurable molecular-based logic gates. *Science* 285: 391–394, 1999.
109. Collin JP, Dietrich-Buchecker CO, Gaviña P, Jimenez-Molero MC, and Sauvage JP. Shuttles and muscles: linear molecular machines based on transition metals. *Acc Chem Res* 34: 477–487, 2001.
110. Collin JP, Gaviña P, and Sauvage JP. Electrochemically induced molecular motions in copper-complexed threaded systems: from the unstoppered compound to the semi-rotaxane and the fully blocked rotaxane. *New J Chem* 21: 525–528, 1997.
111. Collin JP, Jouvenot D, Koizumi M, and Sauvage JP. A ruthenium(II)-complexed rotaxane whose ring incorporates a 6,6′-diphenyl-2,2′-bipyridine: synthesis and light-driven motions. *Eur J Inorg Chem*: 1850–1855, 2005.
112. Connors KA. The stability of cyclodextrin complexes in solution. *Chem Rev* 97: 1325–1357, 1997.
113. Córdova E, Bissell RA, Spencer N, Ashton PR, Stoddart JF, and Kaifer AE. Novel rotaxanes based on the inclusion complexation of biphenyl guests by cyclobis(paraquat-p-phenylene). *J Org Chem* 58: 6550–6552, 1993.
114. Coutouli-Argyropoulou E, Kelaidopoulou A, Sideris C, and Kokkinidis G. Electrochemical studies of ferrocene derivatives and their complexation by beta-cyclodextrin. *J Electroanal Chem* 477: 130–139, 1999.
115. Cramer F. *Chaos and Order*. Weinheim, Germany: VCH, 1993.
116. Credi A and Tian H. (Eds). *Adv Funct Mater* 17: special issue on Molecular Machines and Switches, 2007, pp. 671–840.
117. Credi A, Dumas S, Silvi S, Venturi M, Arduini A, Pochini A, and Secchi A. Viologen-calix[6]arene pseudorotaxanes. Ion-pair recognition and threading/dethreading molecular motions. *J Org Chem* 69: 5881–5887, 2004.
118. Credi A, Montalti M, Balzani V, Langford SJ, Raymo FM, and Stoddart JF. Simple molecular-level machines. Interchange between different threads in pseudorotaxanes. *New J Chem* 22: 1061–1065, 1998.
119. Credi A. Artificial molecular motors powered by light. *Aust J Chem* 59: 157–169, 2006.
120. Credi A. Photochemical molecular devices based on pseudorotaxanes, rotaxanes, and catenanes. In: *Handbook of Photochemistry and Photobiology*, Volume 3, edited by Abdel-Mottaleb MSA and Nalwa HS. Stevenson Ranch, CA: American Scientific Publishers, 2003, pp. 319–353.
121. Cummins D, Boschloo G, Ryan M, Corr D, Rao SN, and Fitzmaurice D. Ultrafast electrochromic windows based on redox-chromophore modified nanostructured semiconducting and conducting films. *J Phys Chem B* 104, 11449–11459, 2000.
122. David E, Born R, Kaganer E, Joselevich E, Dürr H, and Willner I. Photoinduced electron transfer in supramolecular assemblies composed of one-shell and two-shell dialkoxybenzene-tethered Ru(II)-tris(bipyridine) derivatives and a bipyridinium cyclophane. *J Am Chem Soc* 119: 7778–7790, 1997.
123. Dawson RE, Lincoln SF, and Easton CJ. The foundation of a light driven molecular muscle based on stilbene and alpha-cyclodextrin. *Chem Commun* 34: 3980–3982, 2008.
124. De Santis G, Fabbrizzi L, Iacopino D, Pallavicini P, Perotti A, and Poggi A. Electrochemically switched anion translocation in a multicomponent coordination compound. *Inorg Chem* 36: 827–832, 1997.
125. DeIonno E, Tseng HR, Harvey DD, Stoddart JF, and Heath JR. Infrared spectroscopic characterization of [2]rotaxane molecular switch tunnel junction devices. *J Phys Chem B* 110: 7609–7612, 2006.
126. Devonport W, Blower MA, Bryce MR, and Goldenberg LM. A redox-active tetrathiafulvalene [2]pseudorotaxane: spectroelectrochemical and cyclic voltammetric studies of the highly-reversible complexation/decomplexation process. *J Org Chem* 62: 885–887, 1997.
127. Diehl MR, Steuerman DW, Tseng HR, Vignon SA, Star A, Celestre PC, Stoddart JF, and Heath JR. Single-walled carbon nanotube based molecular switch tunnel junctions. *Chem Phys Chem* 4: 1335–1339, 2003.
128. Drechsler U, Erdogan B, and Rotello VM. Nanoparticles: scaffolds for molecular recognition. *Chem Eur J* 10: 5570–5579, 2004.
129. Durola F and Sauvage JP. Fast electrochemically induced translation of the ring in a copper-complexed [2]rotaxane:

the biisoquinoline effect. *Angew Chem Int Ed* 46: 3537–3540, 2007.
130. Edwards SA. *The Nanotech Pioneers.* Weinheim, Germany: Wiley-VCH, 2006.
131. Eelkema R, Pollard MM, Katsonis N, Vicario J, Broer DJ, and Feringa BL. Rotational reorganization of doped cholesteric liquid crystalline films. *J Am Chem Soc* 128: 14397–14407, 2006.
132. Fabbrizzi L, Gatti F, Pallavicini P, and Zambarbieri E. Redox-driven intramolecular anion translocation between transition metal centres. *Chem Eur J* 5: 682–690, 1999.
133. Fabbrizzi L, Licchelli M, and Pallavicini P. Transition metals as switches. *Acc Chem Res* 32: 846–853, 1999.
134. Fabbrizzi L, Licchelli M, Pallavicini P, and Sacchi D. Supramolecular functions related to the redox activity of transition metals. *Supramol Chem* 13: 569–582, 2001.
135. Feng M, Gao L, Du SX, Deng ZT, Cheng ZH, Ji W, Zhang DQ, Guo XF, Lin X, Chi LF, Zhu DB, Fuchs H, and Gao HJ. Observation of structural and conductance transition of rotaxane molecules at a submolecular scale. *Adv Funct Mater* 17: 770–776, 2007.
136. Feringa BL. (Ed). *Molecular Switches*. Weinheim, Germany: Wiley-VCH, 2001.
137. Ferri V, Elbing M, Pace G, Dickey, Zharnikov M, Samorì P, Mayor M, and Rampi MA. Light-powered electrical switch based on cargo-lifting azobenzene monolayers. *Angew Chem Int Ed* 47: 3407–3409, 2008.
138. Feynman RP. There's plenty of room at the bottom. *Eng Sci* 23: 22–36, 1960. See also: www.feynmanonline.com.
139. Fioravanti G, Haraszkiewicz N, Kay ER, Mendoza SM, Bruno C, Marcaccio M, Wiering PG, Paolucci F, Rudolf P, Brouwer AM, and Leigh DA. Three state redox-active molecular shuttle that switches in solution and on a surface. *J Am Chem Soc* 130: 2593–2601, 2008.
140. Flood AH, Peters AJ, Vignon SA, Steuerman DW, Tseng HR, Kang S, Heath JR, and Stoddart JF. The role of physical environment on molecular electromechanical switching. *Chem Eur J* 10: 6558–6564, 2004.
141. Flood AH, Ramirez RJA, Deng WQ, Muller RP, Goddard WA, and Stoddart JF. Meccano on the nanoscale—a blueprint for making some of the world's tiniest machines. *Aust J Chem* 57: 301–322, 2004.
142. Fujita M, Tominaga M, Hori A, and Therrien B. Coordination assemblies from a Pd(II)-cornered square complex. *Acc Chem Res* 38: 369–378, 2005.
143. Fyfe MCT and Stoddart JF. Synthetic supramolecular chemistry. *Acc Chem Res* 30: 393–401, 1997.
144. Garaudée S, Silvi S, Venturi M, Credi A, Flood AH, and Stoddart JF. Shuttling dynamics in an acid-base-switchable [2]rotaxane. *Chem Phys Chem* 6: 2145–2152, 2005.
145. Gaviña P and Sauvage JP. Transition-metal template synthesis of a rotaxane incorporating two different coordinating units in its thread. *Tetrahedron Lett* 38: 3521–3524, 1997.
146. Gibson HW and Marand H. Polyrotaxanes—molecular composites derived by physical linkage of cyclic and linear species. *Adv Mater* 5: 11–21, 1993.
147. Godínez LA, Patel S, Criss CM, and Kaifer AE. Calorimetric studies on the complexation of several ferrocene derivatives by alpha-cyclodextrin and beta-cyclodextrin—effects of urea on the thermodynamic parameters. *J Phys Chem* 99: 17449–17455, 1995.
148. González B, Casado CM, Alonso B, Cuadrado I, Móran M, Wang Y, and Kaifer AE. Synthesis, electrochemistry and cyclodextrin binding of novel cobaltocenium-functionalized dendrimers. *Chem Commun*: 2569–2570, 1998.
149. Goodsell DS. *Bionanotechnology—Lessons from Nature*. Hoboken, NJ: Wiley, 2004.
150. Gosztola D, Niemczyk MP, Svec W, Lukas AS, and Wasielewski MR. Excited doublet states of electrochemically generated aromatic imide and diimide radical anions. *J Phys Chem A* 104: 6545–6551, 2000.
151. Granqvist CG. Electrochromic materials: out of a niche. *Nat Mater* 5: 89–90, 2006.
152. Green JE, Choi JW, Boukai A, Bunimovich Y, Johnston-Halperin E, Delonno E, Luo Y, Sheriff BA, Xu K, Shin YS, Tseng HR, Stoddart JF, and Heath JR. A 160-kilobit molecular electronic memory patterned at 10(11) bits per square centimetre. *Nature* 445: 414–417, 2007.
153. Grill L, Rieder KH, Moresco F, Stojkovic S, Gourdon A, and Joachim C. Exploring the interatomic forces between tip and single molecules during STM manipulation. *Nano Lett* 6: 2685–2689, 2006.
154. Gunter MJ. Superstructured porphyrins as effectors in dynamic supramolecular assemblies: receptors, rotaxanes and catenanes. *Eur J Org Chem*: 1655–1673, 2004.
155. Guo X, Zhou Y, Feng M, Xu Y, Zhang D, Gao H, Fan Q, and Zhu D. Tetrathiafulvalene-, 1,5-dioxynaphthalene-, and cyclobis(paraquat-p-phenylene)-based [2]rotaxanes with cyclohexyl and alkyl chains as spacers: synthesis, Langmuir-Blodgett films, and electrical bistability. *Adv Funct Mater* 17: 763–769, 2007.
156. Hamilton DG, Davies JE, Prodi L, and Sanders JKM. Synthesis, structure and photophysics of neutral pi-associated [2]catenanes. *Chem Eur J* 4: 608–620, 1998.
157. Harada A. Cyclodextrin-based molecular machines. *Acc Chem Res* 34: 456–464, 2001.
158. Heath JR, Stoddart JF, and Williams RS. More on molecular electronics. *Science* 303: 1136–1137, 2004.
159. Heim C, Affeld A, Nieger M, and Vögtle F. Size complementarity of macrocyclic cavities and stoppers in amide-rotaxanes. *Helv Chim Acta* 82: 746–759, 1999.
160. Hernandez JV, Kay ER, and Leigh DA. A reversible synthetic rotary molecular motor. *Science* 306: 1532–1537, 2004.
161. Huang TJ, Brough B, Ho CM, Liu Y, Flood AH, Bonvallet PA, Tseng HR, Stoddart JF, Ballaer M, and Magonov S. A nanomechanical device based on linear molecular motors. *Appl Phys Lett* 85: 5391–5393, 2004.
162. Huang TJ, Tseng HR, Sha L, Lu W, Brough B, Flood AH, Yu BD, Celestre PC, Chang JP, Stoddart JF, and Ho CM. Mechanical shuttling of linear motor-molecules in condensed phases on solid substrates. *Nano Lett* 4: 2065–2071, 2004.
163. Hübner GM, Natchsheim G, Qian YL, Seel C, and Vögtle F. The spatial demand of dendrimers: deslipping of rotaxanes. *Angew Chem Int Ed* 39: 1269–1272, 2000.
164. Ikeda T, Saha S, Aprahamian I, Leung KCF, Williams A, Deng WQ, Flood AH, Goddard WA III, and Stoddart JF. Toward electrochemically controllable tristable three-station [2]catenanes. *Chem Asian J* 2: 76–93, 2007.
165. ITRS Roadmap for Semiconductors, 2009 Edition. www.itrs.net. Accessed August 2010.
166. Jäger R and Vögtle F. A new synthetic strategy towards molecules with mechanical bonds: nonionic template synthesis of amide-linked catenanes and rotaxanes. *Angew Chem Int Ed Engl* 36: 930–944, 1997.
167. Jang SS, Jang YH, Kim YH, Goddard WA III, Choi JW, Heath JR, Laursen BW, Flood AH, Stoddart JF, Nørgaard K, and

Bjørnholm T. Molecular dynamics simulation of amphiphilic bistable [2]rotaxane Langmuir monolayers at the air/water interface. *J Am Chem Soc* 127: 14804–14816, 2005.
168. Jang SS, Jang YH, Kim YH, Goddard III WA, Flood AH, Laursen BW, Tseng HR, Stoddart JF, Jeppesen JO, Choi JW, Steuerman DW, DeIonno E, and Heath JR. Structures and properties of self-assembled monolayers of bistable [2]rotaxanes on Au(111) surfaces from molecular dynamics simulations validated with experiment. *J Am Chem Soc* 127: 1563–1575, 2005.
169. Jang YH, Hwang SG, Kim YH, Jang SS, and Goddard WA III. Density functional theory studies of the [2]rotaxane component of the Stoddart-Heath molecular switch. *J Am Chem Soc* 126: 12636–12645, 2004.
170. Jeon WS, Kim E, Ko YH, Hwang I, Lee JW, Kim SY, Kim HJ, and Kim K. Molecular loop lock: A redox-driven molecular machine based on a host-stabilized charge-transfer complex. *Angew Chem Int Ed* 44: 87–91, 2005.
171. Jeon WS, Ziganshina AY, Lee JW, Ko YH, Kang JK, Lee C, and Kim K. A [2]pseudorotaxane-based molecular machine: Reversible formation of a molecular loop driven by electrochemical and photochemical stimuli. *Angew Chem Int Ed* 42: 4097–4100, 2003.
172. Jeppesen JO, Nielsen KA, Perkins J, Vignon SA, Di Fabio A, Ballardini R, Gandolfi MT, Venturi M, Balzani V, Becher J, and Stoddart JF. Amphiphilic bistable rotaxanes. *Chem Eur J* 9: 2982–3007, 2003.
173. Jeppesen JO, Perkins J, Becher J, and Stoddart JF. Slow shuttling in an amphiphilic bistable [2]rotaxane incorporating a tetrathiafulvalene unit. *Angew Chem Int Ed* 40: 1216–1219, 2001.
174. Jiménez-Molero MC, Dietrich-Buchecker C, and Sauvage JP. Towards synthetic molecular muscles: contraction and stretching of a linear rotaxane dimer. *Angew Chem Int Ed* 39: 3284–3287, 2000.
175. Johansen O, Mau AWH, and Sasse WHF. The 9-anthracenecarboxylate anion as sensitizer for the photoreduction of water. *Chem Phys Lett* 94: 107–112, 1983.
176. Jones RAL. *Soft Machines—Nanotechnology and Life*. Oxford: OUP, 2005.
177. Juris A, Balzani V, Barigelletti F, Campagna S, Belser P, and von Zelewsky A. Ru(II) polypyridine complexes: photophysics, photochemistry, eletrochemistry, and chemiluminescence. *Coord Chem Rev* 84: 85–277, 1988.
178. Kaifer AE. Interplay between molecular recognition and redox chemistry. *Acc Chem Res* 32: 62–71, 1999.
179. Kaifer AE. *Supramolecular Electrochemistry*. Weinheim, Germany: Wiley-VCH, 1999.
180. Katz E, Baron R, Willner I, Richke N, and Levine RD. Temperature-dependent and friction-controlled electrochemically induced shuttling along molecular strings associated with electrodes. *Chem Phys Chem* 6: 2179–2189, 2005.
181. Katz E, Lioubashevsky O, and Willner I. Electromechanics of a redox-active rotaxane in a monolayer assembly on an electrode. *J Am Chem Soc* 126: 15520–15532, 2004.
182. Kay ER, Leigh DA, and Zerbetto F. Synthetic molecular motors and mechanical machines. *Angew Chem Int Ed* 46: 72–191, 2007.
183. Kelly LA and Rodgers MAJ. Intermolecular and intramolecular oxidative quenching of mixed-ligand tris(bipyridyl)ruthenium(ii) complexes by methyl viologen. *J Phys Chem* 99: 13132–13140, 1995.
184. Kelly TR. (Ed). *Top Curr Chem* 262: special volume on Molecular Machines, 2005, pp. 1–236.
185. Kern JM, Raehm L, Sauvage JP, Divisia-Blohorn B, and Vidal PL. Controlled molecular motions in copper-complexed rotaxanes: an XAS study. *Inorg Chem* 39: 1555–1560, 2000.
186. Kim HJ, Jeon WS, Ko YH, and Kim K. Inclusion of methylviologen in cucurbit[7]uril. *Proc Natl Acad Sci USA* 99: 5007–5011, 2002.
187. Kim K. Mechanically interlocked molecules incorporating cucurbituril and their supramolecular assemblies. *Chem Soc Rev* 31: 96–107, 2002.
188. Kim YH and Goddard WA III. Efficiency of pi-pi tunneling in [2]rotaxane molecular electronic switches. *J Phys Chem C* 111: 4831–4837, 2007.
189. Kim YH, Jang SS, and Goddard WA III. Possible performance improvement in [2]catenane molecular electronic switches. *Appl Phys Lett* 88: art. n. 163112, 2006.
190. Kim YH, Jang SS, Jang YH, and Goddard WA III. First-principles study of the switching mechanism of [2]catenane molecular electronic devices. *Phys Rev Lett* 94: art. n. 156801, 2005.
191. Kinbara K and Aida T. Toward intelligent molecular machines: Directed motions of biological and artificial molecules and assemblies. *Chem Rev* 105: 1377–1400, 2005.
192. Kocer A, Walko M, Meijberg W, and Feringa BL. A light-actuated nanovalve derived from a channel protein. *Science* 309: 755–758, 2005.
193. Korybut-Daszkiewicz B, Wieckowska A, Bielewicz R, Domagala S, and Wozniak K. An electrochemically controlled molecular shuttle. *Angew Chem Int Ed* 43: 1668–1672, 2004.
194. Kottas GS, Clarke LI, Horinek D, and Michl J. Artificial molecular rotors. *Chem Rev* 105: 1281–1376, 2005.
195. Koumura N, Zijlstra RWJ, van Delden RA, Harada N, and Feringa BL. Light-driven monodirectional molecular rotor. *Nature* 401: 152–155, 1999.
196. Kropf M, Joselevich E, Dürr H, and Willner I. Photoinduced electron transfer in supramolecular assemblies composed of alkoxyanisyl-tethered ruthenium(II)-tris(bipyridazine) complexes and a bipyridinium cyclophane electron acceptor. *J Am Chem Soc* 118: 655–665, 1996.
197. Lagona J, Mukhopadhyay P, Chakrabarti S, and Isaacs L. The cucurbit[n]uril family. *Angew Chem Int Ed* 44: 4844–4870, 2005.
198. Lehn JM. *Supramolecular Chemistry: Concepts and Perspectives*. Weinheim, Germany: VCH, 1995.
199. Lehn J-M. Toward complex matter: Supramolecular chemistry and self-organization. *Proc Natl Acad Sci USA* 99: 4763–4768, 2002.
200. Leigh DA, Morales MAF, Pérez EM, Wong JKY, Saiz CG, Slawin AMZ, Carmichael AJ, Haddleton DM, Brouwer AM, Buma WJ, Wurpel GWH, Leon S, and Zerbetto F. Patterning through controlled submolecular motion: rotaxane-based switches and logic gates that function in solution and polymer films. *Angew Chem Int Ed* 44: 3062–3067, 2005.
201. Leigh DA, Troisi A, and Zerbetto F. Reducing molecular shuttling to a single dimension. *Angew Chem Int Ed* 39: 350–353, 2000.
202. Létinois-Halbes U, Hanss D, Beierle JM, Collin JP, and Sauvage JP. A fast-moving [2]rotaxane whose stoppers are remote from the copper complex core. *Org Lett* 7: 5753–5756, 2005.
203. Liscio A, Palermo V, Gentilini D, Nolde F, Müllen K, and Samorì P. Quantitative measurement of the local surface potential of pi-conjugated nanostructures: a Kelvin probe

force microscopy study. *Adv Funct Mater* 16: 1407–1416, 2006.
204. Liu Y, Flood AH, Bonvallet PA, Vignon SA, Northrop BH, Tseng HR, Jeppesen JA, Huang TJ, Brough B, Ballaer M, Magonov S, Solares SD, Goddard WA III, Ho CM, and Stoddart JF. Linear artificial molecular muscles. *J Am Chem Soc* 127: 9745–9759, 2005.
205. Livoreil A, Dietrich-Buchecker CO, and Sauvage JP. Electrochemically triggered swinging of a [2]-catenate. *J Am Chem Soc* 116: 9399–9400, 1994.
206. Livoreil A, Sauvage JP, Armaroli N, Balzani V, Flamigni L, and Ventura B. Electrochemically and photochemically driven ring motions in a disymmetrical copper [2]-catenate. *J Am Chem Soc* 119: 12114–12124, 1997.
207. Lo Nostro P, Lopes JR, Ninham BW, and Baglioni P. Effect of cations and anions on the formation of polypseudorotaxanes. *J Phys Chem B* 106: 2166–2174, 2002.
208. Loeb SJ. Rotaxanes as ligands: from molecules to materials. *Chem Soc Rev* 36: 226–235, 2007.
209. Lu T, Zhang L, Gokel GW, and Kaifer AE. The first surface-attached catenane—self-assembly of a 2-component monolayer. *J Am Chem Soc* 115: 2542–2543, 1993.
210. Luo Y, Collier CP, Jeppesen JO, Nielsen KA, Delonno E, Ho G, Perkins J, Tseng HR, Yamamoto T, Stoddart JF, and Heath JR. Two-dimensional molecular electronics circuits. *Chem Phys Chem* 3: 519–531, 2002.
211. Mann S. Life as a nanoscale phenomenon. *Angew Chem Int Ed* 47: 5306–5320, 2008.
212. Mateo-Alonso A, Guldi DM, Paolucci F, and Prato M. Fullerenes: Multitask components in molecular machinery. *Angew Chem Int Ed* 46: 8120–8126, 2007.
213. McDonagh AM, Bayly SR, Riley DJ, Ward MD, McCleverty JA, Cowin MA, Morgan CN, Varrazza R, Penty RV, and White IH. A variable optical attenuator operating in the near-infrared region based on an electrochromic molybdenum complex. *Chem Mater* 12: 2523–2524, 2000.
214. Mecklenburg SL, Opperman KA, Chen PY, and Meyer TJ. Designed intramolecular competition in a chromophore-biquencher complex. *J Phys Chem* 100: 15145–15151, 1996.
215. Melosh NA, Boukai A, Diana F, Gerardot B, Badolato A, Petroff PM, and Heath JR. Ultrahigh-density nanowire lattices and circuits. *Science* 300: 112–115, 2003.
216. Mirzoian A and Kaifer AE. Electrochemically controlled self-complexation of cyclodextrin-viologen conjugates. *Chem Commun*: 1603–1604, 1999.
217. Mirzoian A and Kaifer AE. Reactive pseudorotaxanes: Inclusion complexation of reduced viologens by the hosts beta-cyclodextrin and heptakis(2,6-di-O-methyl)-beta-cyclodextrin. *Chem Eur J* 3: 1052–1057, 1997.
218. Monk PMS. *The Viologens—Physicochemical Properties, Synthesis and Application of the salts of 4,4′-Bipyridine*. Chichester, United Kingdom: Wiley, 1998.
219. Moon K and Kaifer AE. Dimeric molecular capsules under redox control. *J Am Chem Soc* 126, 15016–15017, 2004.
220. Moon K, Grindstaff J, Sobransingh D, and Kaifer AE. Cucurbit[8]uril-mediated redox-controlled self-assembly of viologen-containing dendrimers. *Angew Chem Int Ed* 43: 5496–5499, 2004.
221. Mortimer RJ. Electrochromic materials. *Chem Soc Rev* 26: 147–156, 1997.
222. Mortimer RJ. Organic electrochromic materials. *Electrochim Acta* 44: 2971–2981, 1999.
223. Nabeshima T, Furusawa H, and Yano Y. Redox control for the recognition of Ag^+ ions in a macrocycle containing 2 SH-groups or an S-S bridge inside the cavity. *Angew Chem Int Ed Engl* 33: 1750–1751, 1994.
224. Nguyen TD, Leug KCF, Liong M, Pentecost CD, Stoddart JF, and Zink JI. Construction of a pH-driven supramolecular nanovalve. *Org Lett* 8: 3363–3366, 2006.
225. Nguyen TD, Liu Y, Saha S, Leug KCF, Stoddart JF, and Zink JI. Design and optimization of molecular nanovalves based on redox-switchable bistable rotaxanes. *J Am Chem Soc* 129: 626–634, 2007.
226. Nguyen TD, Tseng HR, Celestre PC, Flood AH, Liu Y, Stoddart JF, and Zink JI. A reversible molecular valve. *Proc Natl Acad Sci USA* 102: 10029–10034, 2005.
227. Nielsen MB, Hansen JG, and Becher J. Self-complexing tetrathiafulvalene-based donor-acceptor macrocycles. *Eur J Org Chem*: 2807–2815, 1999.
228. Nielsen MB, Nielsen SB, and Becher J. "Self-complexing" tetrathiafulvalene macrocycles; a tetrathiafulvalene switch. *Chem Commun*: 475–476, 1998.
229. Niemz A and Rotello VM. From enzyme to molecular device. Exploring the interdependence of redox and molecular recognition. *Acc Chem Res* 32: 44–52, 1999.
230. Nikitin K, Lestini E, Lazzari M, Altobello S, and Fitzmaurice D. A tripodal [2]rotaxane on the surface of gold. *Langmuir* 23: 12147–12153, 2007.
231. Norgaard K, Jeppesen JO, Laursen BA, Simonsen JB, Weygand MJ, Kjaer K, Stoddart JF, and Bjornholm T. Evidence of strong hydration and significant tilt of amphiphilic [2]rotaxane molecules in langmuir films studied by synchrotron X-ray reflectivity. *J Phys Chem B* 109: 1063–1066, 2005.
232. Norgaard K, Laursen BW, Nygaard S, Kjaer K, Tseng HR, Flood AH, Stoddart JF, and Bjornholm T. Structural evidence of mechanical shuttling in condensed monolayers of bistable rotaxane molecules. *Angew Chem Int Ed* 44: 7035–7039, 2005.
233. Nygaard S, Leung KCF, Aprahamian I, Ikeda T, Saha S, Laursen BW, Kim SY, Hansen SW, Stein PC, Flood AH, Stoddart JF, and Jeppesen JO. Functionally rigid bistable [2]rotaxanes. *J Am Chem Soc* 129: 960–970, 2007.
234. Pallavicini P, Boiocchi M, Dacarro G, and Mangano C. Enhanced kinetic inertness in the electrochemical interconversion of Cu(I) double helical to Cu(II) monomeric complexes. *New J Chem* 31: 927–935, 2007.
235. Patel K, Angelos S, Dichtel WR, Coskun A, Yang YW, Zink JI, and Stoddart JF. Enzyme-responsive snap-top covered silica nanocontainers. *J Am Chem Soc* 130: 2382–2383, 2008.
236. Pease AR and Stoddart JF. Computing at the molecular level. *Struct Bond* 99: 189–236, 2001.
237. Pease AR, Jeppesen JO, Stoddart JF, Luo Y, Collier CP, and Heath JR. Switching devices based on interlocked molecules. *Acc Chem Res* 34: 433–444, 2001.
238. Percec V, Rudick JG, Peterca M, and Heiney PA. Nanomechanical function from self-organizable dendronized helical polyphenylacetylenes. *J Am Chem Soc* 130: 7503–7508, 2008.
239. Petty MC. *Langmuir-Blodgett Films—An Introduction*. Cambridge: Cambridge University Press, 1996.
240. Pijper D and Feringa BL. Molecular transmission: controlling the twist sense of a helical polymer with a single light-driven molecular motor. *Angew Chem Int Ed* 46: 3693–3696, 2007.
241. Pluth MD and Raymond KN. Reversible guest exchange mechanisms in supramolecular host-guest assemblies. *Chem Soc Rev* 36: 161–171, 2007.

242. Poleschak I, Kern JM, and Sauvage JP. A copper-complexed rotaxane in motion: pirouetting of the ring on the millisecond timescale. *Chem Commun* 4: 474–476, 2004.
243. Raehm L, Kern JM, and Sauvage JP. A transition metal containing rotaxane in motion: Electrochemically induced pirouetting of the ring on the threaded dumbbell. *Chem Eur J* 5: 3310–3317, 1999.
244. Rapenne G. Synthesis of technomimetic molecules: towards rotation control in single-molecular machines and motors. *Org Biomol Chem* 3: 1165–1169, 2005.
245. Raymo FM and Stoddart JF. Interlocked macromolecules. *Chem Rev* 99: 1643–1663, 1999.
246. Raymo FM, Houk KN, and Stoddart JF. The mechanism of the slippage approach to rotaxanes. Origin of the "all-or-nothing" substituent effect. *J Am Chem Soc* 120: 9318–9322, 1998.
247. Rekharsky MV and Inoue Y. Complexation and chiral recognition thermodynamics of 6-amino-6-deoxy-beta-cyclodextrin with anionic, cationic, and neutral chiral guests: counterbalance between van der Waals and coulombic interactions. *J Am Chem Soc* 124: 813–826, 2002.
248. Rouvray DH. That fuzzy feeling in chemistry. *Chem Brit* 31: 544–546, 1995.
249. Rouvray DH. Fuzzy logic: A new tool for chemical process control. *Chem Ind* January 20: 60–62, 1997.
250. Rouvray DH. *Fuzzy Logic in Chemistry*. London: Academic Press, 1997.
251. Ruben M, Payer D, Landa A, Comisso A, Gattinoni C, Lin N, Collin JP, Sauvage JP, De Vita A, and Kern K. 2D supramolecular assemblies of benzene-1,3,5-triyl-tribenzoic acid: temperature-induced phase transformations and hierarchical organization with macrocyclic molecules. *J Am Chem Soc* 128: 15644–15651, 2006.
252. Ruthkosky M, Kelly CA, Zaros MC, and Meyer GJ. Long-lived charge-separated states following excitation of Cu(I) donor-acceptor compounds. *J Am Chem Soc* 119: 12004–12005, 1997.
253. Saha S, Flood AH, Stoddart JF, Impellizzeri S, Silvi S, Venturi M, and Credi A. A redox-driven multicomponent molecular shuttle. *J Am Chem Soc* 129: 12159–12171, 2007.
254. Saha S, Leung KCF, Nguyen TD, Stoddart JF, and Zink JI. Nanovalves. *Adv Funct Mater* 17: 685–693, 2007.
255. Samorì P. (Ed). *Scanning Probe Microscopies Beyond Imaging—Manipulation of Molecules and Nanostructures*. Weinheim, Germany: Wiley-VCH, 2006.
256. Sauvage JP. (Ed). *Struct Bond* 99: special volume on Molecular Machines and Motors, 2001, pp. 1–302.
257. Sauvage JP. Transition metal-complexed catenanes and rotaxanes as molecular machine prototypes. *Chem Commun* 12: 1507–1510, 2005.
258. Sauvage JP and Dietrich-Buchecker CO. (Eds). *Molecular Catenanes, Rotaxanes and Knots*. Weinheim, Germany: Wiley-VCH, 1999.
259. Schalley CA, Beizai K, and Vögtle F. On the way to rotaxane-based molecular motors: studies in molecular mobility and topological chirality. *Acc Chem Res* 34: 465–476, 2001.
260. Schalley CA, Weilandt T, Bruggemann J, and Vögtle F. Hydrogen-bond-mediated template synthesis of rotaxanes, catenanes, and knotanes. *Top Curr Chem* 248: 141–200, 2004.
261. Schliwa M. (Ed). *Molecular Motors*. Weinheim, Germany: Wiley-VCH, 2003.
262. Schmidt PM, Brown RS, and Luong JHT. Inclusion complexation of tetrathiafulvalene in cyclodextrins and bioelectroanalysis of the glucose-glucose oxidase reaction. *Chem Eng Sci* 50: 1867–1876, 1995.
263. Seiler M, Dürr H, Willner I, Joselevich E, Doron A, and Stoddart JF. Photoinduced electron-transfer in supramolecular assemblies composed of dialkoxybenzene-tethered Ruthenium(ii) trisbipyridine and bipyridinium salts. *J Am Chem Soc* 116: 3399–3404, 1994.
264. Service RF. Molecular electronics—next-generation technology hits an early midlife crisis. *Science* 302: 556–556, 2003.
265. Service RF. More on molecular electronics—response. *Science* 303: 1137–1137, 2004.
266. Shen YB, Walters KA, Abboud K, and Schanze KS. Intramolecular charge transfer in pyridinium-substituted Ru-polypyridine complexes. *Inorg Chim Acta* 300: 414–426, 2000.
267. Shipway AN and Willner I. Electronically transduced molecular mechanical and information functions on surfaces. *Acc Chem Res* 34: 421–432, 2001.
268. Silvi S, Venturi M, and Credi A. Artificial molecular shuttles: from concepts to devices. *J Mater Chem* 19: 2279, 2009.
269. Simmel FC and Dittmer WU. DNA nanodevices. *Small* 1: 284–299, 2005.
270. Sobransingh D and Kaifer AE. Electrochemically switchable cucurbit[7]uril-based pseudorotaxanes. *Org Lett* 8: 3247–3250, 2006.
271. Sotomayor M and Schulten K. Single-molecule experiments *in vitro* and *in silico*. *Science* 316: 1144–1148, 2007, special section on Single Molecules.
272. Steinberg-Yfrach G, Rigaud JL, Durantini EN, Moore AL, Gust D, and Moore TA. Light-driven production of ATP catalysed by F_0F_1-ATP synthase in an artificial photosynthetic membrane. *Nature* 392: 479–482, 1998.
273. Steuerman DW, Tseng HR, Peters AJ, Flood AH, Jeppesen JO, Nielsen KA, Stoddart JF, and Heath JR. Molecular-mechanical switch-based solid-state electrochromic devices. *Angew Chem Int Ed* 43: 6486–6491, 2004.
274. Stewart DR, Ohlberg DAA, Beck PA, Chen Y, Williams RS, Jeppesen JO, Nielsen KA, and Stoddart JF. Molecule-independent electrical switching in Pt/organic monolayer/Ti devices. *Nano Lett* 4: 133–136, 2004.
275. Stoddart JF. (Ed). *Acc Chem Res* 34(6): special issue on Molecular Machines, 2001, pp. 409–522.
276. Summers A. *The Bipyridinium Herbicides*. New York: Academic Press, 1980.
277. Thiem HJ, Brandl M, and Breslow R. Molecular modeling calculations on the acylation of beta-cyclodextrin by ferrocenylacrylate esters. *J Am Chem Soc* 110: 8612–8616, 1988.
278. Thompson SE and Parthasarathy. Moore's law: the future of Si microelectronics. *Mater Today* 9: 20–25, 2006.
279. Tseng HR, Vignon SA, and Stoddart JF. Toward chemically controlled nanoscale molecular machinery. *Angew Chem Int Ed* 42: 1491–1495, 2003.
280. Tseng HR, Vignon SA, Celestre PC, Perkins J, Jeppesen JO, Di Fabio A, Ballardini R, Gandolfi MT, Venturi M, Balzani V, and Stoddart JF. Redox-controllable amphiphilic [2]rotaxanes. *Chem Eur J* 10: 155–172, 2004.
281. Tseng HR, Wu D, Fang N, Zhang X, and Stoddart JF. The metastability of an electrochemically controlled nanoscale machine on gold surfaces. *Chem Phys Chem* 5: 111–116, 2004.
282. Ulman A. *Characterization of Organic Thin Films*. Boston: Butterworth-Heinemann, 1995.
283. van den Heuvel MGL and Dekker C. Motor proteins at work for nanotechnology. *Science* 317: 333–336, 2007.
284. van den Heuvel MGL, de Graaff MP, and Dekker C. Molecular sorting by electrical steering of microtubules in kinesin-coated channels. *Science* 312: 910–914, 2006.

285. Venturi M, Credi A, and Balzani V. Electrochemistry of coordination compounds: an extended view. *Coord Chem Rev* 185–186: 233–256, 1998.
286. Vives G, Gonzales A, Jaud J, Launay JP, and Rapenne G. Synthesis of molecular motors incorporating para-phenylene-conjugated or bicyclo[2.2.2]octane-insulated electroactive groups. *Chem Eur J* 13: 5622–5631, 2007.
287. Wang B and Král P. Chemically tunable nanoscale propellers of liquids. *Phys Rev Lett* 98: art. n. 266102, 2007.
288. Wang W and Kaifer AE. Electrochemical switching and size selection in cucurbit[8]uril-mediated dendrimer self-assembly. *Angew Chem Int Ed* 45: 7042–7046, 2006.
289. Wang Y, Alvarez J, and Kaifer AE. Redox control of host-guest recognition: a case of host selection determined by the oxidation state of the guest. *Chem Commun*: 1457–1458, 1998.
290. Wang Y, Mendoza S, and Kaifer AE. Electrochemical reduction of cobaltocenium in the presence of beta-cyclodextrin. *Inorg Chem* 37: 317–320, 1998.
291. Ward TR, Lutz A, Parel SP, Ensling J, Gütlich P, Buglyó P, and Orvig C. An iron-based molecular redox switch as a model for iron release from enterobactin via the salicylate binding mode. *Inorg Chem* 38: 5007–5017, 1999.
292. Weber N, Hamann C, Kern JM, and Sauvage JP. Synthesis of a copper [3]rotaxane able to function as an electrochemically driven oscillatory machine in solution, and to form SAMs on a metal surface. *Inorg Chem* 42: 6780–6792, 2003.
293. Weiss PS. More on molecular electronics. *Science* 303: 1136–1137, 2004.
294. Wendell DW, Patti J, and Montemagno CD. Using biological inspiration to engineer functional nanostructured materials. *Small* 2: 1324–1329, 2006.
295. Whelan CM, Gatti F, Leigh DA, Rapino S, Zerbetto F, and Rudolf P. Adsorption of fumaramide [2]rotaxane and its components on a solid substrate: a coverage-dependent study. *J Phys Chem B* 110: 17076–17081, 2006.
296. Willner I, Pardo-Yssar V, Katz E, and Ranjit KT. A photoactivated "molecular train" for optoelectronic applications: light-stimulated translocation of a beta-cyclodextrin receptor within a stoppered azobenzone-alkyl chain supramolecular monolayer assembly on a Au-electrode. *J Electroanal Chem* 497: 172–177, 2001.
297. Willner I. (Ed). *Org Biomol Chem* 4(18): special issue on DNA-based Nanoarchitectures and Nanomachines, 2006.
298. Wong EW, Collier CP, Belohradsky M, Raymo FM, Stoddart JF, Kuekes PJ, Williams RS, and Heath JR. Fabrication and transport properties of single-molecule-thick electrochemical junctions. *J Am Chem Soc* 122: 5831–5840, 2000.
299. Wu J, Leung KCF, Benitez D, Han JY, Cantrill SJ, Fang L, and Stoddart JF. An acid-base-controllable [c2]daisy chain. *Angew Chem Int Ed* 47: 7470–7474, 2008.
300. Wu JS, Toda K, Tanaka A, and Sanemasa I. Association constants of ferrocene with cyclodextrins in aqueous medium determined by solubility measurements of ferrocene. *Bull Chem Soc Jpn* 71: 1615–1618, 1998.
301. Yamamoto T, Tseng HR, Stoddart JF, Balzani V, Credi A, Marchioni F, and Venturi M. Redox-induced ring shuttling and evidence for folded structures in long and flexible two-station rotaxanes. *Collect Czech Chem Commun* 68: 1488–1514, 2003.
302. Yonemoto EH, Riley RL, Kim YL, Atherton SJ, Schmehl RH, and Mallouk TE. Photoinduced electron-transfer in covalently linked ruthenium tris(bipyridyl) viologen molecules—observation of back electron-transfer in the Marcus inverted region. *J Am Chem Soc* 114: 8081–8087, 1992.
303. Yonemoto EH, Saupe GB, Schmehl RH, Hubig SM, Riley RL, Iverson BL, and Mallouk TE. Electron-transfer reactions of ruthenium trisbipyridyl-viologen donor-acceptor molecules—comparison of the distance dependence of electron-transfer rates in the normal and Marcus inverted regions. *J Am Chem Soc* 116: 4786–4795, 1994.
304. Yoshizawa M, Kumazawa K, and Fujita M. Room-temperature and solution-state observation of the mixed-valence cation radical dimer of tetrathiafulvalene, $[(TTF)_2]^+$, within a self-assembled molecular cage. *J Am Chem Soc* 127: 13456–13457, 2005.
305. Yu H, Luo Y, Beverly K, Stoddart J F, Tseng HR, and Heath JR. The molecule-electrode interface in single-molecule transistors. *Angew Chem Int Ed* 24: 5706–5711, 2003.
306. Zelikovich L, Libman J, and Shanzer A. Molecular redox switches based on chemical triggering of iron translocation in triple-stranded helical complexes. *Nature* 374: 790–792, 1995.
307. Zhang L, Macías A, Lu T, Gordon JI, Gokel GW, and Kaifer AE. Calixarenes as hosts in aqueous-media—inclusion complexation of ferrocene derivatives by a water-soluble calix[6]arene. *J Chem Soc Chem Commun*: 1017–1019, 1993.
308. Zhao SS and Luong JHT. Bioelectrocatalysis of a water-soluble tetrathiafulvalene 2-hydroxypropyl-beta-cyclodextrin complex. *Anal Chim Acta* 282: 319–327, 1993.
309. Ziganshina AY, Ko YO, Jeon WS, and Kim K. Stable pi-dimer of a tetrathiafulvalene cation radical encapsulated in the cavity of cucurbit[8]uril. *Chem Commun*: 806–807, 2004.

Address correspondence to:
Prof. Alberto Credi
Dipartimento di Chimica "G. Ciamician"
Università di Bologna
Via Selmi 2–40126 Bologna
Italy

E-mail: alberto.credi@unibo.it

Date of first submission to ARS Central, April 1, 2010; date of final revised submission, June 21, 2010; date of acceptance, June 23, 2010.

Abbreviations Used

BPY^{2+} = 4,4′-bipyridinium
CD = cyclodextrin
CT = charge-transfer
DABCO = diazabicyclo[2.2.2]octane
DOB = dioxybenzene
DON = dioxynaphthalene
LB = Langmuir-Blodgett
NDI = naphthalene diimide
NMR = nuclear magnetic resonance
PMI = pyromellitic imide
ptz = phenothiazine
SAM = self-assembled monolayer
SCE = saturated calomel electrode
TTF = tetrathiafulvalene
TTFP = monopyrrolotetrathiafulvalene
XPS = X-ray photoelectron spectroscopy

This article has been cited by:

1. Albert C. Fahrenbach, Zhixue Zhu, Dennis Cao, Wei-Guang Liu, Hao Li, Sanjeev K. Dey, Subhadeep Basu, Ali Trabolsi, Youssry Y. Botros, William A. Goddard, J. Fraser Stoddart. 2012. Radically Enhanced Molecular Switches. *Journal of the American Chemical Society* **134**:39, 16275-16288. [CrossRef]
2. Paola Ceroni, Alberto Credi, Margherita VenturiElectrochemical Methods 371-457. [CrossRef]
3. G. Z. Cohen, V. Fleurov, K. Kikoin. 2012. Cotunneling mechanism of single-electron shuttling. *The European Physical Journal B* **85**:2. . [CrossRef]
4. Shuai-Fan Wu, Xiang Ma. 2011. Vinylbipyridinium dication–triphenylureidocalix[6]arene pseudorotaxane. *Tetrahedron Letters* . [CrossRef]